

**Bactericidal Properties of Blackened Titanium Dioxide on Glass Filter:
A Proof of Concept for Water Decontamination**

Sara Currie

Thesis submitted to the University of Ottawa
in partial Fulfillment of the requirements for the degree of Master of Chemistry

Department of Chemistry and Biomolecular Sciences
Faculty of Science
University of Ottawa

Submitted to thesis committee on January 8, 2025
© Sara Currie, Ottawa, Canada, 2025

ABSTRACT

Water scarcity remains a pressing global challenge, disproportionately affecting rural communities lacking access to effective water treatment systems. This thesis explores the development and optimization of a solar-powered water purification technology employing blackened titanium dioxide (bTiO₂) as a photocatalyst to address bacterial contamination. This work builds on the "Water Project," a collaborative initiative aimed at sustainably purifying river water in Kenya using abundant sunlight for community-scale applications. Beyond sunny regions, this technology holds great potential in areas like northern Canada or anywhere under a boil water advisory, where white LEDs can serve as an effective substitute for sunlight.

Heterogeneous bTiO₂, synthesized directly onto glass filter supports, demonstrates robust photocatalytic activity under white light, facilitating the generation of reactive oxygen species (ROS) for bacterial inactivation. The material's properties, including extended spectral absorption (300-800 nm) and reduced bandgap energy (from 3.3 eV to 2.18 eV), enable efficient solar-driven disinfection. Two bacterial strains, *Escherichia Coli* (Gram-negative) and *Staphylococcus Aureus* (Gram-positive), were chosen as representative contaminants due to their prevalence in Kenyan river water and health implications.

A key innovation in this study is the development and application of a fluorescence-based viability assay using PicoGreen. This novel method offers rapid and reliable evaluation of bacterial viability within 10 minutes, significantly faster than traditional colony counting methods. Importantly, the research uncovers a novel dependency of PicoGreen fluorescence on the bacterial inactivation pathway. The assay is highly sensitive to lysis-mediated inactivation, where cellular membranes are disrupted, but demonstrates limited fluorescence response with apoptotic cells, where ROS-mediated DNA damage and fragmentation occur without significant loss of membrane integrity. While PicoGreen has been shown to produce false negatives under certain conditions, it has never demonstrated false positives, ensuring that bacterial inactivation is never overestimated. This reliability makes the method worthy of further study, as a false positive would undermine the validity of disinfection processes, whereas a false negative only highlights the need for further refinement. These findings provide critical insights into the mechanism-specific applicability of fluorescence-based quantification methods.

This thesis employs batch and flow systems to assess bacterial inactivation, with outcomes quantified using the PicoGreen assay. The thesis achieved notable bacterial inactivation with bTiO₂, particularly during Flow 3.0 tests that incorporated oxygen bubbles to enhance turbulence and ROS generation. *E. Coli* inactivation reached 99.8 %, exceeding the WHO standard¹ of 99 % within 30 minutes, while *S. Aureus* achieved 98.5 %, narrowly missing the benchmark by 0.5 %. However, the spatial limitations of batch systems prompted the development of three flow systems, including a single-pass configuration with gas bubbling to enhance turbulence and ROS availability. Flow systems significantly improve bacterial interaction with the catalyst, achieving two-log bacterial reductions within 30 minutes, meeting World Health Organization (WHO) guidelines for water disinfection.

Beyond establishing that our new catalyst can kill bacteria under white light and flow conditions, we also investigated mechanistic insights into bacterial inactivation and the behavior of PicoGreen using fluorescence lifetime imaging microscopy (FLIM). Results indicate that ROS-induced oxidative stress is the primary inactivation pathway, leading to cellular damage and membrane disruption. Scanning electron microscopy (SEM) imaging highlights the importance of flow systems in mitigating biofilm formation on the catalyst surface.

This work advances the application of solar-activated photocatalysis for sustainable water purification. The findings underscore the potential of bTiO₂ in delivering accessible, efficient, and environmentally friendly solutions to global water challenges, while the novel fluorescence assay contributes to streamlined monitoring of water quality in real-time applications.

ACKNOWLEDGEMENTS

My deepest gratitude goes out to my incredible supervisors, Dr. Juan Scaiano and Dr. Adam Shuhendler. This research journey would not have been possible without Dr. Scaiano welcoming me into his chemistry fold back in 2019. Tito, your leadership, marked by compassion and curiosity, has been nothing short of inspiring. It has been both an honor and a privilege to be part of the Scaiano Lab for over five years. Your mentorship extended far beyond lectures and scientific guidance—you offered friendship and camaraderie that I will always treasure. I'll hold our book club conversations close to my heart forever.

The Scaiano Lab is a wellspring of knowledge and support, and I owe much of my progress to the generosity of my colleagues. A special thank you to Daliane Regis Correa da Silva and Jazmin Silvero for always taking the time to answer my questions and guiding me through my biology journey as a young chemist. To Neeraj Joshi, thank you for your willingness to teach me how to use any piece of equipment I needed and for always being a supportive sounding board.

Dr. Shuhendler, thank you for your invaluable guidance in biology and for challenging me to tackle the difficult tasks, especially during moments of self-doubt. Because of your encouragement, I've grown not only in knowledge but also in confidence, far beyond what I thought possible when I first embarked on this degree.

I couldn't have completed this journey without the unwavering support of my parents. Mom and Dad, thank you for dropping off meals at my apartment, listening to me vent, and offering endless encouragement. Your love and support mean the world to me, and I'm forever grateful.

To Liam, thank you for standing by me through my most stressful moments, my late nights in the lab, and for showing endless patience and understanding. Your love and support have been my anchor, and I love you more than words can express.

Table of Contents

1.0 INTRODUCTION	1
1.1 General Introduction	1
1.2 Blackened Titanium Dioxide	2
1.3 Reactive Oxygen Species	5
1.4 Bacteria	7
1.4.1 Gram Positive and Negative Bacteria	7
1.4.2 Bacterial Growth	8
1.4.3 Bacterial Inactivation	8
1.4.4 Quantification of Bacteria – Current Technologies	10
1.4.5 Quantification of Bacteria – Novel Fluorescence Tests	10
1.5 Goals of Thesis	11
2.0 METHODS	12
2.0.1 Materials	12
2.1 Blackened Titanium Dioxide Synthesis	12
2.2 Media preparation	16
2.2.1 Luria-Bertani (LB) broth	16
2.2.2 HEPES Media	16
2.2.3 0.85% NaCl	16
2.2.4 DL-Lactate Minimal Media	16
2.2.4 LB Agar Plates	17
2.3 Bacteria Incubation and Preparation	17
2.4 Plating and Colony Counting	18
2.5 Optical Density Growth Assay	18
2.6 Fluorescent Dye Testing	20
2.7 SEM Imaging	21
2.8 Fluorescence assay	22
2.8.1 Batch Experiments	22
2.8.2 Flow Experiments – Recycled, Flow 1.0	23
2.8.3 Flow Experiments – Single Pass, Flow 2.0	24

2.8.4 Flow Experiments – Single Pass with Gas, Flow 3.0	26
2.8.5 Fluorescence Experiments - Analysis.....	27
2.9 <i>FLIM</i>	27
2.10 <i>Statistical Analysis- ANOVA and T-Tests</i>	29
3.0 <i>RESULTS</i>	30
3.1 <i>Optical Density Growth Assay</i>	30
3.2 <i>SEMImages</i>	35
3.3 <i>Fluorescent Dye Testing</i>	41
3.4 <i>Fluorescence Batch Experiments</i>	48
3.5 <i>Fluorescence Flow Experiments Results</i>	51
3.5.1 Flow 1.0, Recycled Solution	51
3.5.2 Flow 2.0, Single Pass.....	54
3.5.3 Flow 3.0, Single Pass with Gas	57
3.6 <i>FLIM Studies</i>	61
4.0 <i>DISCUSSION</i>	66
4.1 <i>Optical Density Growth Assay</i>	66
4.2 <i>SEMImages</i>	68
4.3 <i>Fluorescent Dyes</i>	69
4.4 <i>Fluorescence Tests for Batch Experiments</i>	70
4.5 <i>Fluorescence Tests for Flow Experiments (Flow 1.0, 2.0, and 3.0)</i>	71
4.6 <i>Fluorescence Lifetime Imaging Microscopy (FLIM) Tests</i>	74
5.0 <i>CONCLUSIONS</i>	77
6.0 <i>APPENDIX</i>	80
<i>REFERENCES</i>	99

LIST OF FIGURES AND TABLES

- Figure 1** schematic representation of the photocatalytic mechanism of titanium dioxide (TiO₂) upon absorption of photons with energy equal to or greater than the band gap, an electron (e⁻) is excited from the valence band (VB) to the conduction band (CB), leaving behind a hole (h⁺) in the vb. The excited electron can participate in reduction reactions, while the hole can drive oxidation reactions. Particularly, the promoted electron can react with dissolved O₂ to create reactive oxygen species (ROS), facilitating the degradation of contaminants in water purification processes. 3
- Figure 2** characterization spectra of blackened titanium dioxide. Diffuse reflectance spectra (a) and x-ray diffraction (XRD) (b), as well as the absorbance spectra (c) of white and black TiO₂ catalysts on glass filter. The lines in (b) are representative of the known anatase XRD pattern according to ICDD card number 01-073-1764. Figures (a) and (b) are used with permission from the authors and were published recently in catalysis². Brunauer-Emmett Teller (BET) measurements (from adsorption-desorption of n₂ at 77k) for bTiO₂ on glass filter showed a specific surface area of 25.0 m²/g and an average crystal size of 15.4 nm. The crystal size of the TiO₂ materials (nm) was calculated using the Scherrer equation ($l = k\lambda/\beta \cdot \cos\theta$), where crystalline Factor (k)=0.9, λ cuka = 0.154 and the fwhm (β) was measured from the XRD diffractograms². 4
- Figure 3** Proposed band gap comparison diagram between white and black TiO₂ adapted from b. Wang et al., 2017⁹. 5
- Figure 4** Strips of white (top) and blackened (bottom) TiO₂ on glass filter. Catalyst strips are 25-26 cm long and are shown here after synthesis and five washes with Milli-Q water. 14
- Figure 5** UV-Visible spectrum taken of Milli-Q water used to rinse excess tio₂ off glass filters. A baseline of pure Milli-Q water was established at absorbance 0. Small 47 mm, 100 nm filters were used from pall corporation²⁹. Each rinse was performed with approximately 10 ml of milli- q water, swirled, and sampled in the Cary 60 UV-Vis spectrometer. 15
- Figure 6** 96 well plate setup for calibration curve and exposure samples. In column 2 wells of the 96 wellplate, calibration curves were set up by diluting Live bacteria (od₆₀₀ = 0.030) to 50 %, 25 %, 12.5 %, 6.25 %, 3.12 %, and 1.56 % of its experimental concentration with DL-Lactate minimal media. We will call this column “concentrated calibration curve”. 20µl from each of the “concentrated calibration curve” wells was placed in column 3 of the wellplate and diluted with 180 µl of lb media, totalling 200 µl. This was repeated in triplicate to create the “calibration curve”. Experimental aliquots were plated in cells B6 through G11 (labelled in orange). 20 µl from each timed aliquot was added to a well and diluted with 180 µl of lb media for a total of 200 µl. This was repeated in triplicate. Blank wells contained only lb media. Water was plated around the outside of the wellplate where space allowed to minimize evaporation of experimental wells during the 16-hour incubation and growth measurements. 20
- Figure 7** Experimental batch setup diagram with photograph inset (a). Created with biorender.com 23
- Figure 8** Flow 1.0 set up diagram with photograph inset (a). Equipment used was a VWR mini variable flow peristaltic pump, a glass tube (39 cm long, 0.57 cm (interior diameter), silicone tubing (0.85 cm interior diameter), a strip of bTiO₂ (30 cm long, 0.5 cm wide), and a 150 ml beaker for recycling flow. The beaker contained 70 ml of bacterial solution. Total residence time was 20.0 minutes, with a flow speed of 3.43 ml/minute. The active residence time (inside glass tube) was three minutes. Figure created with biorender.com. 24
- Figure 9** single pass flow 2.0 set up diagram with photograph inset (a). Total volume of this system (not including

the syringe chamber) was 20.70 ml, where 0.70 ml was dead volume and 20 ml was active volume inside the quartz tube. The tent lamp consisted of two white LED flood lamps positioned on two faces of a triangular prism, with an aluminum foil covered piece of particle board on the third face to improve the tube's exposure to photons (**figure 35**). The quartz tube was held at a 45-degree angle using clamps, and solution filled it from the bottom to the top. Figure created with biorender.com. 26

Figure 10 flow 3.0 set up with gas flow either air or pure oxygen, and photograph inset (a). For the air, benchtop air flow was supplied, and for oxygen, a cylinder of compressed oxygen was used. Both had a rate of 1.22 ml/minute, giving a champagne-bubble-like appearance in the flow system. Figure created with biorender.com 27

Figure 11 growth assay calibration curve graph 1. OD₆₀₀ was monitored via wellplate reader over the course of 16 hours. Data after 8 hours demonstrates a plateau, so was discarded. *E. Coli* live cells (OD₆₀₀ 0.003) were diluted with dead cells (prepared as described in section 2.3 bacteria incubation and preparation.) Longer lag times correspond to smaller fractions of live cells compared to dead cells. Inset datapoints refer to the time when each sample reaches the threshold value of OD₆₀₀ 0.1 versus the Log(percent live cells). Inset trendlines were used to calculate the percent inactive bacteria for experimental and control conditions. 32

Figure 12 Growth assay results for *E. Coli* exposure to bTiO₂ and white LED light (**figure 36 (a)**). Aliquots were plated, incubate at 37°C, and OD₆₀₀ were read in a wellplate reader every 20 minutes for 16 hours. Datapoints after 8 hours show a plateau so were discarded. Longer lag times correspond to a higher percentage inactive or dead cells. 33

Figure 13 Growth assay calibration curve graph 2. OD₆₀₀ was monitored via wellplate reader over the course of 16 hours. Data after 8 hours demonstrates a plateau, so was discarded. *S. Aureus* live cells (OD₆₀₀ 0.003) were diluted with dead cells (prepared as described in section 2.3 bacteria Incubation and preparation.) Longer lag times correspond to smaller fractions of live cells compared to dead cells. Inset datapoints refer to the time when each sample reaches the threshold value of OD₆₀₀ 0.1 versus the Log(percent live cells). Inset trendlines were used to calculate the percent inactive bacteria for experimental and control conditions. 34

Figure 14 growth assay results for *S. Aureus* exposure to bTiO₂ and white LED light (**figure 36 (a)**). Aliquots were plated, incubate at 37°C, and OD₆₀₀ were read in a wellplate reader every 20 minutes for 16 hours. Datapoints after 8 hours show a plateau so were discarded. Longer lag times correspond to a higher percentage inactive or dead cells. 35

Figure 15 SEM images of catalyst strips prior to use in experiments. Glass filter before synthesis of catalyst (a), bTiO₂ on glass filter support before use (b), bTiO₂ on glass filter support after 30-minute exposure to DL-Lactate media (c), and same conditions as (c), but with higher magnification (d). 37

Figure 16 SEM images of catalyst strip after 1.5 hours in solution, shown at various magnifications. Small catalyst strips were placed in 30 ml of DL-Lactate bacterial solution (10⁶ CFU/ml) and oscillated at room temperature under dark conditions for 1.5 hours. They were not rinsed. 38

Figure 17 SEM images of catalyst strip after 1.5 hours in solution followed by rinse, shown at various magnifications. Small catalyst strips were placed in 30 ml of DL-Lactate bacterial solution (10⁶ CFU/ml) and oscillated at room temperature under dark conditions for 1.5 hours. They were rinsed one time with 50 ml Milli-Q water. 39

Figure 18 SEM images of catalyst strip after 3 hours in solution, shown at various magnifications. Small catalyst were placed in 30 ml of DL-Lactate bacterial solution (10⁶ CFU/ml) and oscillated at room temperature

under dark conditions for 3 hours. They were not rinsed.

40

Figure 19 SEM images of catalyst strip after 3 hours in solution followed by rinse. Small catalyst strips were placed in 30 ml of DL-Lactate bacterial solution (10^6 CFU/ml) and oscillated at room temperature under dark conditions for 3 hours. They were rinsed one time with 50 ml Milli-Q water.

41

Figure 20 Fluorescent dye molecule structures. Excitation (ex) and emission (em) wavelengths included, according to measurements at 6.4 μ m in DL-Lactate media.

42

Figure 21 Excitation spectra for all fluorescent dyes tested. Dyes were DAPI, Ethidium Bromide, Hoechst 33342, Hoechst 33258, Propidium Iodide, Sybr Green, Sybr Gold, and PicoGreen. All dyes were diluted to 6.4 μ m in DL-Lactate media, and monitored using an M5 microplate reader which performed an excitation sweep with data collected every 2 nm. Spectra were collected with high concentrations of both bacteria (2.4×10^7 CFU/ml), and averaged.

43

Figure 22 Emission spectra for all fluorescent dyes tested. Only peaks are included for spectra simplification. Dyes were DAPI, Ethidium Bromide, Hoechst 33342, Hoechst 33258, Propidium Iodide, Sybr Green, Sybr Gold, and PicoGreen. All dyes were diluted to 6.4 μ m in DL-Lactate media, and monitored using an M5 Microplate reader which performed an emission sweep with data collected every 2 nm. All dyes were excited at their respective wavelengths (**figure 21**). Spectra were collected with high concentrations of both bacteria (2.4×10^7 CFU/ml), and averaged.

44

Figure 23 Calibration curves of all fluorescent dyes tested, using both *E. Coli*, and *S. Aureus* [(a)-(p)]. Data is normalized to the 0 % dead cells fluorescence value (RFU) for each trial.

47

Figure 24 *E. Coli* (a) and *S. Aureus* (b) inactivation batch test results measured with PicoGreen fluorescence. Bacteria in DL-Lactate media (30 ml, OD₆₀₀ 0.003) was oscillated at room temperature either under light or dark conditions (**figure 7** experimental batch setup diagram) red bars represent experimental conditions; bTiO₂ on glass filter (GF) support and white LED light (**figure 36**). All other conditions were represented other colours (bTiO₂ dark, GF light and dark, and nothing - no catalyst and no GF). Bacteria were exposed to conditions for 180 minutes with 1 ml aliquots taken at minutes 0, 5, 10, 20, 40, 60, 80, 100, 120, 140, 160, and 180 minutes. Dilute PicoGreen (50 μ l) was added to each 1 ml aliquot for a total concentration of 6.4 μ m, left at room temperature in the dark for ten minutes, and fluorescence was read. Aliquots were taken in triplicate with error bars representing standard deviation. Statistical analysis using ANOVA and Tukey's HSD test ($p < 0.05$) showed that bTiO₂ significantly reduced viability compared to GF and 'nothing' conditions.

50

Figure 25 *E. Coli* (a) and *S. Aureus* (b) inactivation batch test results measured with plating and colony counting. Bacteria in DL-Lactate media (30 ml, OD₆₀₀ 0.003) was oscillated at room temperature either under light or dark conditions (**figure 7** experimental batch setup diagram) red bars represent experimental conditions; bTiO₂ on glass filter (GF) support and white LED light (**figure 36**). All other conditions were represented other colours (bTiO₂ dark, GF light and Dark, and nothing - no catalyst and no GF). Bacteria were exposed to conditions for 180 minutes with 1 ml aliquots taken at minutes 0, 5, 10, 20, 40, 60, 80, 100, 120, 140, 160, and 180. Drops of working solution (10 μ l) in various dilutions were plated, incubated for 14h and counted. Aliquots were taken in triplicate with error bars representing standard deviation. Statistical analysis using ANOVA and Tukey's HSD test ($p < 0.05$) showed that bTiO₂ and white light significantly reduced viability compared to control conditions.

51

Figure 26 *E. Coli* (a) and *S. Aureus* (b) inactivation flow 1.0 test results measured with PicoGreen fluorescence. Bacteria in DL-Lactate media (70 ml, OD₆₀₀ 0.003) was pumped at 6 ml/min from a beaker over catalyst or glass filter at room temperature under either light or dark conditions (**figure 8**) upon exiting the flow tube, solution was returned to the beaker to be recycled. One millilitre aliquots were collected from the beaker. Aliquot times represent the number of minutes after the first millilitre of solution returned to the recycling beaker. Red bars represent experimental conditions; bTiO₂ on glass filter (GF) support and white LED light (**figure 36**). All other conditions were represented other colours (bTiO₂ dark, GF light and dark). Dilute PicoGreen (50 µl) was added to each 1 ml aliquot for a total dye concentration of 6.4 µM, left at room temperature in the dark for ten minutes, and fluorescence was read. Aliquots were taken in triplicate with error bars representing standard deviation. Statistical analysis using ANOVA and Tukey's HSD test (p < 0.05) showed that bTiO₂ reduced viability compared to control conditions for *E. Coli*.

54

Figure 27 *E. Coli* (a) and *S. Aureus* (b) inactivation flow 1.0 test results measured with plating and colony counting. Bacteria in DL-Lactate media (70 ml, OD₆₀₀ 0.003) was pumped at 6 ml/min from a beaker over catalyst or glass filter at room temperature under either light or dark conditions (**figure 8**). Upon exiting the flow tube, solution was returned to the beaker to be recycled. One millilitre aliquots were collected from the beaker. Aliquot times represent the number of minutes after the first millilitre of solution returned to the recycling beaker. Red bars represent experimental conditions; bTiO₂ on glass filter (GF) support and white LED light (**figure 36**). All other conditions were represented other colours (bTiO₂ dark, GF light and dark). Drops of working solution (10 µl) in various dilutions were plated, incubated for 14h and counted. Drops were plated in triplicate with error bars representing standard deviation. Statistical analysis using ANOVA and Tukey's HSD test (p < 0.05) showed that bTiO₂ and white light significantly increased bacterial inactivation compared to control conditions.

55

Figure 28 Flow 2.0 bacterial inactivation at various flow speeds, under white LED and bTiO₂ measured by PicoGreen. *E. Coli* and *S. Aureus* working solutions (OD₆₀₀ 0.003-0.006) were flowed through a 20 ml quartz tube at varying flow rates. Experiments were conducted under a "tent lamp" white LED light source (**figure 36**) in the presence of bTiO₂ on glass filter support. Dilute PicoGreen (50 µl) was added to each 1 ml aliquot for a total dye concentration of 6.4 µM, followed by resting in the dark at room temperature for 10 minutes prior to fluorescence measurement. Statistical analysis using ANOVA and Tukey's HSD Test (p < 0.05) showed that both flow speeds of 0.35 and 0.66 ml/min significantly increased bacterial inactivation compared to 1.33 ml/min. Note that the absence of bars for 0.35 and 1.33 ml/min at times longer than 15 minutes signifies that the measurement was not performed (as opposed to the reading being zero).

57

Figure 29 Control experiments for flow 2.0 bacterial inactivation, measured by PicoGreen, under bTiO₂ (dark conditions) and glass filter (GF) support in both dark and light conditions. *E. Coli* and *S. Aureus* working solutions (OD₆₀₀ 0.003-0.006) were flowed through a 20 ml quartz tube at varying flow rates. For bTiO₂ controls (**figure 29**), experiments were conducted in the absence of illumination, while for GF controls, experiments were conducted under both "tent lamp" white LED light (**figure 36**) and dark conditions. Dilute PicoGreen (50 µl) was added to each 1 ml aliquot for a total dye concentration of 6.4 µM, followed by rest in the dark at room temperature for 10 minutes prior to fluorescence measurement. Statistical analysis using ANOVA and Tukey's HSD Test (p < 0.05) showed that bTiO₂ and white light significantly increased bacterial inactivation compared to all control conditions at any speed.

59

Figure 30 flow 3.0 *E. Coli* and *S. Aureus* inactivation measured by PicoGreen with air or oxygen bubbled. *E. Coli* was flowed at 0.66 ml/min (30 minutes exposure time) with air (a) or oxygen (c) bubbled at 1.33 ml/min. *S. Aureus* was flowed under the same conditions with air (b) or oxygen (d). Dilute PicoGreen (50 µl) was added to each 1 ml aliquot for a total dye concentration of 6.4 µM, followed by resting in the dark at room temperature for 10 minutes prior to fluorescence measurement. Aliquots were measured in triplicate with error

X

bars representing standard deviation. Statistical analysis using ANOVA and Tukey's HSD test ($p < 0.05$) showed that bTiO₂ and white light significantly increased bacterial inactivation compared to control conditions.

62

Figure 31 Flow 3.0 colony counting results for *E. Coli* and *S. Aureus* inactivation under white light illumination with bTiO₂ in the presence of either air (a) or oxygen (b). Drops of working solution (10 μ l) in various dilutions were plated, incubated for 14h and counted. Drops were plated in triplicate with error bars representing standard deviation.

63

Figure 32 *E. Coli* inactivation by various methods using white light microscopy and FLIM. Percent inactive (dead) cells was verified using plating and colony counting.

66

Figure 33 *S. Aureus* inactivation by various methods using white light microscopy and FLIM. Percent inactive (dead) cells was verified using plating and colony counting.

67

Figure 34 Sample average decay histograms for *E. Coli* live (a) and heat-treated cells (c), and *S. Aureus* live (b) and heat-treated cells (d). Instrument response function (IRF) was $\tau = 0.36$ ns (e).

69

Figure 35 Radar plots with decision factors for dye selection. Factors include price (information sourced from Sigma Aldrich), sensitivity (found using normalized RFU, **figure 23**), ease of storage, and safety (toxicity, temperature, and light conditions located on MSDS sheet, Sigma Aldrich). Plotted with Kaleidagraph v5.0.

74

Figure 36 Intensity spectra for 'flood lamp' (a) 'tent lamp' (b), and UVC lamp (c). Measured using Luzchem spr-01-235-850nm spectroradiometer. The 'flood lamp' was used for growth assay, fluorescence batch, and fluorescence flow 1.0 Experiments. The bottom of the 'tent lamp' was coated with aluminum foil, and this setup was used for fluorescence flow 2.0 and 3.0 experiments. The UVC lamp was used exclusively for FLIM test cell inactivation at a distance of 5.0 cm, spectrum used was from Luzchem⁵³. A 2% filter was used to prevent overexposure for (a) and (b).

I

Figure 37 Growth assay calibration curve graph 3. OD₆₀₀ was monitored via wellplate reader over the course of 16 hours. *E. Coli* live cells (OD₆₀₀ 0.003) were diluted with dead cells (prepared as described in section 2.3 bacteria incubation and preparation.) Longer lag times correspond to smaller fractions of live cells compared to dead cells. Inset datapoints refer to the time when each sample reaches the threshold value of OD₆₀₀ 0.1 versus the Log(percent live cells). Inset trendlines were used to calculate the percent inactive bacteria for experimental and control conditions.

II

Figure 38 Growth assay results for *E. Coli* exposure to bTiO₂ under dark conditions. Aliquots were plated, incubate at 37°C, and OD₆₀₀ were read in a wellplate reader every 20 minutes for 16 hours. Datapoints after 8 hours show a plateau so were discarded. Times when each sample crossed the OD₆₀₀ threshold of 0.1 were noted and compared to the respective calibration curve to determine percent bacterial inactivation.

III

Figure 39 Growth assay results for *E. Coli* exposure to glass filter under white LED conditions (**figure 35 (a)**). Aliquots were plated, incubate at 37°C, and OD₆₀₀ were read in a wellplate reader every 20 minutes for 16 hours. Datapoints after 8 hours show a plateau so were discarded. Times when each sample crossed the OD₆₀₀ threshold of 0.1 were noted and compared to the respective calibration curve to determine percent bacterial inactivation.

IV

Figure 40 Growth assay calibration curve graph 4. OD₆₀₀ was monitored via wellplate reader over the course of 16 hours. Data after 8 hours demonstrates a plateau, so was discarded. *E. Coli* live cells (OD₆₀₀ 0.003) were diluted with dead cells (prepared as described in section 2.3 bacteria incubation and preparation.) Longer lag times correspond to smaller fractions of live cells compared to dead cells. Inset datapoints refer to the time when each sample reaches the threshold value of OD₆₀₀ 0.1 versus the Log(percent live cells). Inset trendlines were used to calculate the percent inactive bacteria for experimental and control conditions.

V

Figure 41 Growth assay results for *E. Coli* without catalyst or glass filter under white LED conditions (**figure 36 (a)**). Aliquots were plated, incubate at 37°C, and OD₆₀₀ were read in a wellplate reader every 20 minutes for 16 hours. Datapoints after 8 hours show a plateau so were discarded. Times when each sample crossed the OD₆₀₀ threshold of 0.1 were noted and compared to the respective calibration curve to determine percent bacterial inactivation.

VI

Figure 42 Growth assay results for *E. Coli* exposure to glass filter under dark conditions. Aliquots were plated, incubate at 37°C, and OD₆₀₀ were read in a wellplate reader every 20 minutes for 16 hours. Datapoints after 8 hours show a plateau so were discarded. Times when each sample crossed the OD₆₀₀ threshold of 0.1 were noted and compared to the respective calibration curve to determine percent bacterial inactivation.

VI

Figure 43 Growth assay calibration curve graph 5. OD₆₀₀ was monitored via wellplate reader over the course of 16 hours. Data after 8 hours demonstrates a plateau, so was discarded. *E. Coli* live cells (OD₆₀₀ 0.003) were diluted with dead cells (prepared as described in section 2.3 bacteria incubation and preparation.) Longer lag times correspond to smaller fractions of live cells compared to dead cells. Inset datapoints refer to the time when each sample reaches the threshold value of OD₆₀₀ 0.1 versus the Log(percent live cells). Inset trendlines were used to calculate the percent inactive bacteria for experimental and control conditions.

VII

Figure 44 Growth assay results for *E. Coli* without catalyst or glass filter under dark conditions. Aliquots were plated, incubate at 37°C, and OD₆₀₀ were read in a wellplate reader every 20 minutes for 16 hours. Datapoints after 8 hours show a plateau so were discarded. Times when each sample crossed the OD₆₀₀ threshold of 0.1 were noted and compared to the respective calibration curve to determine percent bacterial inactivation.

VIII

Figure 45 Growth assay calibration curve graph 6. OD₆₀₀ was monitored via wellplate reader over the course of 16 hours. Data after 8 hours demonstrates a plateau, so was discarded. *S. Aureus* live cells (OD₆₀₀ 0.003) were diluted with dead cells (prepared as described in section 2.3 bacteria incubation and preparation.) Longer lag times correspond to smaller fractions of live cells compared to dead cells. Inset datapoints refer to the time when each sample reaches the threshold value of OD₆₀₀ 0.1 versus the Log(percent live cells). Inset trendlines were used to calculate the percent inactive bacteria for experimental and control conditions.

IX

Figure 46 Growth assay results for *S. Aureus* exposure to glass filter under dark conditions. Aliquots were plated, incubate at 37°C, and OD₆₀₀ were read in a wellplate reader every 20 minutes for 16 hours. Datapoints after 8 hours show a plateau so were discarded. Times when each sample crossed the OD₆₀₀ threshold of 0.1 were noted and compared to the respective calibration curve to determine percent bacterial inactivation.

X

Figure 47 Growth assay calibration curve graph 7. OD₆₀₀ was monitored via wellplate reader over the course of 16 hours. Data after 8 hours demonstrates a plateau, so was discarded. *S. Aureus* live cells (OD₆₀₀ 0.003) were diluted with dead cells (prepared as described in section 2.3 bacteria incubation and preparation.) Longer lag times correspond to smaller fractions of live cells compared to dead cells. Inset datapoints refer to the time when each sample reaches the threshold value of OD₆₀₀ 0.1 versus the log(percent live cells). Inset trendlines were used to calculate the percent inactive bacteria for experimental and control conditions.

XI

Figure 48 Growth assay results for *S. Aureus* exposure to bTiO₂ under dark conditions. Aliquots were plated, incubated at 37°C, and OD₆₀₀ were read in a wellplate reader every 20 minutes for 16 hours. Datapoints after 8 hours show a plateau so were discarded. Times when each sample crossed the OD₆₀₀ threshold of 0.1 were noted and compared to the respective calibration curve to determine percent bacterial inactivation.

XII

Figure 49 Growth assay results for *S. Aureus* exposure to glass filter under white LED conditions (**figure 35 (a)**). Aliquots were plated, incubate at 37°C, and OD₆₀₀ were read in a wellplate reader every 20 minutes for 16 hours. Datapoints after 8 hours show a plateau so were discarded. Times when each sample crossed the OD₆₀₀ threshold of 0.1 were noted and compared to the respective calibration curve to determine percent bacterial inactivation.

XII

Figure 50 Growth assay calibration curve graph 8. OD₆₀₀ was monitored via wellplate reader over the course of 16 hours. Data after 8 hours demonstrates a plateau, so was discarded. *S. Aureus* live cells (OD₆₀₀ 0.003) were diluted with dead cells (prepared as described in section 2.3 bacteria incubation and preparation.) Longer lag times correspond to smaller fractions of live cells compared to dead cells. Inset datapoints refer to the time when each sample reaches the threshold value of OD₆₀₀ 0.1 versus the Log(percent live cells). Inset trendlines were used to calculate the percent inactive bacteria for experimental and control conditions.

XIII

Figure 51 Growth assay results for *S. Aureus* without catalyst or glass filter under white LED conditions (**figure 36 (a)**). Aliquots were plated, incubate at 37°C, and OD₆₀₀ were read in a wellplate reader every 20 minutes for 16 hours. Datapoints after 8 hours show a plateau so were discarded. Times when each sample crossed the OD₆₀₀ threshold of 0.1 were noted and compared to the respective calibration curve to determine percent bacterial inactivation.

XIV

Figure 52 Growth assay results for *S. Aureus* without catalyst or glass filter under dark conditions. Aliquots were plated, incubate at 37°C, and OD₆₀₀ were read in a wellplate reader every 20 minutes for 16 hours. Datapoints after 8 hours show a plateau so were discarded. Times when each sample crossed the OD₆₀₀ threshold of 0.1 were noted and compared to the respective calibration curve to determine percent bacterial inactivation.

XIV

Figure 53 Sample average decay histograms for *E. Coli* treated with UVC (**figure 36 (c)**) (a), isopropanol (c), and bTiO₂ and white light (**figure 36 (b)**) (e), as well as *S. Aureus* treated with UVC (**figure 36 (c)**) (b), isopropanol (d), and bTiO₂ and white light (**figure 36 (b)**) (f).

XVIII

Table 1 Cary 60 UV-Vis spectrometer settings. As used in single scans. Quartz cuvettes were used for all measurements in the instrument.	15
Table 2 Bacterial calibration curve preparation. Total volumes for each sample were 1 ml.	21
Table 3 Flow rate and residence time for flow 2.0 and 3.0 single pass experiments.	25
Table 4 PicoGreen fluorescence test analysis conditions on the SpectraMax M5 microplate reader ³³	28
Table 5 FLIM settings used for imaging dyed bacteria. Bidirectional scans were used for all images.	29
Table 6 Growth assay experimental condition results. Inactivation of <i>E. Coli</i> and <i>S. Aureus</i> under white LED light (figure 36) with bTiO ₂ strips. No bacterial inactivation (or bacterial growth) is represented by “NI”.	36
Table 7 Optical density (OD ₆₀₀) to colony forming unit (CFU/ml) conversion table. Based on <i>E. Coli</i> conversion factor OD ₆₀₀ of 1.0 = 8 × 10 ⁸ cells/ml and <i>S. Aureus</i> conversion factor OD ₆₀₀ of 1.0 = 1.6 × 10 ⁸ cells/ml. Conversion factors were verified via plating and colony counting in triplicate.	48
Table 8 Flow rates and equivalent residence times for flow 2.0 and 3.0 experimental setups.	57
Table 9 One-way ANOVA results for all batch fluorescence tests. Comparisons used are from Tukey’s HSD test, where ANOVA results which rejected the null hypothesis (p < 0.05) indicated significant differences among treatment group means. PG is data measured with PicoGreen (figure 24), and plating indicates data measured by plating and colony counting (figure 25).	XV
Table 10 One-way ANOVA results for all flow 1.0 fluorescence tests. Comparisons used are from Tukey’s HSD test, where ANOVA results which rejected the null hypothesis (p < 0.05) indicated significant differences among treatment group means. PG is data measured with PicoGreen (figure 26), and plating indicates data measured by plating and colony counting (figure 27).	XVI
Table 11 One-way ANOVA results for all flow 3.0 fluorescence tests measured with PicoGreen (PG) (figure 30). Comparisons used are from Tukey’s HSD test, where ANOVA results which rejected the null hypothesis (p < 0.05) indicated significant differences among treatment group means.	XVI
Table 12 Two-way ANOVA results for all flow 2.0 fluorescence tests measured with PicoGreen (PG) (figure 28 , figure 29). Comparisons used are from Tukey’s HSD test, where ANOVA results which rejected the null hypothesis (p < 0.05) indicated significant differences among treatment group means. Values in ml are aliquots, compared to residence times of 15, 30 or 60 minutes. Only comparisons with significant statistical differences are included in the table, all other values (controls and other experimental values) were found to be insignificant(p > 0.05).	XVII

LIST OF ABBREVIATIONS AND UNITS

Unit or Abbreviation	Meaning
°C	Degrees Celsius
CFU	Colony Forming Units (colonies per millilitre)
DNA	Deoxyribonucleic acid
GF	Glass Filter strips
HEPES	4-(2-hydroxyethyl)-1-piperazineethanesulfonic acid
LB	Lysogeny broth media
Milli-Q Water	Water passed through ion exchange, organic filtration cartridges, and a UV sanitizer in a Millipore water purifier
OD ₆₀₀	Optical Density at 600nm, read on a spectrophotometer
ROS	Reactive oxygen species
W/m ²	Watts per meter squared, unit of irradiation
bTiO ₂	Blackened Titanium Dioxide, on Glass Filter strips
g	Grams
kV	Kilovolt
mL	Millilitre
mW	Milliwatt
ms	Milliseconds
ns	Nanosecond
pH	Potential of Hydrogen
ps	Picosecond
s	Seconds
τ_{avg}	Average fluorescence lifetime in nanoseconds
μ L	Microlitre

1.0 INTRODUCTION

1.1 General Introduction

Water scarcity is an escalating global challenge, impacting a growing proportion of the world's population as demand increases and resources diminish¹. The lack of clean water is a critical issue, particularly in rural areas without access to adequate water treatment systems. In 2017, the Scaiano Lab initiated a government-commissioned project with Kenya and South Africa to develop a water purification technology designed for small community use. Collaborating with the Edith Amuhaya and Tebello Nyokong Labs at United States International University – Africa and Rhodes University, we conceptualized a solution that harnesses Kenya's abundant sunlight and freshwater rivers. This innovative purification system would pump contaminated water from rivers, process it through the device, and deliver potable water, all powered entirely by natural sunlight.

The 'Water Project,' as we have named it, has involved the contributions of numerous graduate and undergraduate students over the years and has demonstrated significant success to date. The project employs a three-pronged approach to address organic, biological, and heavy metal contaminants. Our innovative heterogeneous blackened titanium dioxide catalyst (bTiO₂) has shown effectiveness in degrading organic contaminants such as dyes and estrogens² and has also proven its potential as a proof-of-concept for tackling biological contaminants. I have personally studied the degradation of organic dyes (methylene blue, crocin) in 2019-2020 for an honours project with Dr. Scaiano³, and this work was continued by Nelson Rutajoga for applications in estrogen degradation. This thesis will focus on the issue of bacterial contamination, as the study of heavy metals and organic contaminants lies outside our scope.

1.2 Blackened Titanium Dioxide

The Water Project was born from a desire to make clean water accessible; this means creating a system that is affordable and easy to maintain. Heterogeneous catalysis is the obvious choice here, as supported catalysts can be more easily handled by people without a scientific background. They also allow for flow systems to work without excessive filters or settling time for powders. Blackened Titanium Dioxide has been proven in our studies to work for over a year of testing² without needing to be replaced. When it does need to be replaced, it is as simple as using tweezers to remove the old strip of bTiO₂ on glass filter and placing a new one in the flow tubes.

Titanium Dioxide is a cheap and safe material⁴, having been used for decades in cosmetics, sunscreen, hygiene products, food, and even for antibacterial purposes in operating room paint and tiles. This multi-product use is due to TiO₂'s effective light scattering properties and whitening capabilities, along with its semiconductor ability to generate ROS under illumination. It is a cheap and abundant semiconductor, with research grade TiO₂ costing just over \$100.00 CAD per 10 kilograms⁵.

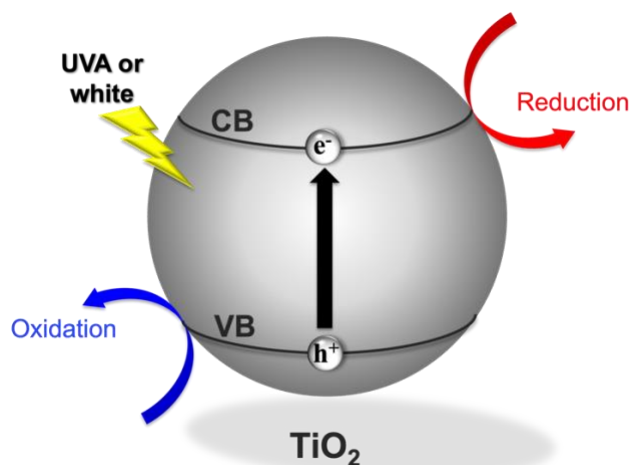


Figure 1 Schematic representation of the photocatalytic mechanism of titanium dioxide (TiO_2). Upon absorption of photons with energy equal to or greater than the band gap, an electron (e^-) is excited from the valence band (VB) to the conduction band (CB), leaving behind a hole (h^+) in the VB. The excited electron can participate in reduction reactions, while the hole can drive oxidation reactions. Particularly, the promoted electron can react with dissolved O_2 to create reactive oxygen species (ROS), facilitating the degradation of contaminants in water purification processes.

Both white and black TiO_2 participate in the semiconductor activity shown in **Figure 1**, with the main difference being white TiO_2 does not absorb visible light, only UV. Blackened TiO_2 (or bTiO_2) will absorb visible light. Kenya receives 4-6 kWh per square meter per day of solar radiation⁶, which makes a solar activated photocatalyst extremely attractive. Comparatively, Ottawa receives an annual average of 4.26 kWh per square meter per day of solar radiation, with the winter months getting as low as 1.92 kWh per square meter per day⁷. Despite the lower energy of visible photons compared to UV photons, the solar spectrum contains 10 times more visible radiation than UVA radiation⁸, making visible illumination the preferred photodegradation pathway. Therefore, since the black TiO_2 is more than half as active under white light as it is under UVA, black TiO_2 is a viable catalyst.

Titanium dioxide presents in two main different crystalline phases, rutile and anatase. Both are photocatalytically active, with transition from anatase to rutile crystal structure achievable by heating to 550-1000 °C. Due to the borosilicate glass filter support's melting point of 600 °C, we explored anatase phase TiO₂. Additionally, rutile is the thermodynamically stable form of TiO₂, so limiting the heating allowed us to prevent rutile formation. White TiO₂ absorbs in the UV region under 400 nm, and blackened TiO₂ absorbs in both the UV and Visible regions, between 300-800 nm (**Figure 2**).

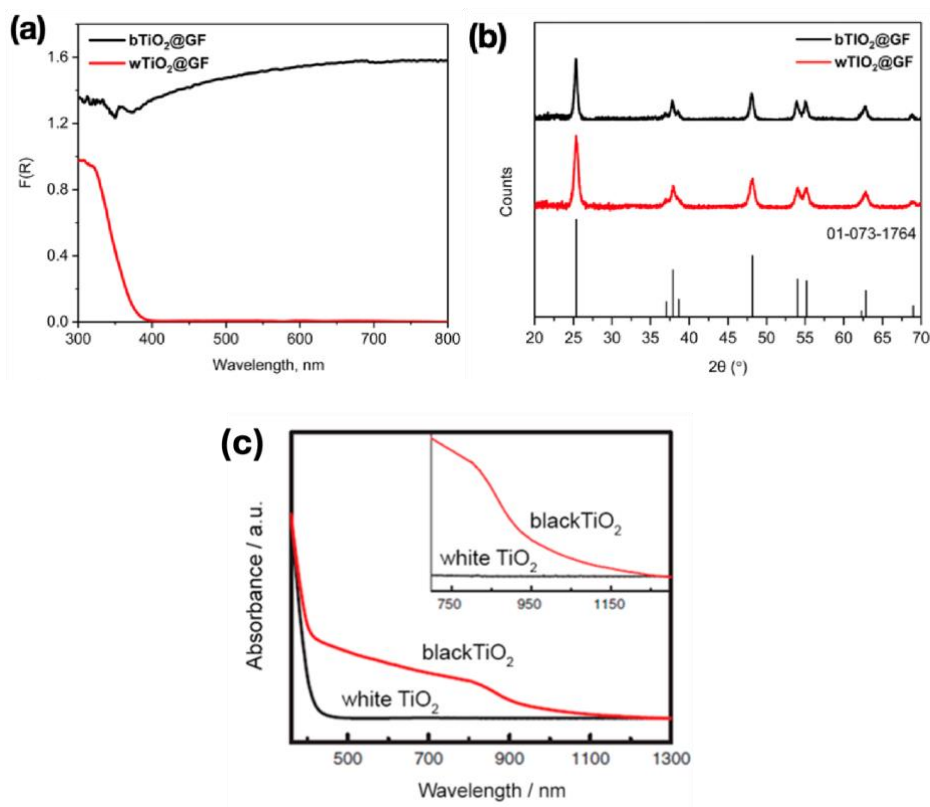


Figure 2 Characterization spectra of blackened titanium dioxide. Diffuse reflectance spectra (a) and x-ray diffraction (XRD) (b), as well as the absorbance spectra (c) of white and black TiO₂ catalysts on glass filter. The lines in (b) are representative of the known anatase XRD pattern according to ICDD card number 01-073-1764. Figures (a) and (b) are used with permission from the authors and were published recently in *Catalysis*². Brunauer-Emmett-Teller (BET) measurements (from adsorption-desorption of N₂ at 77K) for bTiO₂ on glass filter showed a specific surface area of 25.0 m²/g and an average crystal size of 15.4 nm. The crystal size of the

TiO₂ materials (nm) was calculated using the Scherrer equation ($L = K\lambda/\beta \cdot \cos\theta$), where crystalline factor (K)=0.9, λ Cuka = 0.154 and the FWHM (β) was measured from the XRD diffractograms².

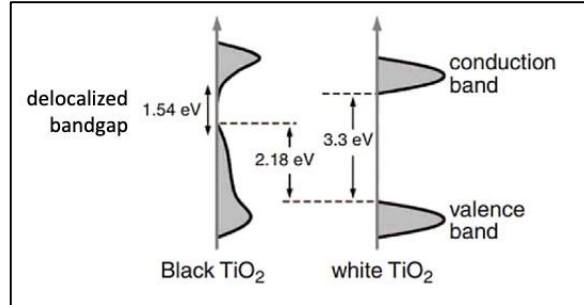


Figure 3 Proposed band gap comparison diagram between white and black TiO₂. Adapted from B. Wang et al., 2017⁹.

As TiO₂ on Glass Filter undergoes blackening, a small fraction of the particles exposed to the ethanol environment during heating are reduced from Ti⁴⁺ to Ti³⁺. Consequently, the bandgap of reduced TiO₂ particles is shrunk from 3.3 eV to 2.18 eV (**Figure 3**). Due to the gaseous phase of the ethanol, only the outermost layer of TiO₂ particles undergo this reduction, allowing the inner particles to remain white and in a 4⁺ oxidation state. It is therefore important to be gentle when handling the bTiO₂ on Glass Filter to maintain the highest degree of catalytic activity under visible light.

1.3 Reactive Oxygen Species

Reactive oxygen species (ROS) are oxygen species that have both beneficial and detrimental roles in bacterial and mammalian physiology. They are either endogenous or exogenous.

Endogenous ROS are formed naturally inside bacterial cells. They can be made via aerobic metabolism in the electron transport chain, or via enzymatic activity¹⁰.

Exogenous reactive oxygen species (ROS) are generally detrimental to cell viability and can be formed through host cell immune responses or environmental stressors. These stressors include host immune cell ROS production, UV radiation (including photodynamic therapy), antibiotics, or exposure to oxidizing agents such as bTiO₂, peroxides, and ozone. The types of ROS vary in their reactivity and lifetimes in aqueous environments. Superoxide anions ($\cdot\text{O}_2^-$) have a short lifetime of approximately 1–10 microseconds due to rapid dismutation¹¹, giving them the ability to travel 54.8 nm to 173.2 nm from their site of generation before quenching. Hydrogen peroxide (H_2O_2) is more stable, with a half-life ranging from milliseconds to hours depending on the presence of catalase or peroxidases¹², which allows them to travel 1,732.1 nm to 0.329 cm from their site of generation. Hydroxyl radicals ($\cdot\text{OH}$) are highly reactive and extremely short-lived, persisting for less than 1 nanosecond¹², which allows them to travel 1.7 nm from their site of generation. Singlet oxygen ($^1\text{O}_2$) has a lifetime of 2–4 microseconds in water due to its rapid quenching by solvent molecules¹³, and can consequently travel 77.5 nm to 109.5 nm from where they are generated. All distances travelled are calculated using **Equation 1** in an aqueous media.

$$\Delta x = \sqrt{(2D\tau)}$$

***Equation 1** Einstein's Equation for Molecular Diffusion. D represents the diffusion coefficient, estimated to be $1.5 \times 10^{-5} \text{ cm}^2 \text{ s}^{-1}$ for all molecules here. Δx is distance travelled before quenching in centimetres. τ represents the lifetime of each species in seconds.*

Beneficial ROS production improves physiological functions, such as regulating biofilm formation and regulation, sensing, and using ROS to outcompete other microbes¹⁰. Negative impacts of ROS on bacterial cells often include oxidative damage. This includes but is not limited to protein oxidation, lipid peroxidation, DNA damage, and metabolic inhibition. Protein oxidation causes structural disruption to protein formation, damaging the cell. Lipid

peroxidation degrades the cellular membrane by attacking phospholipids and causing leakage of intracellular components. DNA is damaged by the breaking of single stranded and double stranded DNA, as well as modifying bases (for example, formation of 8-oxoguanine). Metabolic inhibition disrupts enzymes and cofactors, impairing energy production in the cell¹⁰. Negative (exogenous) ROS effects will lead to cell death.

Bacterial cells facing ROS damage employ defence mechanisms. Enzymes and antioxidants can transform superoxides into hydrogen peroxides, followed by a neutralization of the peroxide species. DNA is repaired by excising damaged bases and nucleotides. Intracellular iron is also highly regulated to prevent excessive Fenton reaction and consequent hydroxyl radical production from occurring¹⁰. Under long-term exposure to exogenous ROS, bacterial cells can develop resistances in the form of antioxidant defences, so it is vital to use fresh bacterial stock for testing proof-of-concept antibacterial technologies. This is not a huge concern for a water purification technology as once the water is treated cells will die and not have a chance to replicate with antioxidant mutations.

1.4 Bacteria

1.4.1 Gram Positive and Negative Bacteria

Bacteria can be classified as either gram positive or gram negative. This classification depends on the strain's response to the gram staining test¹⁴, in which bacterial cells are exposed to four stains consecutively: crystal violet, Gram's iodine, ethanol, and safranin. The crystal violet and iodine penetrate the peptidoglycan of the cell and form a purple complex. Ethanol washes the complex out of cells with thin peptidoglycan (Gram-negative), but not with thicker

peptidoglycan (Gram-positive). Safranin is added afterwards to stain the gram-negative cells pink.

Both gram-negative and gram-positive cells exist in natural water sources. It is thus important to study both types of cells in the context of water decontamination. Wild type *Escherichia Coli* and *Staphylococcus Aureus* were chosen as representative strains of gram-negative and grampositive bacteria, respectively. They were selected due to their statistically significant presence in Kenyan river water^{15,16}, their impact on human health, and the wealth of literature available^{17,18}.

1.4.2 Bacterial Growth

Bacteria grows in four main phases, the lag phase, the log (exponential) phase, the stationary phase, and the death phase¹⁹. During the lag phase, bacteria adapt to their new environment by synthesizing essential enzymes and molecules, but cell division does not occur. This is followed by the log phase, where bacteria grow and divide at their maximum rate, leading to exponential population growth under optimal conditions. In the stationary phase, growth slows as nutrients become limited and waste products accumulate, resulting in a balance between cell division and death. Secondary metabolites, such as antibiotics, are often produced during this phase. Finally, in the death phase, nutrient exhaustion and toxic waste accumulation lead to a decline in the number of viable cells, with the death rate surpassing the growth rate.

1.4.3 Bacterial Inactivation

Bacteria can be inactivated through multiple pathways; however, this thesis will focus on chemical and physical inactivation. Chemical inactivation includes cell exposure to detergents, aldehydes, or alcohols which disrupt the membranes²⁰. Physical inactivation can be completed

by exposing cells to heat, UVC irradiation, sonication, nanostructured surfaces, supercritical fluids, or other methods²¹. These paths can impact the bacteria directly or by the generation of reactive oxygen species (ROS). Overall, death is often the consequence of a complex multifactorial chain reaction, achieved by a combination of more than one cause. Moreover, sometimes these factors can lead to a quiescent state from which cells are able to return to replication after a long period of not growing. Recently, bacterial death studies have shown that they do not only perish by necrosis type destruction but also through a programmed killing. That would be the equivalent to eukaryotic cell apoptosis²². This suicide can be triggered by chemical or physical conditions that the bacteria cell interprets as not convenient for development. Despite the ongoing debate on using the word apoptosis for bacteria²³, for simplicity's sake apoptosis-like bacterial inactivation will be called "apoptosis" in this thesis.

Particularly, photocatalysis with both white and black TiO₂ is known to produce large amounts of ROS. Therefore, it is expected that bacterial inactivation in this system is mostly because of the oxidation of vital proteins and lipids. However, is yet to be fully understand the location of these degraded molecules and the final faith of the bacteria structure. Once the biocomponents of the membranes and inner parts are oxidized, the body could shrink and collapse or the membrane could break and leaking of inside content like DNA could happen²².

We employed two methods of chemical inactivation though our studies. First, 70% isopropanol was used as an inactivating alcohol for calibration curves and dye selection (**2.6 Fluorescent Dye Testing**). Then, reactive oxygen species were used for experimental cell inactivation (**2.8 Fluorescence assay**). Heating and UVC irradiation (254 nm) were employed for comparison to physical inactivation methods in FLIM studies but were not used with any experimental conditions (**2.9 FLIM**).

1.4.4 Quantification of Bacteria – Current Technologies

Current methodologies in bacterial quantification include coliform tests, viability dyeing, mitochondrial dyeing, apoptosis assays, flow cytometry, Annexin V assays or CellTOX assays. Coliform tests work by identifying coliforms through lactose fermentation (producing gas or acid), selective growth on nutrient media, or fluorescence-based methods. Viability dyes are used to distinguish dead cells from living ones by penetrating cells with compromised membrane integrity, a hallmark of cell death. Mitochondrial dyes, on the other hand, specifically stain intact mitochondrial membranes; however, they lose their staining capability when mitochondria depolarize, a process commonly associated with cell death. Apoptosis assays provide a noninvasive means to generate high-contrast, time-lapse images of individual cells, enabling the detection of apoptosis-associated events such as DNA fragmentation, caspase activation, and the externalization of phosphatidylserine (PS) on the cell surface. Flow cytometry is another valuable technique for distinguishing apoptotic cells from viable cells, based on the reduced DNA content characteristic of apoptotic cells. The Annexin V assay employs fluorescently labeled annexin V to detect the externalization of PS on the plasma membrane, a key indicator of apoptosis²⁴. Finally, CellTOX dye can be used to measure cell death by incubating it with cells following stress-inducing treatments, such as UVB irradiation, allowing for precise quantification of cytotoxic effects²⁴. For the most part, this work will explore only viability dyeing assays.

1.4.5 Quantification of Bacteria – Novel Fluorescence Tests

All the quantification methods discussed in section 1.4.4 Quantification of Bacteria – Current

Technologies require at least 14 hours of incubation, which is not ideal in reference to water purification. Ideally, one could administer a quick, safe, and easy test to determine how effective the catalyst is and when it should be replaced. In just ten minutes, our novel fluorescence test effectively determines percent cell inactivation under specific conditions.

The dyes used were chosen from a 2001 study²⁵ from the Scaiano Group, where eight DNA intercalating dyes were tested on mammalian double and single stranded DNA to determine dye properties. These properties included spectral data, quantum yields and lifetimes. All dyes tested were DNA intercalators, meaning they insert themselves into a strand of DNA, preventing molecular rotation, which causes an increase in fluorescence.

1.5 Goals of Thesis

The primary objectives of this thesis are twofold: first, to evaluate and optimize the bacterial inactivation efficiency of bTiO₂ under white light for water decontamination purposes. Both *E. Coli* (a Gram-negative bacterium) and *S. Aureus* (a Gram-positive bacterium) will be tested to explore the scope of bTiO₂'s antimicrobial capabilities across different bacterial classifications. The ultimate aim is to establish a sustainable, accessible method for water decontamination that is both effective and widely applicable. Second, this thesis seeks to develop and assess the performance of a novel PicoGreen fluorescence-based viability assay. This assay was specifically developed to provide a quicker, easier alternative for assessing bacterial viability during water testing. Bacterial inactivation will be quantified using the newly developed fluorescence assay and validated through traditional plating and colony counting methods to ensure reliability and accuracy.

2.0 METHODS

Blackened Titanium Dioxide (bTiO₂) was synthesized on Glass Filters and then used as a cytotoxic catalyst for water purification. Cell inactivation was measured in three ways, an Optical Density Growth Assay, a novel Fluorescence Assay using PicoGreen, and Fluorescence Lifetime Measurements, also with PicoGreen.

2.0.1 Materials

Materials are listed in order of appearance. Glass filters were purchased from Pall Corporation. Titanium isopropoxide, ethanol, NaOH pellets, Luria-Bertani Broth powder, HEPES powder, NaCl, KCl, MgCl₂•6H₂O, Na₂SO₄, NH₄Cl, Na₂HPO₄, agar powder, and CaCl₂, isopropyl alcohol, untreated polystyrene 96 wellplate, and 60% Sodium DL-Lactate Syrup were all obtained from Sigma-Aldrich. Bacteria used were *Escherichia Coli* (Migula) Castellani and Chalmers (ATCC 25404)²⁶ and *Staphylococcus Aureus* subsp. aureus Rosenbach (ATCC 12600)²⁷.

2.1 Blackened Titanium Dioxide Synthesis

The titanium dioxide catalyst was synthesized directly onto the glass filter support. Glass filters were 330 μm thick and were made of 100 nm diameter glass fibres. Strips cut from small round filters were up to 47 mm long and 1.0 cm wide. Long glass filter strips were 0.6 cm by 21.9 cm. The high porosity of these filters allowed up to 60 % loading by weight of TiO₂ on the filter after rinses.

Titanium Isopropoxide was used as a starting material. It was kept under anhydrous conditions. A strip of glass filter paper was placed in an aluminum foil tray, and saturated with titanium

isopropoxide – approximately 3-5 mL in a glass Pasteur pipette. The aluminum tray was then filled with enough water to cover the filter paper. The glass filter paper was left in the water for 5 minutes per side to ensure all titanium isopropoxide reacted. A Teflon stir rod was used to flip the filter paper over. The filter paper was then removed from the water and placed between two sheets of aluminum foil and ironed with a clothing iron on medium heat (160°C) until dry. Ironing took approximately 15 minutes.

To convert the TiO₂ to anatase the samples were heated. Small glass filters (glass strands were about 100nm in diameter, and the glass filter was 47 mm in diameter) fit in a ceramic crucible which is placed in an oven for 2 hours at 500°C and then heated to 650°C for 5 minutes and immediately removed with tongs. Large filter papers (cut by hand with a size of 0.6 cm by 27.94 cm, Pall Corporation) were too long for the small oven so were placed in a tube furnace for 2 hours at 500°C and then heated to 650°C for 5 minutes. This happened inside a borosilicate tube inside the furnace instead of a small crucible. This furnace used an automatic cool-down feature, after which the sample was removed.

Black anatase was made using previously synthesized anatase, and done using a modification of Chen's method²⁸, developed by master's student at uOttawa, Yiran Li (images in **Figure 4**).

Absolute ethanol (10 mL for small glass wool supports, 15 mL for large supports) was placed in a 50 mL beaker inside a container of 75-100 mL liquid nitrogen, and left for 10 minutes to freeze. The frozen ethanol was then quickly placed in the furnace, beside the quartz boats with strips of white anatase on glass wool. For the larger catalyst supports, a long tube (26 cm ACE borosilicate glass) was used instead of small quartz boats. These ethanol boats/tubes were then placed in a tube furnace and the system was placed under medium vacuum (1×10^{-2} Torr). The heat treatment in a sealed tube was as follows: initial temperature was set to 25°C, then

temperature was increased to 400°C with a rate of 5°C/min and then maintained at 400°C for 3 hours. After heat treatment, the temperature was cooled to 50°C with a rate of 5°C/min. Finally, catalysts were cooled to room temperature and pressure without any further treatment.

All bTiO₂ GF strips were washed with water passed through ion exchange, organic filtration cartridges, and a UV sanitizer in a Millipore water purifier (Milli-Q water). It was determined that only five rinses (**Figure 5**) are necessary for the light scattering effects of excess TiO₂ in the rinse water to disappear. Batch (small) catalyst strips were gently swirled around a vial with Milli-Q water. The flow catalyst (large strip) was rinsed for 20 minutes at a flow rate of 13 mL/min using Milli-Q water. All catalyst was left to dry before use in further experiments.



Figure 4 Strips of white (top) and blackened (bottom) TiO₂ on Glass Filter. Catalyst strips are 25-26 cm long and are shown here after synthesis and five washes with Milli-Q water.

Table 1 Cary 60 UV-Vis spectrometer settings. As used in single scans. Quartz cuvettes were used for all measurements in the instrument.

Instrument: Cary 60
Instrument Version: 2.00
Start (nm): 800.0
Stop (nm): 200.0
X Mode: Nanometers
Y Mode: Absorbance
UV-Vis Scan Rate (nm/min): 4800.000
UV-Vis Data Interval (nm): 1.00
UV-Vis Ave. Time (sec): 0.0125
Beam Mode: Dual
Beam Common interval: 1nm

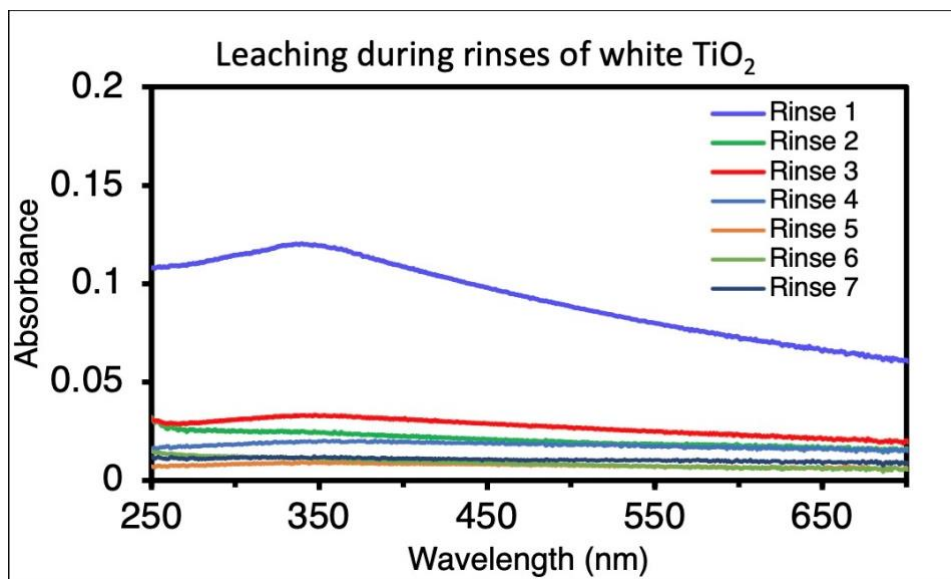


Figure 5 UV-Visible spectrum taken of Milli-Q water used to rinse excess TiO_2 off glass filters. A baseline of pure Milli-Q water was established at absorbance 0. Small 47 mm, 100 nm filters were used from Pall Corporation²⁹. Each rinse was performed with approximately 10 mL of Milli-Q water, swirled, and sampled in the Cary 60 UV-Vis spectrometer.

2.2 Media preparation

2.2.1 Luria-Bertani (LB) broth

Also referred to as LB Media in this thesis, Luria-Bertani Broth is made by adding 25.0 g of premixed powder (containing Tryptone, NaCl and Yeast Extract) to 1000 mL of Milli-Q water. It was then adjusted to a pH of 7.2-7.3 measured using a pH probe and NaOH solution.

2.2.2 HEPES Media

HEPES Media is made by adding 17.69 g of premixed powder to 500 mL of Milli-Q water. It was then adjusted to a pH of 7.2-7.3 measured using a pH probe and NaOH solution.

2.2.3 0.85% NaCl

0.85% NaCl solution is made by adding 8.5 g of NaCl to 1000 mL of Milli-Q water. It was then adjusted to a pH of 7.2-7.3 measured using a pH probe and NaOH solution.

2.2.4 DL-Lactate Minimal Media

In one litre of Milli-Q water was dissolved: 0.68 g NaCl, 0.30 g KCl, 0.285 g $\text{MgCl}_2 \cdot 6\text{H}_2\text{O}$, 0.03975 g Na_2SO_4 , 0.15 g NH_4Cl , and 2.383 g HEPES powder. The pH was adjusted to 7.2-7.3 using concentrated NaOH, then was autoclaved at 121 °C and 1.05 kg/cm² for an hour. After cooling and readjusting pH if necessary, the following were added: 0.0125 g Na_2HPO_4 , and 0.0056 g CaCl_2 . The media was then sectioned into 45 mL aliquots and stored under ambient conditions for up to two months. Directly before use, 0.645 mL of 60% Sodium DL-Lactate Syrup (hereafter referred to as DL-Lactate) was added per 45 mL of media³⁰. This is due to the quick degradation of the DL-Lactate at room temperature if left for over 24 hours.

2.2.4 LB Agar Plates

LB agar plates were prepared by dissolving 12.5 g of LB premixed powder into 500 mL of MilliQ water and adding 7.5 g of agar powder. It was then adjusted to pH of 7.2-7.3 and autoclaved at 121°C and 1.05 kg/cm² for an hour. Under sterile conditions, and while still liquid, the LB agar media was poured into untreated plates³¹ until the bottom was just covered (20 mL in each plate) and was left to solidify at room temperature. Plates were then stored under refrigerated conditions (4°C) for up to 1 month prior to use.

2.3 Bacteria Incubation and Preparation

Bacteria were grown in from -80°C frozen stocks or plates overnight in 15mL of LB media (Luria-Bertani broth) prepared via bottle instructions and adjusted to a pH of 7.2-7.3. Cells were placed in a 37°C oscillating incubator for 14-18 h and removed with a cell count of approximately 1×10^8 CFU/mL. This was verified by plating and counting colonies once per cell line.

Once removed from the incubator, bacterial solutions were placed in 50 mL centrifuge tubes and pelleted in a centrifuge (Beckman Coulter Avanti J-15R Centrifuge) for 10 minutes at 4000 rpm.

The supernatant was removed, and the bacteria was resuspended.

For the Optical Density Assay, all bacteria were resuspended in 20 mL HEPES media, pelleted and resuspended one final time in 5 mL HEPES. Bacteria was then diluted into fresh DL-Lactate media to 5.0×10^7 CFU/mL for use in experiments.

For the Fluorescence Assay and Fluorescence Lifetime Assay, bacteria were resuspended into 2 mL of 0.85 % NaCl solution. One millilitre of bacterial solution was put into each of two

separate 50 mL falcon tubes, which were labelled “live” and “dead”. 20 mL of 0.85 % NaCl was added to the “live” tube, and 20mL of 70 % isopropyl alcohol was added to the “dead” tube. Both tubes were oscillated at room temperature for one hour. Both tubes were then pelleted and resuspended in 10 mL DL-Lactate media, pelleted a final time and resuspended in 5 mL DL-Lactate minimal media. From here, the bacteria were diluted in more DL-Lactate media to the desired final concentration for experiments.

2.4 Plating and Colony Counting

From the experimental dilution of bacteria (varying with different experiments), 100 μ L aliquots of bacteria exposed to the reaction conditions and unexposed to reaction conditions were diluted by a factor of ten. This was repeated until there were 6 serial dilutions of bacteria in LB media, from each of which, 3×10 μ L drops were placed in LB Agar plates and incubated overnight or for 14-16 hours at 37°C. Bacterial colonies (appearing to the naked eye as white spots on the plate) were then counted per drop and multiplied by 100 and by their dilution factor to calculate the number of colonies per millilitre of solution. This was mostly represented in factors of ten (for example, 10^8 CFU/mL).

2.5 Optical Density Growth Assay

The Optical Density Growth Assay was performed by exposing bacteria (*E. Coli* and *S. Aureus*) to bTiO₂ strips in batch and measuring their growth via absorbance (OD₆₀₀) measurements over the course of 16 hours. This protocol was based on a growth-based viability assay developed by Qiu Et Al.³², in which cells exposed to varying amounts of cytotoxic materials were allowed to grow at 37°C, and then compared to a calibration curve.

Bacteria started at a concentration of OD_{600} 0.03, and 30 mL was exposed to a small strip of $bTiO_2$ catalyst for the following times: 5, 10, 15, 20, 40, 60, 80, 100, 120, 140, 160, and 180 minutes. Bacterial solution was oscillated at 60-80 rpm, at 37 °C in a MM-2 MINIM Oscillator. Aliquots were taken at each of the listed times and set aside at room temperature, in the dark, in 1.5 mL Eppendorf tubes while the rest of the exposure occurred. When all aliquots were collected, they were plated in triplicate according to **Figure 6**, in an untreated polystyrene 96 wellplate.

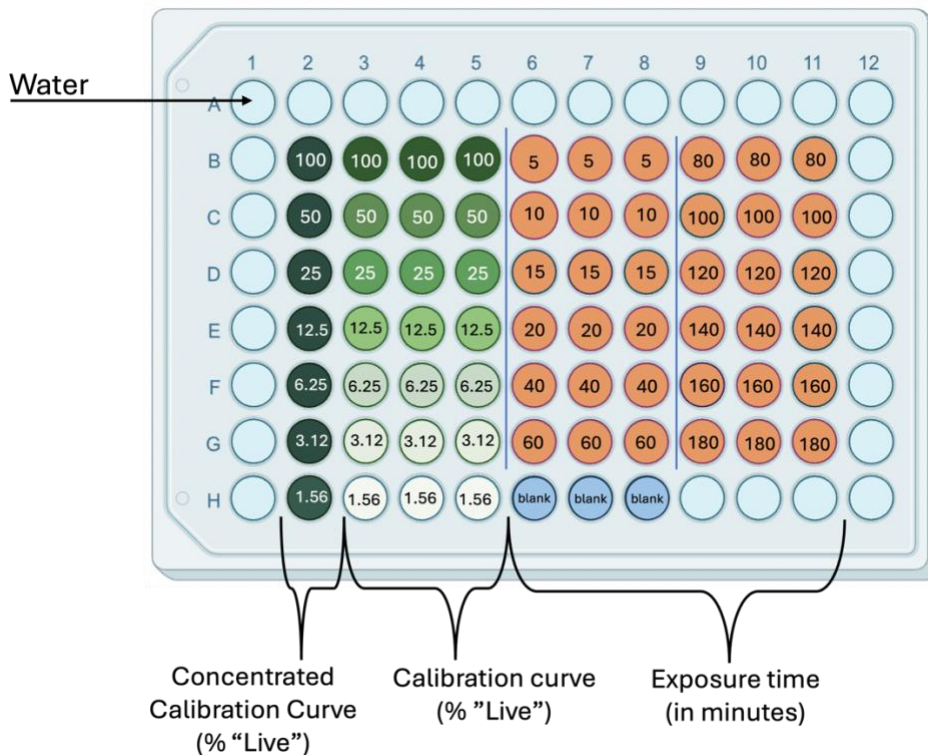


Figure 6 96 Well plate setup for calibration curve and exposure samples. In column 2 wells of the 96 wellplate, calibration curves were set up by diluting live bacteria ($OD_{600} = 0.030$) to 50 %, 25 %, 12.5 %, 6.25 %, 3.12 %, and 1.56 % of its experimental concentration with DL-Lactate Minimal Media. We will call this column “Concentrated Calibration Curve”. 20 μ L from each of the “Concentrated Calibration Curve” wells was placed in column 3 of the wellplate and diluted with 180 μ L of LB media, totalling 200 μ L. This was repeated in triplicate to create the “Calibration Curve”. Experimental aliquots were plated in cells B6 through G11 (labelled in orange). 20 μ L from each timed aliquot was added to a well and diluted with 180 μ L of LB

media for a total of 200 μ L. This was repeated in triplicate. Blank wells contained only LB media. Water was plated around the outside of the wellplate where space allowed to minimize evaporation of experimental wells during the 16-hour incubation and growth measurements.

Once the wellplate (**Figure 6**) was set up with all aliquots in triplicate it was placed in a temperature-controlled plate reader³³ for 16 hours at 37 °C with measurements of OD₆₀₀ taken every 20 minutes. Data was then exported and analyzed using Python code¹.

2.6 Fluorescent Dye Testing

We chose DNA intercalating dyes based on a scoping paper published by the Scaiano Group²⁵. The paper was crucial in elucidating ratios of dye to single and double stranded DNA and their interactions. Each dye chosen was diluted to a concentration of 6.4 μ M. This dye concentration was used for all bacterial concentrations, 10⁶ CFU/mL being the most common, which is equivalent to 6.06×10^{-6} moles intracellular DNA/mL *E. Coli*³⁴, and 5.80×10^{-10} moles intracellular DNA/mL *S. Aureus*³⁵.

Bacterial samples were prepared using the “live” and “dead” isopropanol method described in 2.3 Bacteria Incubation and Preparation, and calibration curves were prepared as described in **Table 2**.

¹ Code written by MSc student Julia Ong.

Table 2 Bacterial calibration curve preparation. Total volumes for each sample were 1mL.

Volume “live” Bacteria (μL)	Volume “dead” Bacteria (μL)	Percent dead Bacteria Per Sample (%)
1000	0	0
750	250	25
500	500	50
250	750	75
0	1000	100

E. Coli used were diluted in DL-Lactate media to OD₆₀₀ measurements of 0.3, 0.03, 0.015, and 0.003. *S. Aureus* used were diluted in DL-Lactate media to OD₆₀₀ measurements of 0.3, 0.15, 0.075, and 0.015.

After dilution, bacteria were loaded with dye. They were rested for 10 minutes at room temperature in the dark and then read using a quartz cuvette and spectrophotometer in triplicate. The goal was to determine the most sensitive dye, and discover the lowest cell:dye ratio possible for further experimentation. All dyes were kept in -20 °C and dark conditions while not in use.

2.7 SEM Imaging

SEM images were taken of small strips of bTiO₂ on glass filter after 1.5 hour and 3 hours in 30 mL bacterial DL Lactate solution with oscillation, either with a Milli-Q water rinse or without rinsing. Rinse was done by holding catalyst strips with tweezers and running Milli-Q water over the strips one time. Bacteria had a starting concentration of 10⁶ CFU/mL. Samples were fixed using 3 % glutaraldehyde solution³⁶ followed by 10-minute submersions in ethanol with increasing concentration. Ethanol was prepared in five vials, with percent ethanol from 25% to 99.7 % (absolute ethanol). SEM conditions are detailed in Section **3.2 SEM Images**.

2.8 Fluorescence assay

E. Coli and *S. Aureus* were grown according to the bacterial growth methodologies in section 2.3 Bacteria Incubation and Preparation. All strains were then diluted in DL-Lactate media to an OD₆₀₀ of 0.003-0.006, equivalent to 10⁵-10⁶ CFU/mL (verified by plating and colony counting). The bacterial solutions of *E. Coli* and *S. Aureus* were exposed to white light and bTiO₂ using one batch system and three different flow systems. Control experiments for all tests were run under dark conditions with bTiO₂, as well as with glass filter without bTiO₂ under light and dark conditions. For batch tests, additional controls were added: exposure of the working solution to light and dark without any catalyst or glass filter. All tests were run in triplicate. All LED and UVC lamp spectra can be found in the Appendix (**Figure 36**).

2.8.1 Batch Experiments

Each experimental trial used 30 mL of bacterial solution in a 50 mL Erlenmeyer flask³⁷. As shown in **Figure 7**, the flask was placed on a wellplate oscillator and set to 75 rpm. A neutral white LED lamp³⁸ was set 15 cm away from the working solution, and all external light was blocked using blackout curtain.

A small strip of bTiO₂ on GF catalyst was placed in the Erlenmeyer. The working solution was then exposed to the Flood Lamp white LED (**Figure 36**) for up to 180 minutes at room temperature. This lamp emits between 400-700 nm only.

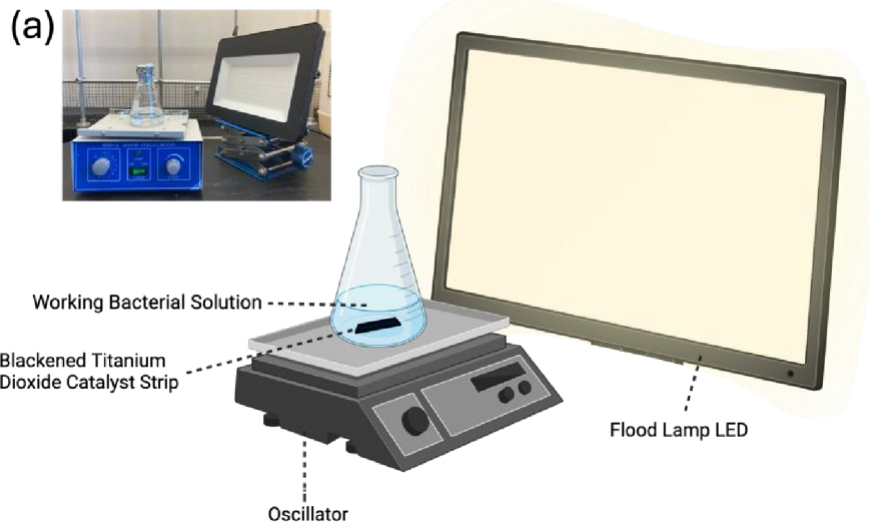


Figure 7 Experimental batch setup diagram with photograph inset (a). Created with BioRender.com

Aliquots were taken from the solution at the following times in minutes: 0, 10, 20, 40, 60, 80, 100, 120, 140, 160, and 180. Once all 1mL aliquots were collected in 1.5 mL Eppendorf tubes, 50 μ L of diluted PicoGreen were added to each Eppendorf tube for a total dye concentration of 6.4 μ M, manually mixed by inverting 15 times, and allowed to sit for 10 minutes in the dark at room temperature. Aliquots with dye were then analyzed according to the parameters outlined in **2.8.5 Fluorescence Experiments - Analysis**.

2.8.2 Flow Experiments – Recycled, Flow 1.0

A peristaltic pump³⁹ was used to create a recycling flow (**Figure 8**), meaning bacterial solution was pumped through the tube containing bTiO₂, and then returned to a beaker to be pumped through again.

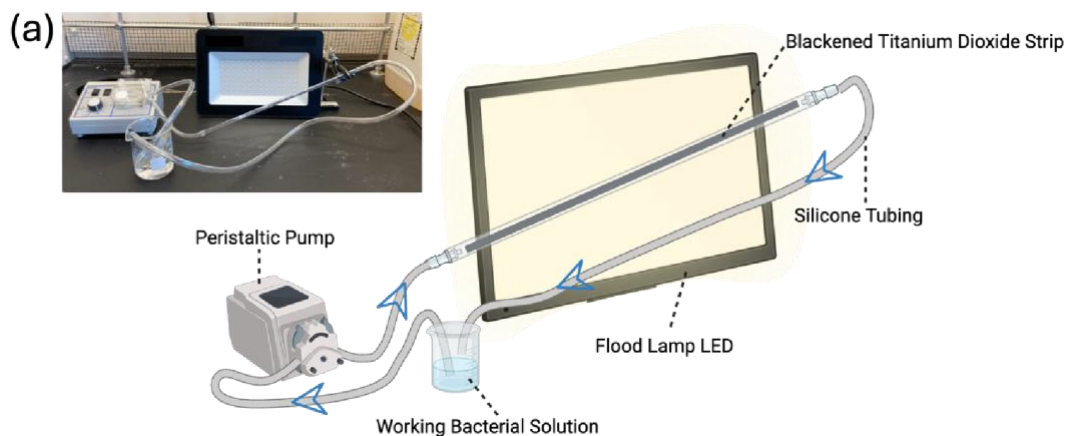


Figure 8 Flow 1.0 set up diagram with photograph inset (a). Equipment used was a VWR mini variable flow peristaltic pump, a glass tube (39 cm long, 0.57 cm interior diameter), silicone tubing (0.85 cm interior diameter), a strip of bTiO₂ (30 cm long, 0.5 cm wide), and a 150 mL beaker for recycling flow. The beaker contained 70 mL of bacterial solution. Total residence time was 20.0 minutes, with a flow speed of 3.43 mL/minute. The active residence time (inside glass tube) was three minutes. Figure created with BioRender.com

1 mL aliquots were collected at the following times in minutes: 0, 10, 20, 40, 60, 80, 100, 120, 140, 160, and 180 minutes. At time 0 minutes the aliquot was collected directly from the end of the tube (single pass), and all aliquots after were collected from the beaker (recycled flow). Once all aliquots were collected in 1.5 mL Eppendorf tubes, 50 μ L of diluted PicoGreen were added to each Eppendorf tube for a total dye concentration of 6.4 μ M, manually mixed by inverting 15 times, and allowed to sit for 10 minutes in the dark at room temperature. Aliquots with dye were then analyzed according to the parameters outlined in 2.8.5 Fluorescence Experiments - Analysis.

2.8.3 Flow Experiments – Single Pass, Flow 2.0

A programmable syringe pump⁴⁰ with a 50 mL syringe⁴¹ was used to flow bacterial solution through a quartz tube⁴² with bTiO₂ catalyst. This tube was irradiated through a triangular prism of lamps (**Figure 9**), referred to in this thesis as the ‘tent lamp’ due to its shape. This lamp emits between 400-700 nm only. Bacterial solution was flowed at the rates listed in **Table 3**.

Table 3 Flow rate and residence time for flow 2.0 and 3.0 single pass experiments.

Flow rate (mL/minute)	Residence Time in Quartz Tube (minutes)
1.33	15
0.66	30
0.35	60

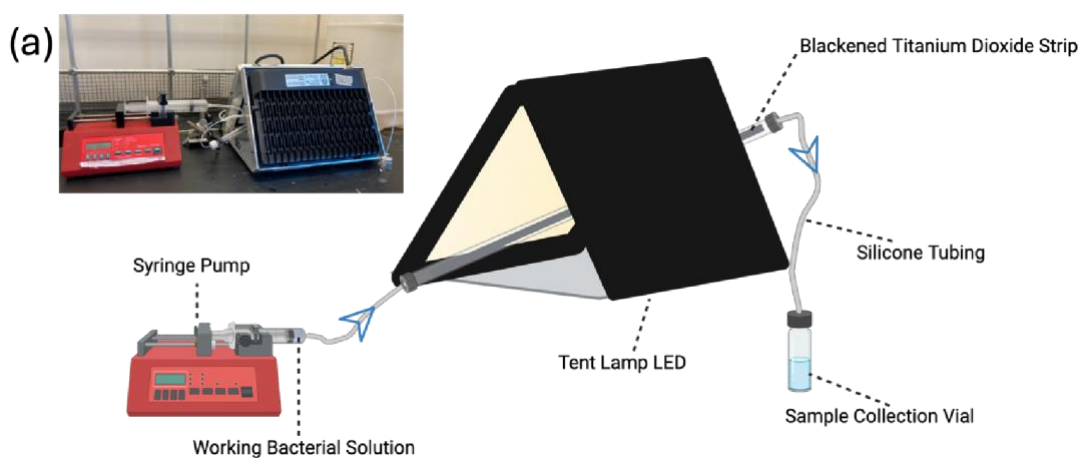


Figure 9 Single pass flow 2.0 set up diagram with photograph inset (a). Total volume of this system (not including the syringe chamber) was 20.70 mL, where 0.70 mL was dead volume and 20 mL was active volume inside the quartz tube. The tent lamp consisted of two white LED flood lamps positioned on two faces of a triangular prism, with an aluminum foil covered piece of particle board on the third face to improve the tube's exposure to photons (**Figure 36**). The quartz tube was held at a 45-degree angle using clamps, and solution filled it from the bottom to the top. Figure created with BioRender.com

1 mL aliquots were collected at the following volumes: 0 mL (first mL to exit the system), 8 mL, 15 mL, 30 mL, 45 mL, 60 mL, 75 mL, 90 mL, 105 mL, and 120 mL. Once all aliquots were collected in 1.5 mL Eppendorf tubes, 50 μ L of diluted PicoGreen were added to each Eppendorf tube for a total dye concentration of 6.4 μ M, manually mixed by inverting 15 times, and allowed to sit for 10 minutes in the dark at room temperature. Aliquots with dye were then analyzed according to the parameters outlined in **2.8.5 Fluorescence Experiments - Analysis**.

2.8.4 Flow Experiments – Single Pass with Gas, Flow 3.0

Bacterial solution was flowed through the quartz tube using the syringe pump with the same set up as flow 2.0 described above. The main difference was the orientation- in flow 3.0 the tube was set vertically to allow inserted gas (air or pure oxygen) to bubble up the reaction tube.

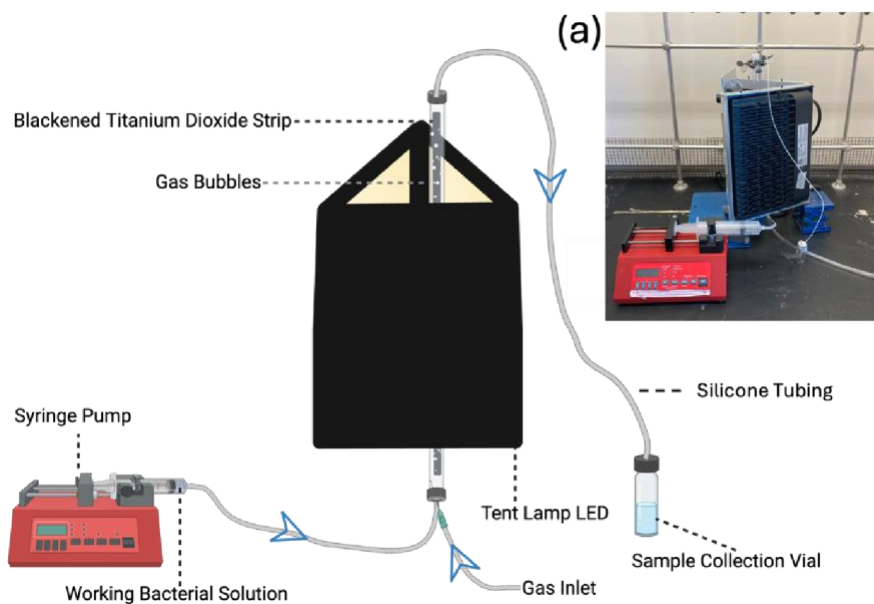


Figure 10 Flow 3.0 set up with gas flow either air or pure oxygen, and photograph inset (a). For the air, benchtop air flow was supplied, and for oxygen, a cylinder of compressed oxygen was used. Both had a rate of 1.22 mL/minute, giving a champagne-bubble-like appearance in the flow system. Figure created with BioRender.com

Only 30 mL residence times, or 0.67 mL/minute flow rates (**Table 3**) were used in accordance with WHO guidelines¹. 1 mL aliquots were collected at the following volumes: 0 mL (first mL to exit the system), 8 mL, 15 mL, 30 mL, 45 mL, and 60 mL. Once all aliquots were collected in 1.5 mL Eppendorf tubes, 50 μ L of diluted PicoGreen were added to each Eppendorf tube for a total dye concentration of 6.4 μ M, manually mixed by inverting 15 times, and allowed to sit for

10 minutes in the dark at room temperature. Aliquots with dye were then analyzed according to the parameters outlined in **2.8.5 Fluorescence Experiments - Analysis**.

2.8.5 Fluorescence Experiments - Analysis

After 10 minutes of resting in the dark at room temperature, each aliquot's fluorescence was read in a quartz cuvette under the following conditions (**Table 4**). It was then compared to the corresponding calibration curve to determine percentage dead bacteria.

Table 4 PicoGreen fluorescence test analysis conditions on the SpectraMax M5 Microplate Reader³³

Instrument: SpectraMax M5 Microplate Reader
Excitation (nm): 480.0
Start (nm): 500.0
Stop (nm): 670.0
X Mode: Nanometers
Y Mode: Emission Sweep
UV-Vis Scan Rate (nm/min): 4800.000
UV-Vis Data Interval (nm): 1.00
UV-Vis Ave. Time (sec): 0.0125
Beam Mode: Automatic
Beam Common interval: 1nm

2.9 FLIM

Images were captured using a Fluorescent Lifetime Imaging Microscopy (FLIM) system (PicoQuant MicroTime 200). The system featured a frequency-doubled picosecond pulsed diode laser (485 ± 10 nm, 70 ps, 40 MHz, LDH-D-C-485, PicoQuant), with the laser beam collimated and focused via a fiber-coupling unit. A 500dcxr beam splitter (Chroma) was employed to direct the excitation light into a 100 \times oil immersion total internal reflection objective (NA 1.45,

Olympus PLAPO). The excitation dose (average power) was approximately 1.5 mW at the microscope, and the resulting images spanned 80 μm on both the x and y axes. Tests were performed on *S. Aureus* and *E. Coli* after exposure to UVC light for 30 minutes, heat (100 °C for 60 seconds), isopropanol (as described in ‘live’ / ‘dead’ calibration curve preparation protocol), light, oxygen, and bTiO₂ exposure for 30 minutes, and entirely live cells.

Samples were loaded into glass-bottom confocal imaging dishes, using 25 μL of bacterial solution, 25 μL of diluted dye (PicoGreen, diluted to a total dye concentration of 6.4 μM). If cells were too concentrated, they were further diluted with 50 μL of freshly prepared DL Lactate media. Confocal dishes were placed on the objective and read under the conditions listed in

Table 5. FLIM data were processed using SymPhoTime software. Regions of interest (ROIs) were defined within each image, and fluorescence decay curves were fitted to a multiexponential model. The goodness-of-fit for one-, two-, and three-component decays was assessed using χ^2 values and residuals. Lifetimes were then averaged over all readings of each sample. T-tests were completed to ensure statistical relevance of the lifetimes observed.

Table 5 FLIM settings used for imaging dyed bacteria. Bidirectional scans were used for all images.

Instrument: PicoQuant MicroTime 200
Origin: X=10.000 μm ; Y=10.000 μm ; Z=80.000 μm
image size: 80.00 μm x 80.00 μm
image pixels: 512 x 512
time per pixel: 0.60 ms
pattern: bidirectional
acceleration: 6 %
learning loops: 20
recording time: 3.54min
laser intensity (photo diode): 11.63

2.10 Statistical Analysis- ANOVA and T-Tests

We employed One-way Analysis of Variance (ANOVA) with repeated measures at a 95% confidence level to assess statistical differences in cytotoxicity and antibacterial performance under varying conditions. Fluorescence Assays analyzed with this method were the Batch assay, Flow 1.0, and Flow 3.0. For antibacterial performance, mean percent bacterial inactivation was analyzed for cellular toxicity.

A Two-way ANOVA (same conditions as above) was adopted for analysis of Fluorescence Assay Flow 2.0 results. This Two-way ANOVA was used to determine differences between treatment groups, including both varying conditions and flow speeds.

ANOVA results which rejected the null hypothesis ($P < 0.05$) indicated significant differences among treatment group means. To identify treatment group differences, *post-hoc* analysis was performed using Tukey's Honest Significant Difference (HSD) test.

Additionally, a T-test at a 95 % confidence level was used to compare average fluorescence lifetimes from FLIM results under various conditions. This was used to determine if there was a meaningful correlation between *S. Aureus* and *E. Coli* fluorescence responses to various methods of bacterial inactivation.

All statistical analyses, including ANOVA and T-tests, were conducted using PRISM version 8 software.

3.0 RESULTS

The results presented in this section highlight the effectiveness of blackened titanium dioxide (bTiO₂) as a photocatalyst for bacterial inactivation in water purification applications. An optimization of batch and flow experiments demonstrated significant bacterial reductions under white light, with *Escherichia Coli* and *Staphylococcus Aureus* serving as representative strains. These experiments validated the potential of bTiO₂ to meet and exceed World Health Organization (WHO) standards for bactericidal processes. Complementary techniques, including fluorescence assays, colony counting, and advanced imaging methods, provided robust and multi-dimensional insights into the mechanisms of bacterial inactivation. Together, these results underscore the viability of bTiO₂ as a sustainable and scalable solution for addressing waterborne bacterial contamination.

It is crucial to have bacteriostatic media while studying benchtop bacterial inactivation. This is due to the short doubling time of both *E. Coli* and *S. Aureus* (20 minutes⁴³) compared to the experimental time (up to three hours). Although it is possible to account for growth, for simplicity's sake, it is preferable to prevent it. DL-Lactate minimal media was found to be the best candidate for inhibiting bacterial growth but not inactivating the cells over the course of hours at room temperature. It was thus used for all subsequent tests for bacterial suspension.

3.1 Optical Density Growth Assay

The Optical Density Growth Assay was chosen to quantify the bactericidal properties of bTiO₂ under white illumination. This method was a good option for a preexisting, high-throughput assay to test multiple conditions. Plots are organized by calibration curve followed by the

corresponding results, which are calculated using the line of best fit from each respective calibration curve inset.

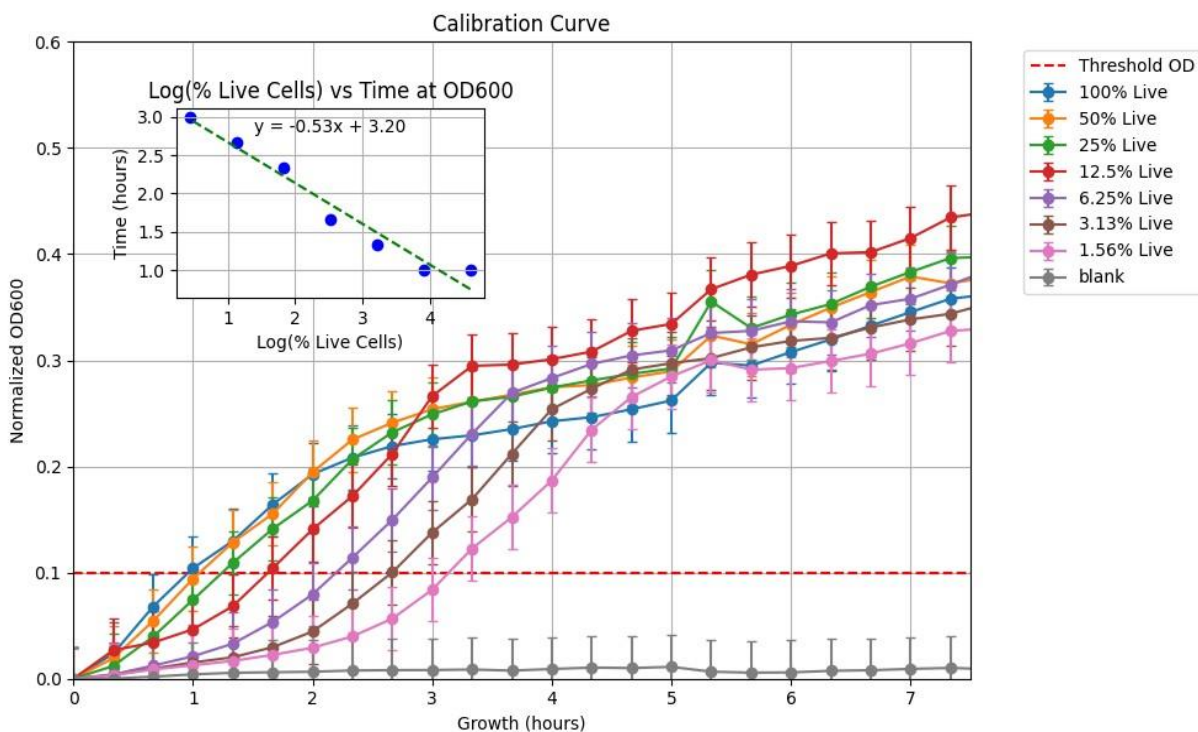


Figure 11 Growth Assay Calibration Curve Graph 1. OD_{600} was monitored via wellplate reader over the course of 16 hours. Data after 8 hours demonstrates a plateau, so was discarded. *E. Coli* live cells (OD_{600} 0.003) were diluted with dead cells (prepared as described in section 2.3 Bacteria Incubation and Preparation.) Longer lag times correspond to smaller fractions of live cells compared to dead cells. Inset datapoints refer to the time when each sample reaches the threshold value of OD_{600} 0.1 versus the log(percent live cells). Inset trendlines were used to calculate the percent inactive bacteria for experimental and control conditions.

Above Calibration Curve Graph corresponds to **Figure 12** Growth assay results for *E. Coli* exposure to bTiO₂ and white LED light (**Figure 36 (a)**). for growth assay with *E. Coli*, bTiO₂ exposure, and white LED light.

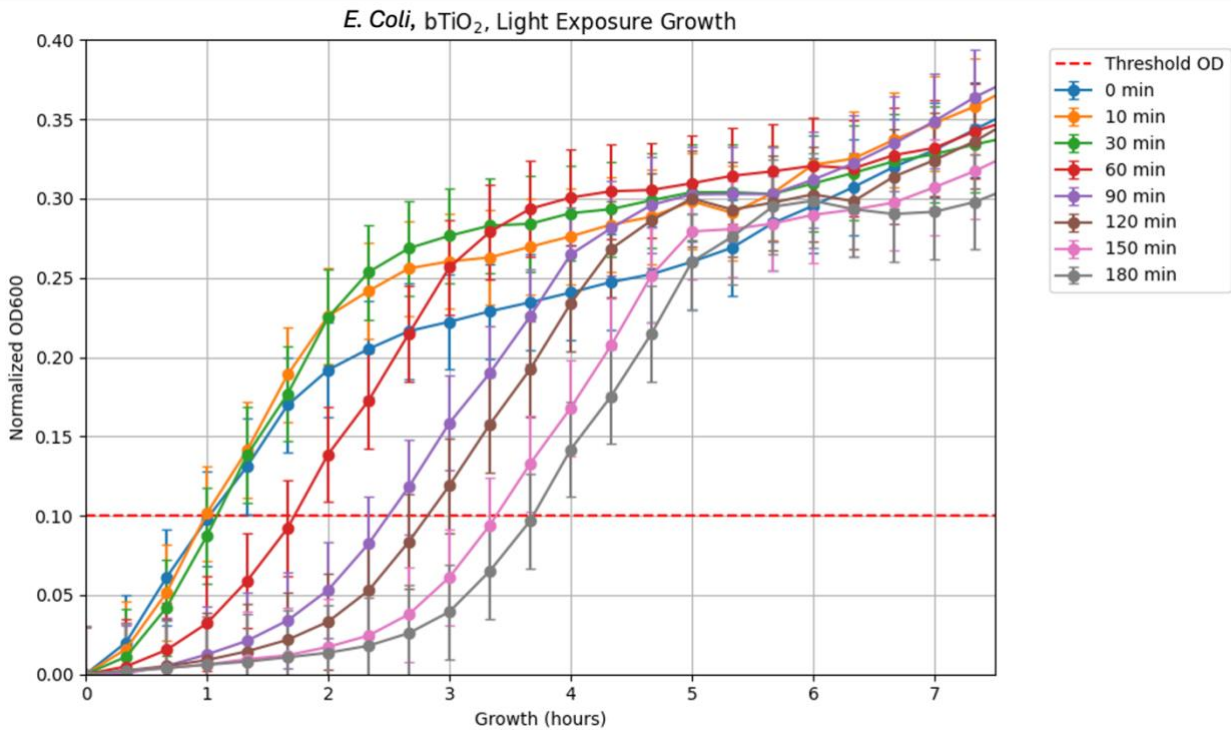


Figure 12 Growth assay results for *E. Coli* exposure to $bTiO_2$ and white LED light (**Figure 36 (a)**). Aliquots were plated, incubate at 37°C, and OD₆₀₀ were read in a wellplate reader every 20 minutes for 16 hours. Datapoints after 8 hours show a plateau so were discarded. Longer lag times correspond to a higher percentage inactive or dead cells.

Aliquots were taken from batch solution at the following times in minutes: 0, 10, 30, 60, 90, 120, 150, and 180 minutes. The highest percent bacterial inactivation was noted at 180 minutes of exposure, with 99.9% bacterial inactivation.

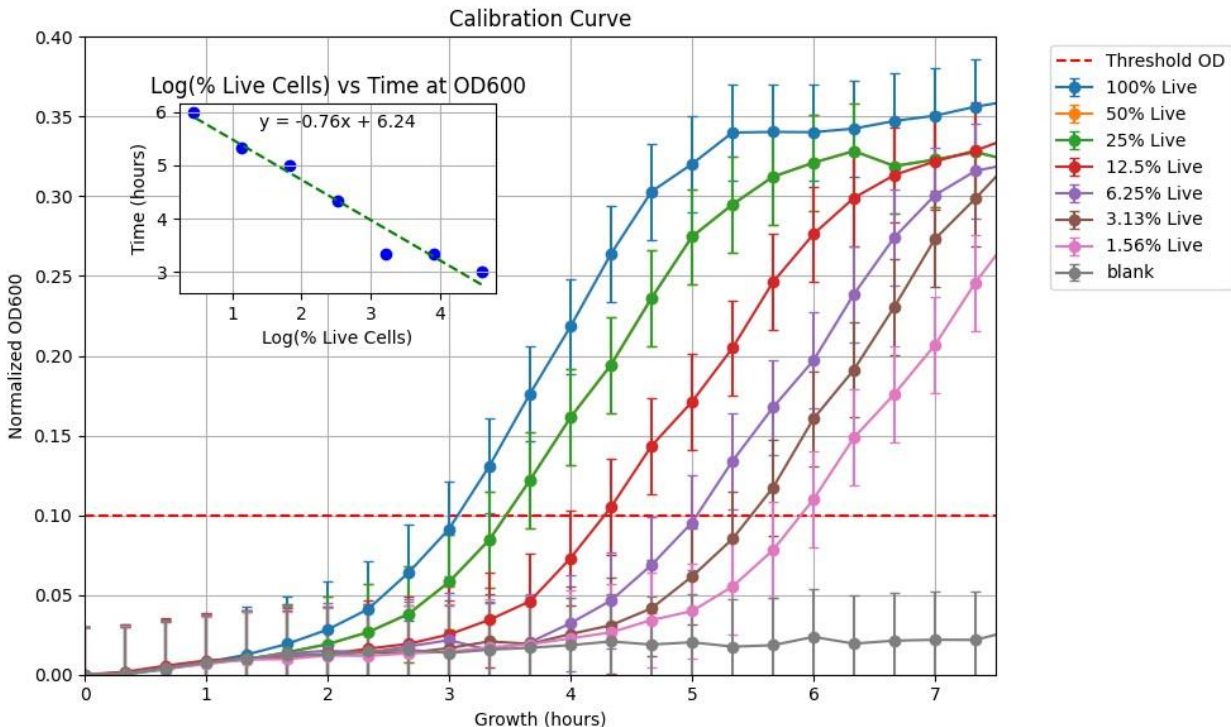


Figure 13 Growth Assay Calibration Curve Graph 2. OD_{600} was monitored via wellplate reader over the course of 16 hours. Data after 8 hours demonstrates a plateau, so was discarded. *S. Aureus* live cells (OD_{600} 0.003) were diluted with dead cells (prepared as described in section 2.3 Bacteria Incubation and Preparation.) Longer lag times correspond to smaller fractions of live cells compared to dead cells. Inset datapoints refer to the time when each sample reaches the threshold value of OD_{600} 0.1 versus the log(percent live cells). Inset trendlines were used to calculate the percent inactive bacteria for experimental and control conditions.

Above graph corresponds to **Figure 14** Growth assay results for *S. Aureus* exposure to bTiO₂ and white LED light (**Figure 36 (a)**). for growth assay with *S. Aureus*, bTiO₂ exposure, and white LED light (**Figure 36**). Inset refers to the time when each sample reaches the threshold value of OD_{600} 0.1 versus the log(percent live cells).

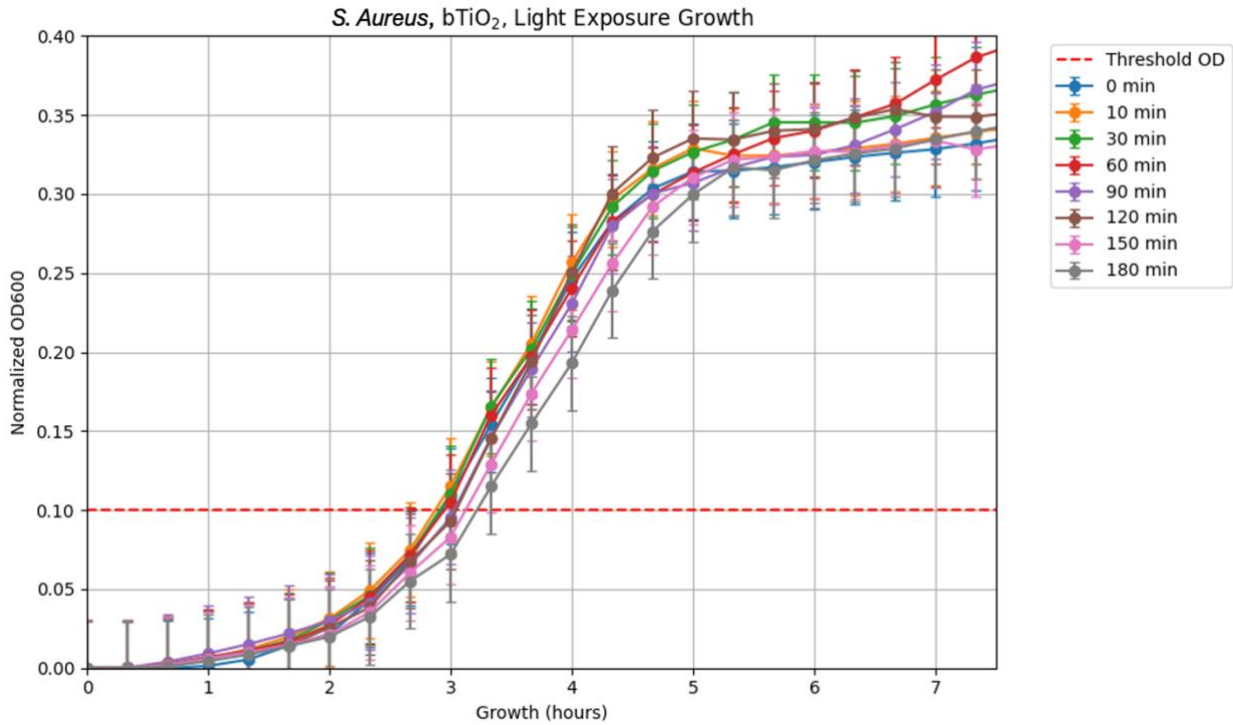


Figure 14 Growth assay results for *S. Aureus* exposure to $bTiO_2$ and white LED light (**Figure 36 (a)**). Aliquots were plated, incubate at 37°C, and OD₆₀₀ were read in a wellplate reader every 20 minutes for 16 hours. Datapoints after 8 hours show a plateau so were discarded. Longer lag times correspond to a higher percentage inactive or dead cells.

Aliquots were taken from batch solution at the following times in minutes: 0, 10, 30, 60, 90, 120, 150, and 180 minutes. The highest percent bacterial inactivation was noted at 180 minutes of exposure, with 65.7% bacterial inactivation.

Table 6 Growth Assay Experimental Condition Results. Inactivation of *E. Coli* and *S. Aureus* under white LED light (**Figure 36**) with $bTiO_2$ strips. No bacterial inactivation (or bacterial growth) is represented by “NI”.

Exposure Time (minutes)	<i>E. Coli</i> Percent Inactivation (%)	<i>S. Aureus</i> Percent Inactivation (%)
0	NI	5.88
10	NI	5.88

30	NI	5.88
60	NI	5.88
90	56.76	5.88
120	89.87	5.88
150	99.44	5.88
180	99.87	65.68

The assay revealed that bacterial inactivation rates under the experimental conditions (bTiO₂ and white light) were 99.9 % for *E. Coli* and 65.6 % for *S. Aureus* after 180 minutes. Controls were performed on both *E. Coli* and *S. Aureus* under light and dark conditions with: bTiO₂, only glass filter, or no glass filter and catalyst. In all control samples, bacterial populations increased by up to 250 %, showing that the controls allowed bacterial growth during room temperature exposure to control conditions rather than killing the bacteria. These results also indicate that the DL-Lactate media was bacteriostatic only at room temperature. Notably, bacterial inactivation was observed exclusively under the target experimental conditions, becoming apparent after 60 minutes for *E. Coli* and after 180 minutes for *S. Aureus*. The delay in bacterial inactivation likely resulted from the experimental design, where the catalyst was swirled in the solution using a small strip. To further investigate these promising findings, SEM imaging was employed to visualize bacterial settling on the catalyst surface, revealing valuable insights into the interaction dynamics and further validating the efficacy of the experimental setup.

3.2 SEM Images

Scanning Electron Microscope (SEM) images were taken of glass filter, freshly made catalyst, and used catalyst before and after rinses. These images were taken with the goal of qualitatively determining the degree of bacterial settling on our catalyst with and without a rinse. All SEM

images were taken at the uOttawa MatChar CORE facility by technician Dr. Yun Liu, using a JSM 7401F (JEOL Ltd., Tokyo, Japan) operated between 2.0-3.0 kV. For all images, round clusters on the bTiO₂ on glass filter are salts precipitated from the minimal media upon dehydration of the catalyst strips for SEM imaging. This is particularly evident in **Figure 15 (c)** and **(d)**. All images containing catalyst have up to 60 % TiO₂ by weight.

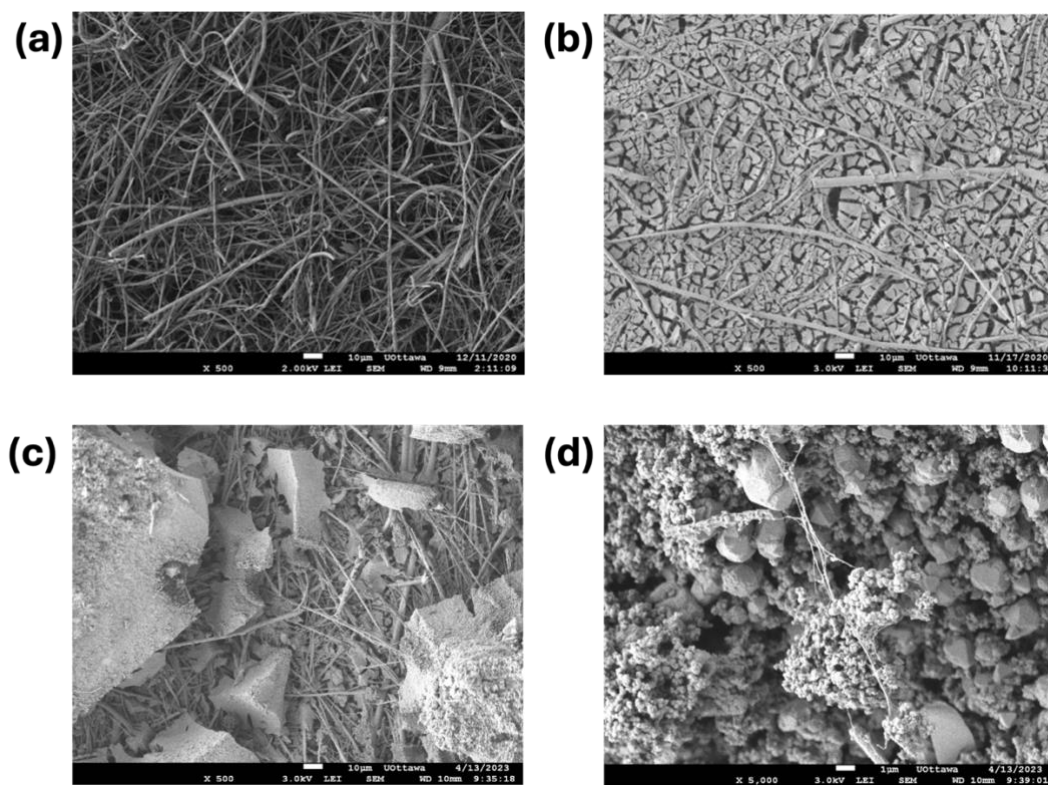


Figure 15 SEM images of catalyst strips prior to use in experiments. Glass filter before synthesis of catalyst (a), bTiO₂ on glass filter support before use (b), bTiO₂ on glass filter support after 30minute exposure to DL Lactate media (c), and same conditions as (c), but with higher magnification (d).

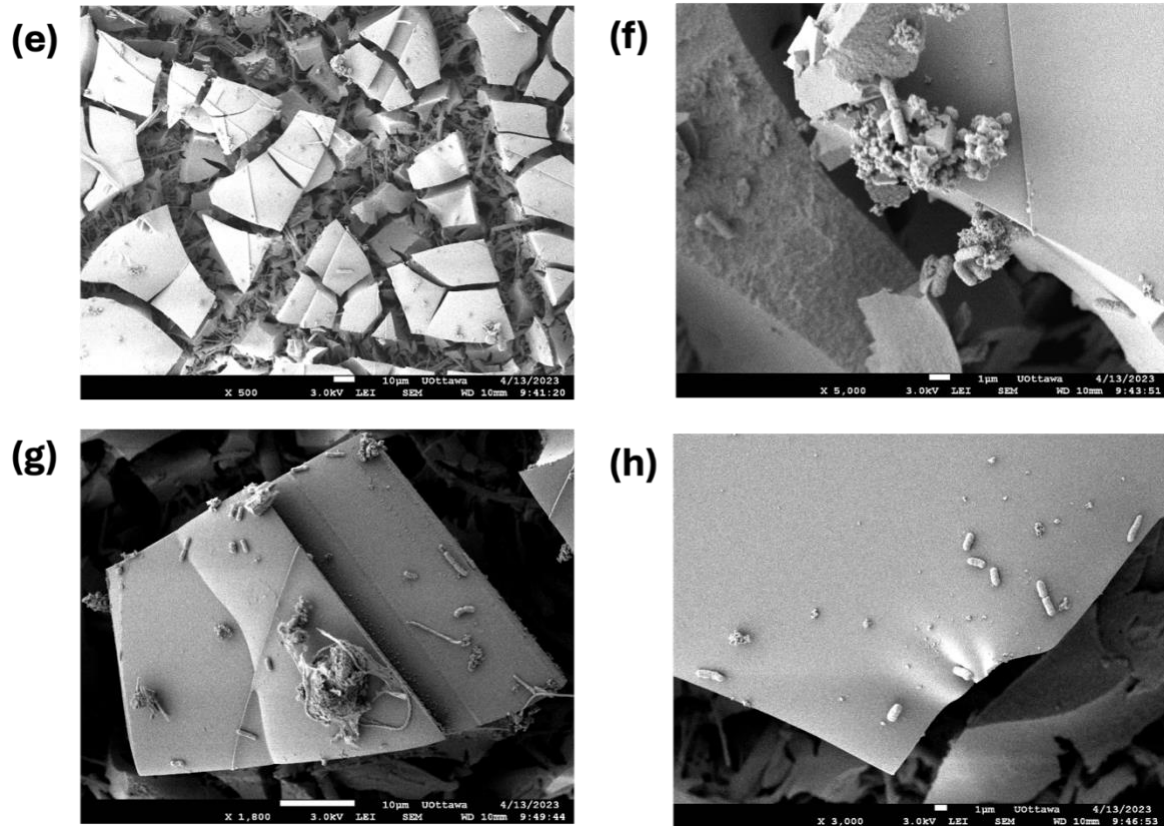


Figure 16 SEM Images of Catalyst Strip after 1.5 hours in solution, shown at various magnifications. Small catalyst strips were placed in 30 mL of DL-Lactate bacterial solution (10^6 CFU/mL) and oscillated at room temperature under dark conditions for 1.5 hours. They were not rinsed.

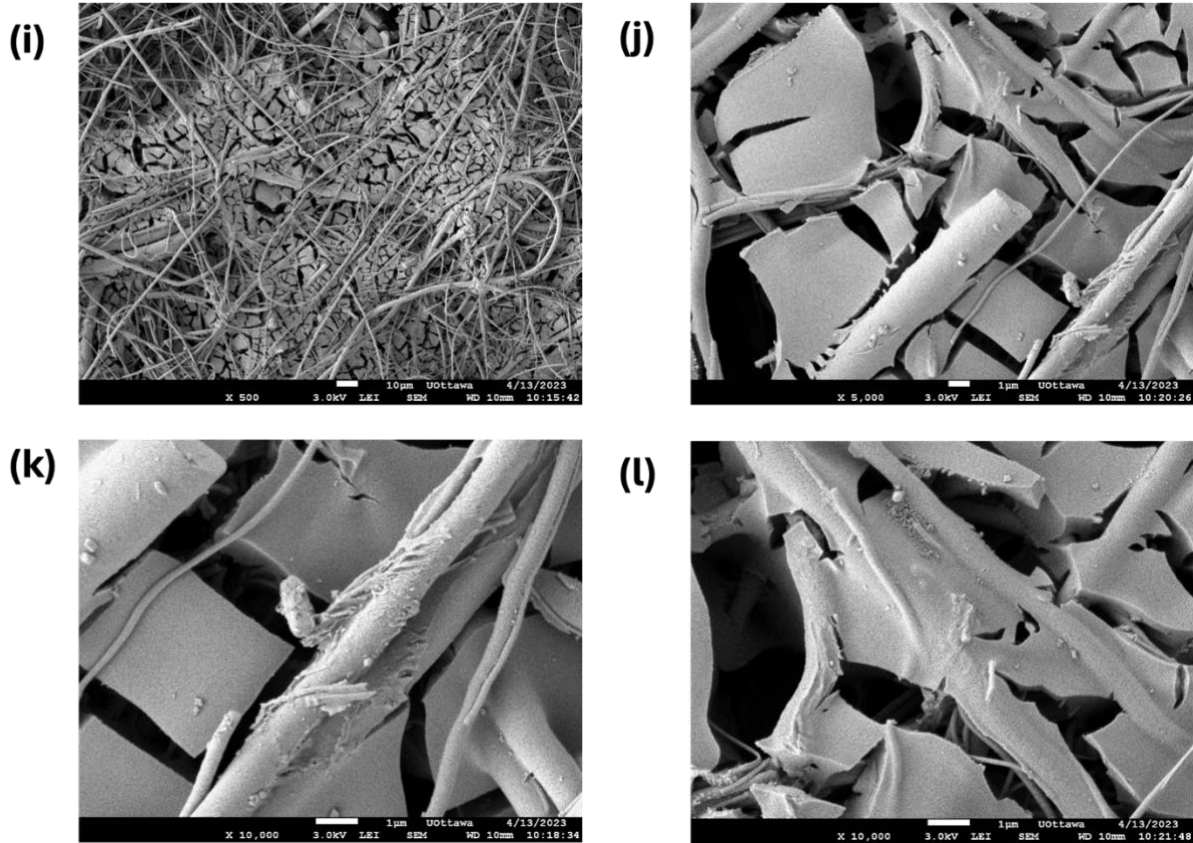


Figure 17 SEM Images of Catalyst Strip after 1.5 hours in solution followed by rinse, shown at various magnifications. Small catalyst strips were placed in 30 mL of DL-Lactate bacterial solution (10^6 CFU/mL) and oscillated at room temperature under dark conditions for 1.5 hours. They were rinsed one time with 50 mL Milli-Q water.

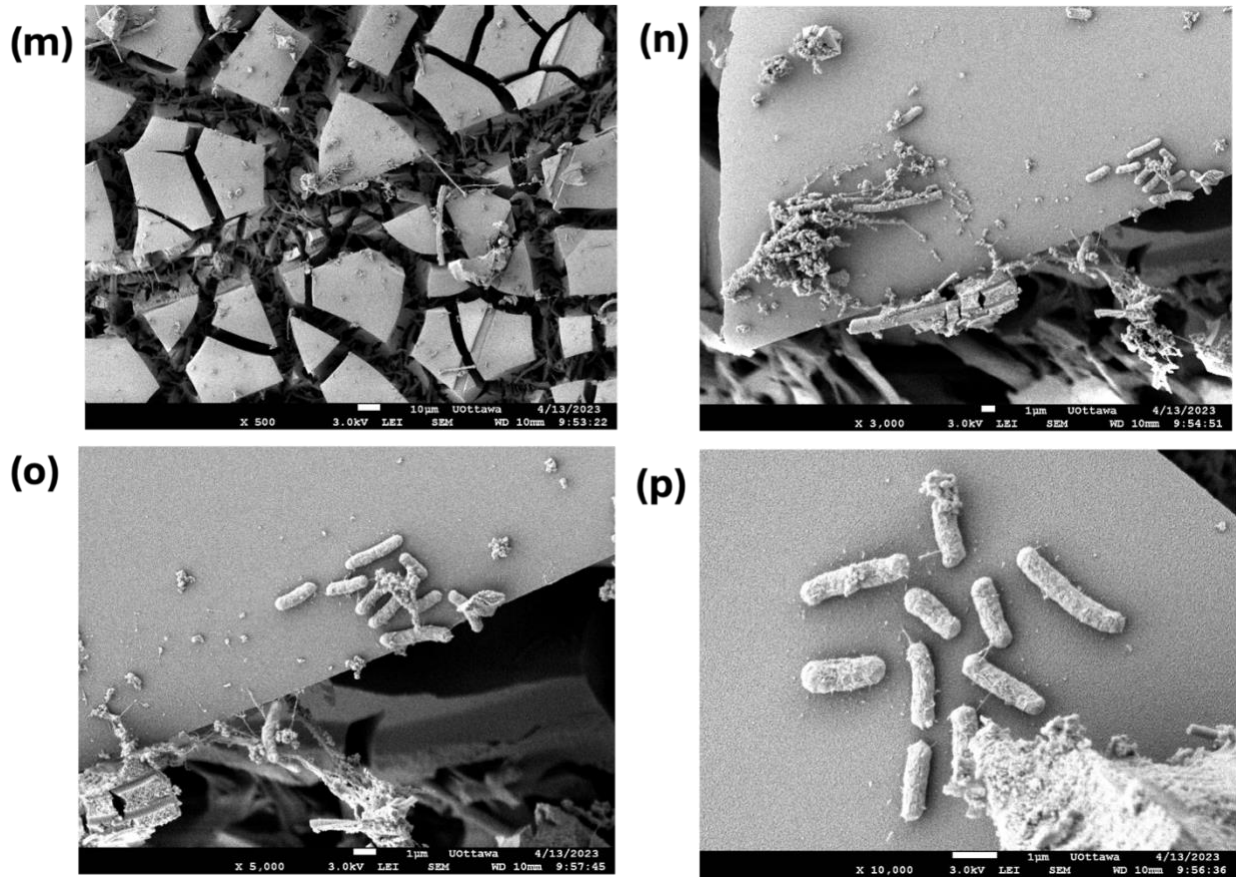


Figure 18 SEM Images of Catalyst Strip after 3 hours in solution, shown at various magnifications. Small catalyst strips were placed in 30 mL of DL-Lactate bacterial solution (10^6 CFU/mL) and oscillated at room temperature under dark conditions for 3 hours. They were not rinsed.

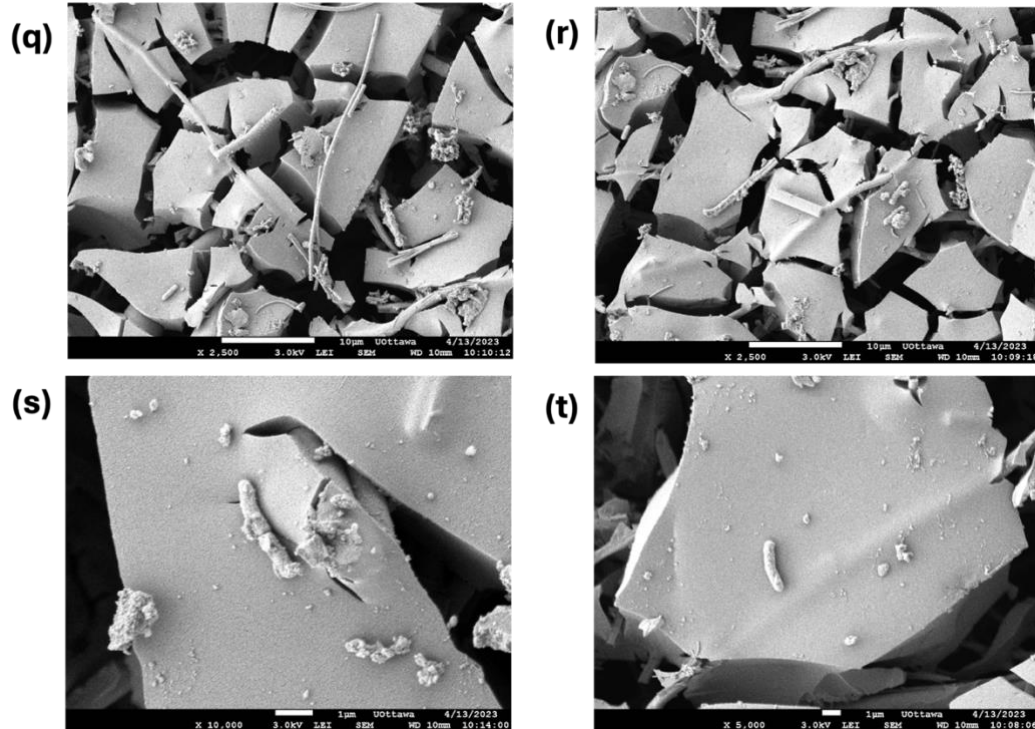


Figure 19 SEM Images of Catalyst Strip after 3 hours in solution followed by rinse. Small catalyst strips were placed in 30 mL of DL-Lactate bacterial solution (10^6 CFU/mL) and oscillated at room temperature under dark conditions for 3 hours. They were rinsed one time with 50 mL Milli-Q water.

Figure 16 and **Figure 18** qualitatively demonstrate that after exposure to bacterial media, unrinsed catalyst strips retain bacteria on their surface. The longer a catalyst strip is exposed to bacterial solution, the more bacteria settle on its surface. This is particularly evident when comparing 1.5 hours of exposure (**Figure 16**) to 3 hours of exposure (**Figure 18**). Over longterm exposure, this could lead to biofilm formation. **Figure 17** and **Figure 19** show rinsed species, with a notable decrease in bacteria present on their surfaces. **Figure 17** has zero to one visible, intact *E. Coli* cell at all magnifications, whereas **Figure 19** shows up to 4 cells with their membranes intact in image (**r**). These findings pushed our research towards a flow model, in the interest of both having a more realistic model, and for the prevention of biofilm formation.

3.3 Fluorescent Dye Testing

All dyes (DAPI, Ethidium Bromide, Hoechst 33342, Hoechst 33258, Propidium Iodide, Sybr Green, Sybr Gold, and PicoGreen) increase fluorescence upon binding to double stranded DNA. We wanted to select the dye that increased in fluorescence the most when exposed to live versus dead cells. To do this, various dilutions of live:dead *E. Coli* and *S. Aureus* were rested with each dye for ten minutes. Fluorescence was taken for each dilution of each dye at various bacterial concentrations. All dyes were diluted to a concentration of 6.4 μM , regardless of the bacterial concentration tested.

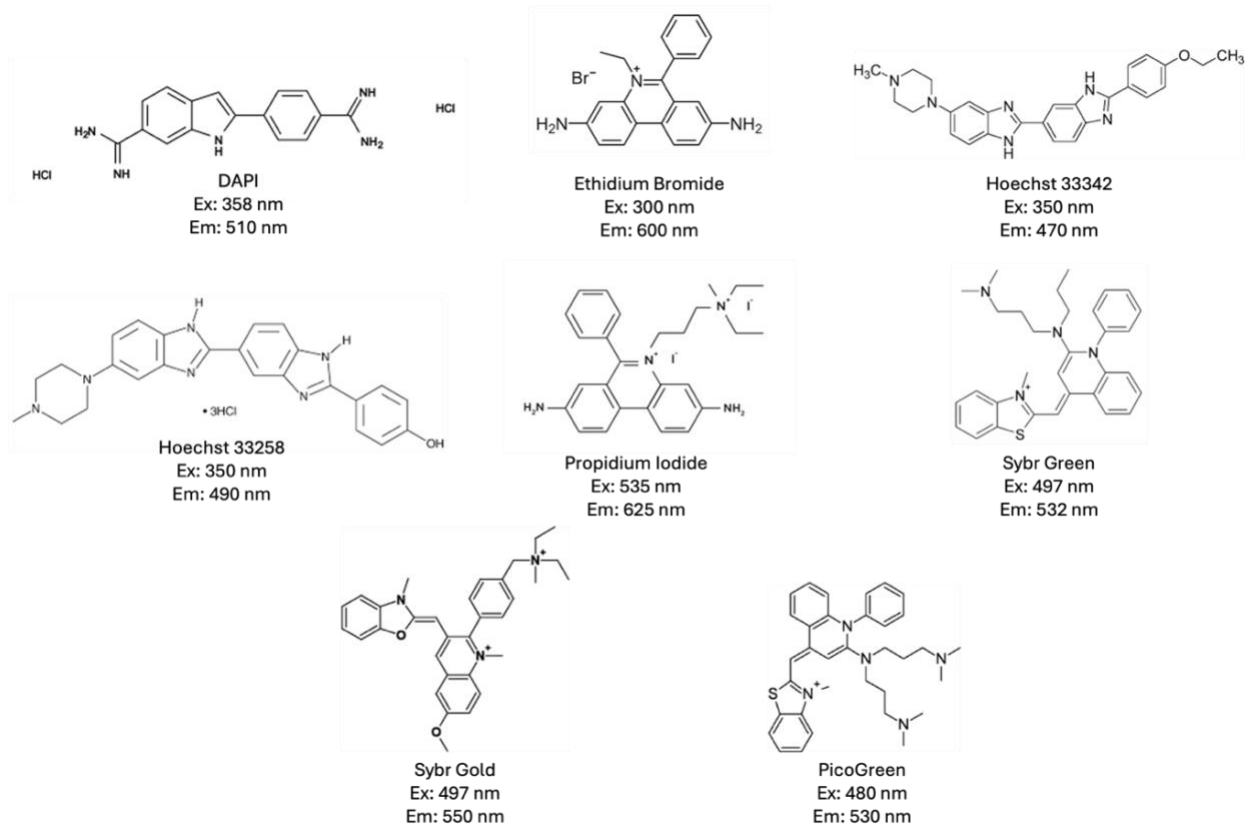


Figure 20 Fluorescent dye molecule structures. Excitation (Ex) and emission (Em) wavelengths included, according to measurements at 6.4 μM in DL-Lactate media.

Fluorescent Dyes Excitation Spectra

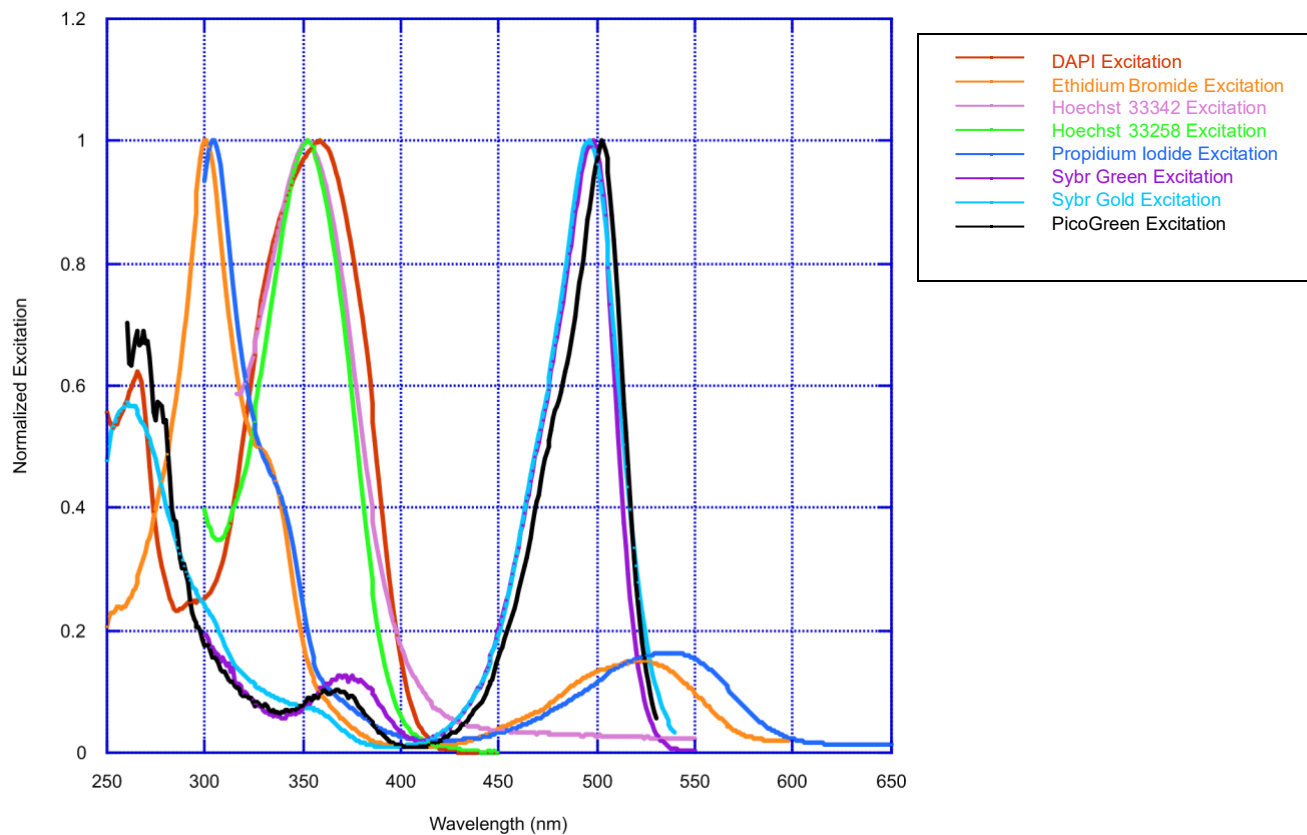


Figure 21 Excitation Spectra for all fluorescent dyes tested. Dyes were DAPI, Ethidium Bromide, Hoechst 33342, Hoechst 33258, Propidium Iodide, Sybr Green, Sybr Gold, and PicoGreen. All dyes were diluted to 6.4 μM in DL-Lactate media, and monitored using an M5 Microplate Reader which performed an excitation sweep with data collected every 2 nm. Spectra were collected with high concentrations of both bacteria (2.4×10^7 CFU/mL), and averaged.

Fluorescent Dyes Emission Spectra

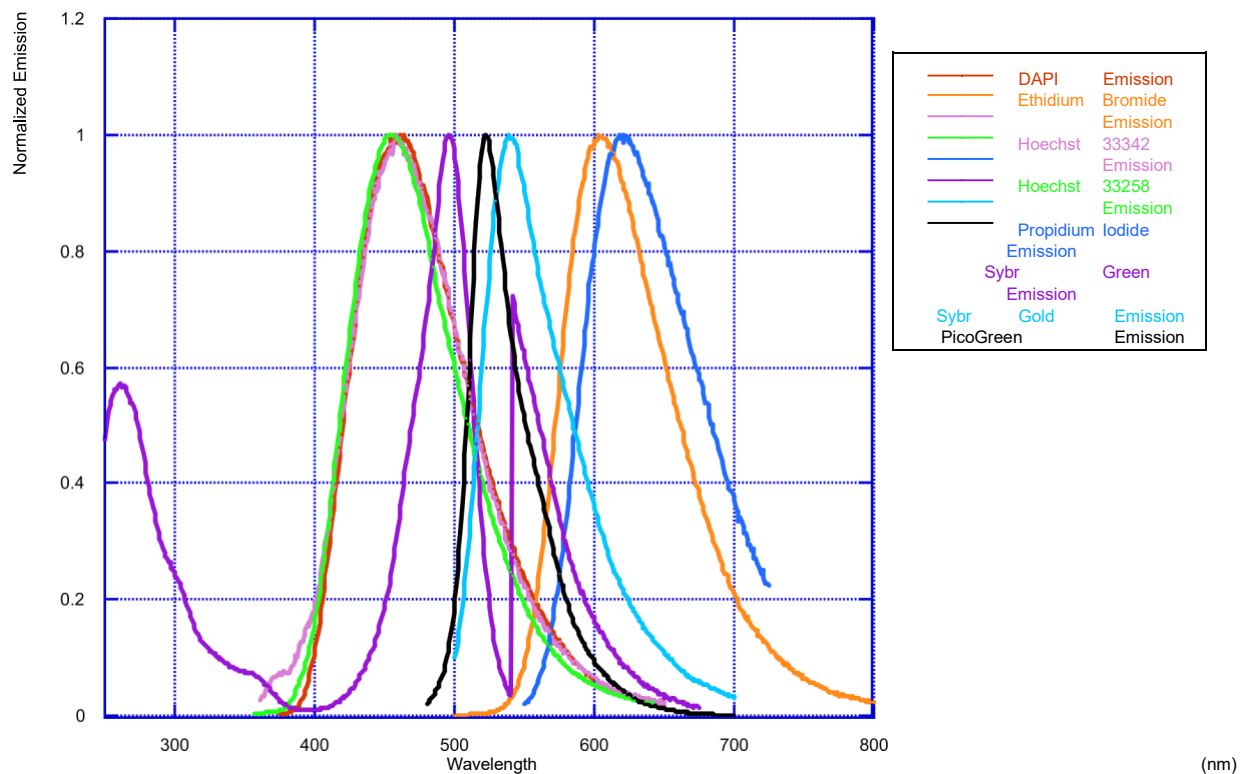
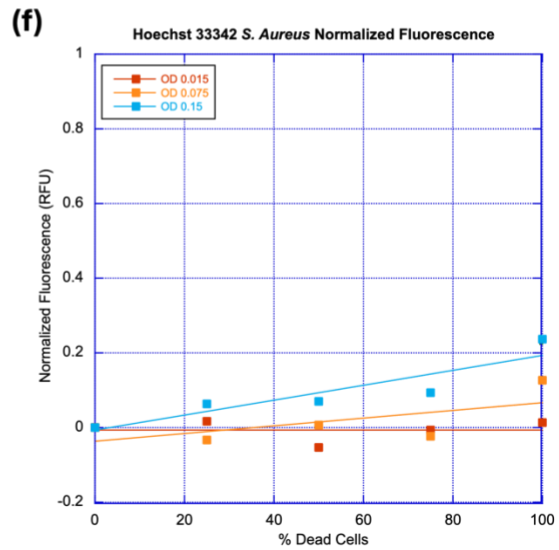
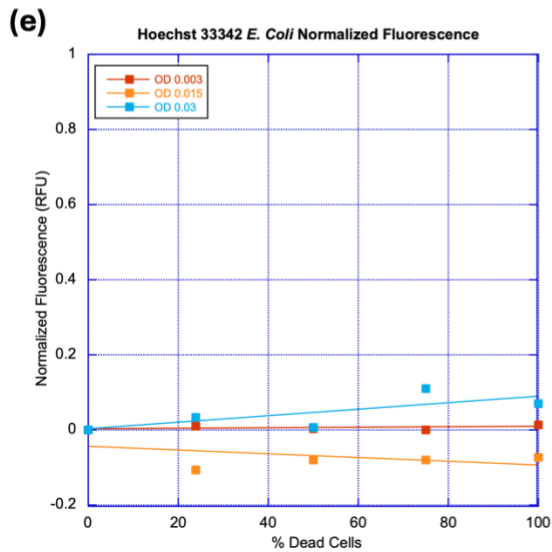
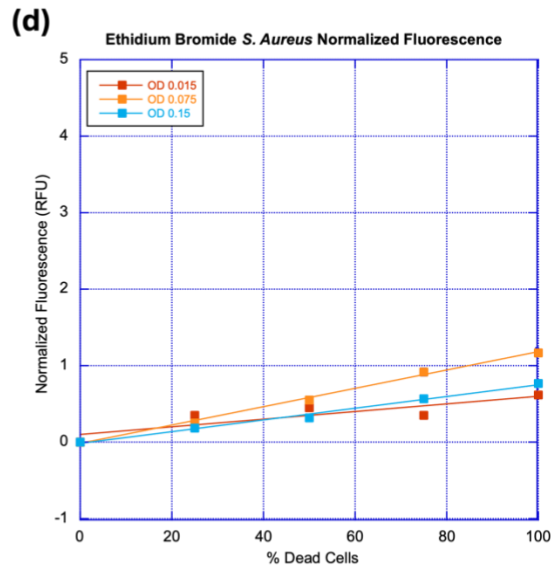
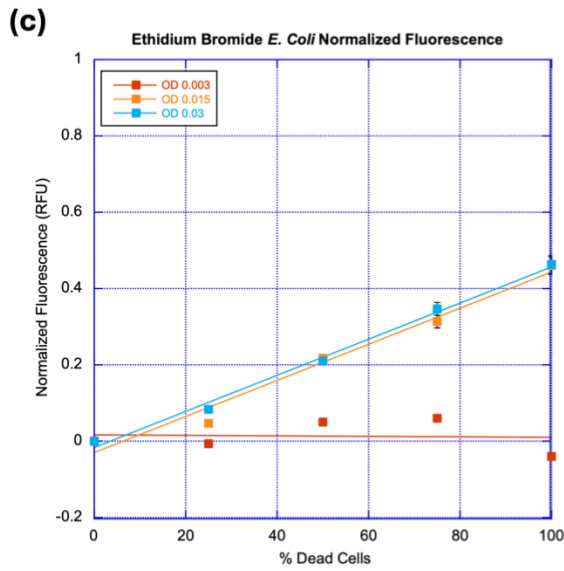
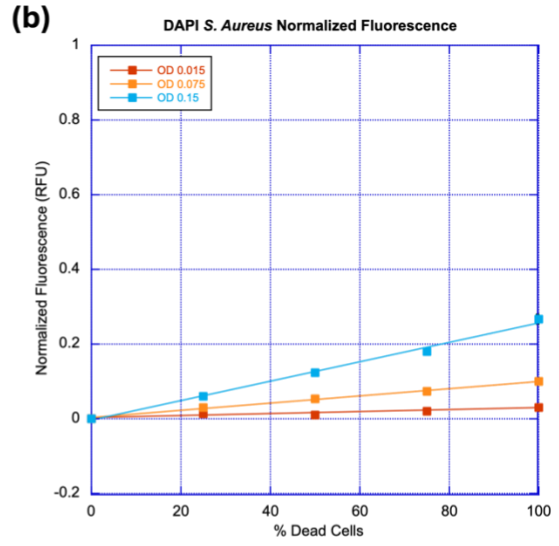
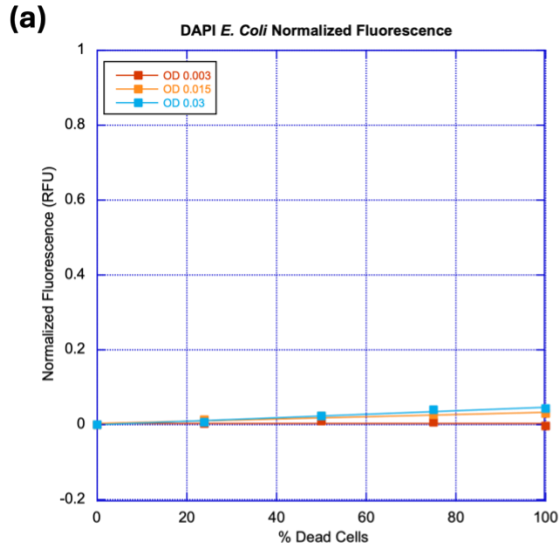
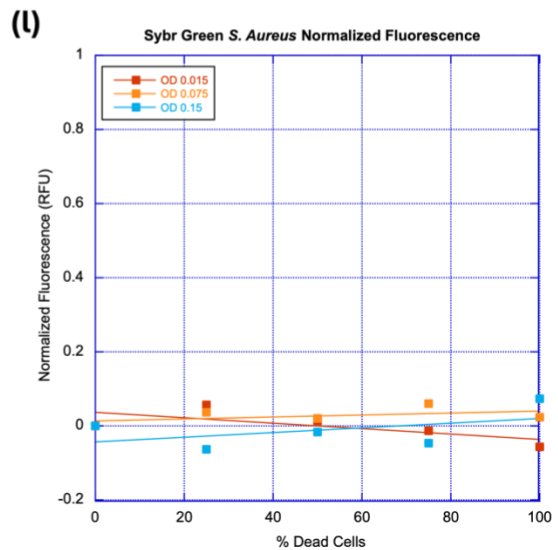
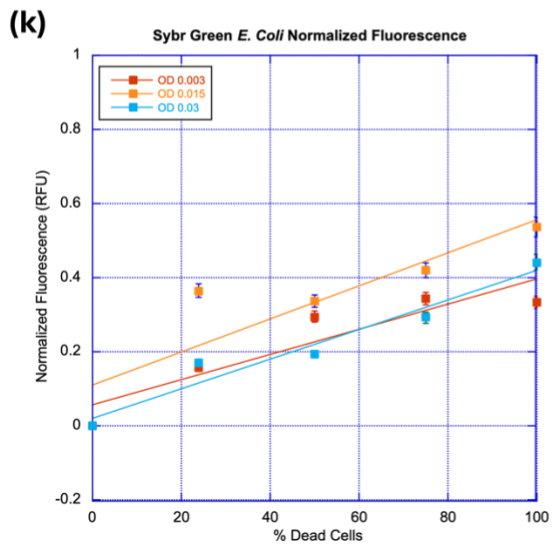
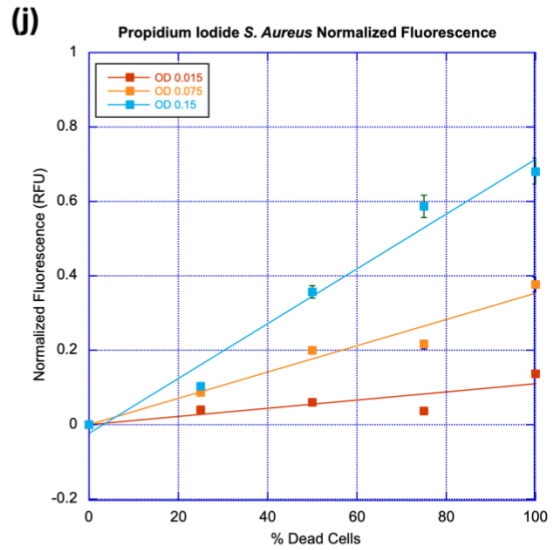
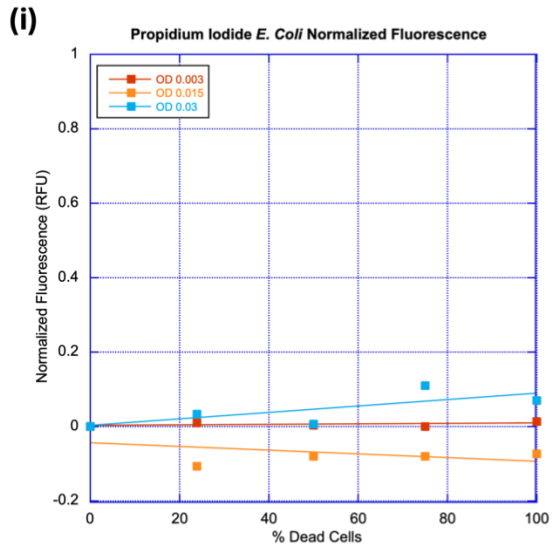
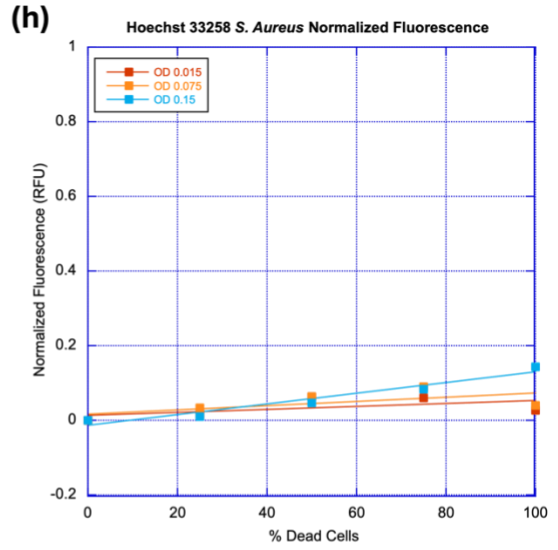
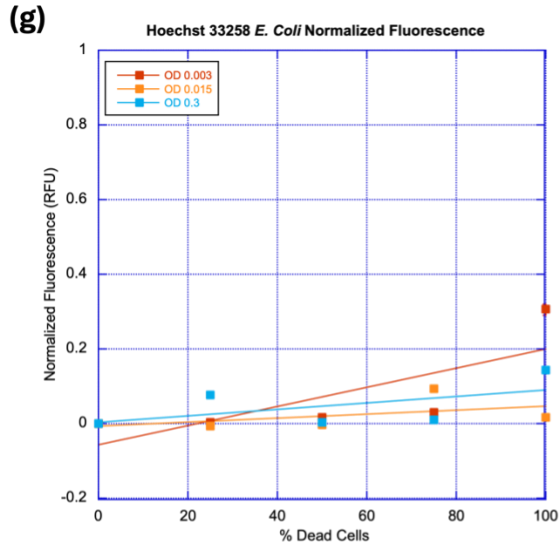


Figure 22 Emission Spectra for all fluorescent dyes tested. Only peaks are included for spectra simplification. Dyes were DAPI, Ethidium Bromide, Hoechst 33342, Hoechst 33258, Propidium Iodide, Sybr Green, Sybr Gold, and PicoGreen. All dyes were diluted to 6.4 μM in DL-Lactate media, and monitored using an M5 Microplate Reader which performed an emission sweep with data collected every 2 nm. All dyes were excited at their respective wavelengths (**Figure 21**). Spectra were collected with high concentrations of both bacteria (2.4×10^7 CFU/mL), and averaged.

Fluorescence changes for **Figure 23** were recorded in relative fluorescence units (RFU). The average RFU values from each triplicate were normalized against the RFU of the 0% dead cell control and adjusted to remove baseline fluorescence. Normalized fluorescence values lower than one correspond to a less than 100% increase in fluorescence between the live versus dead cells.





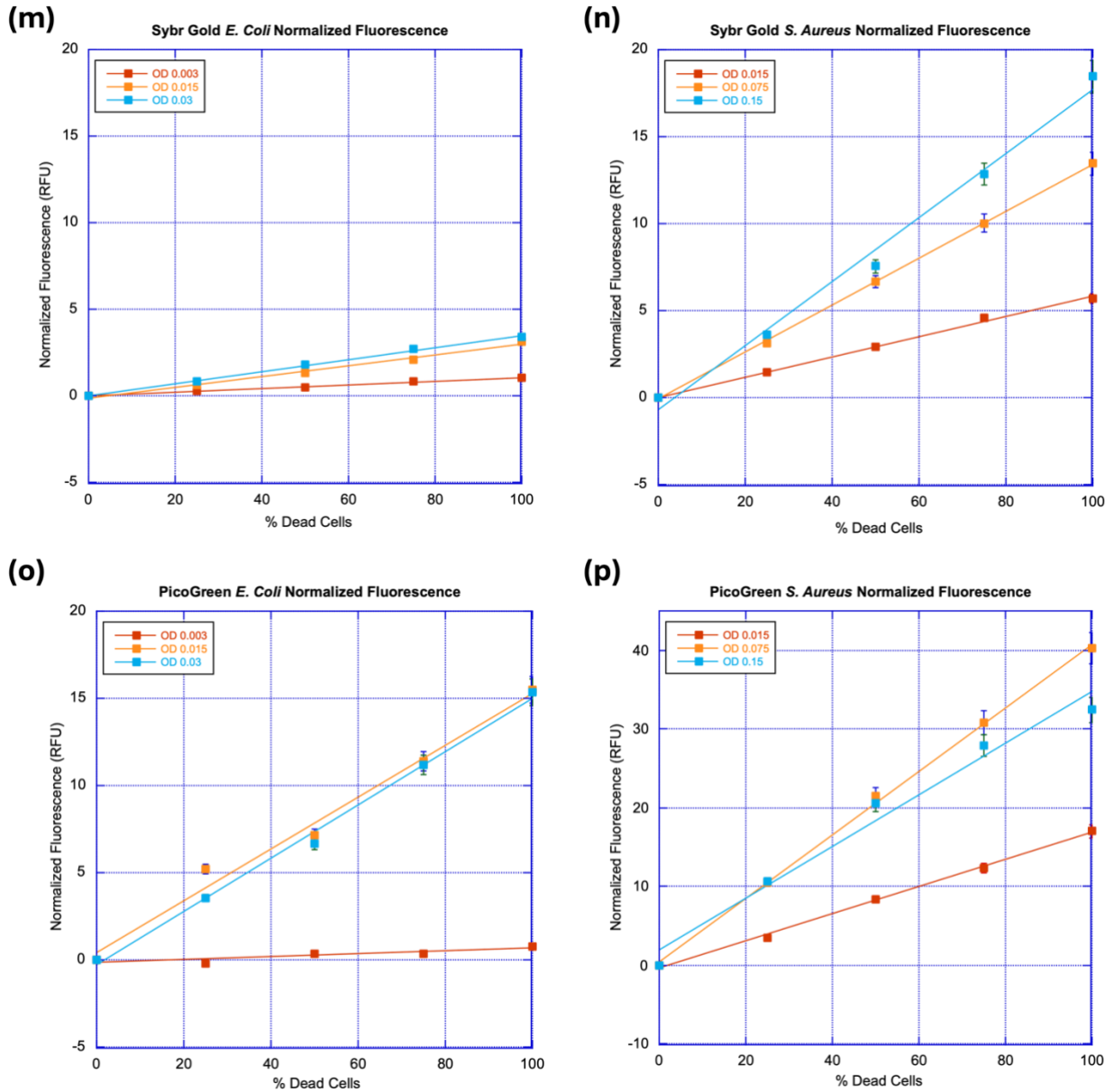


Figure 23 Calibration curves of all fluorescent dyes tested, using both *E. Coli*, and *S. Aureus* [(a)-(p)]. Data is normalized to the 0 % dead Cells fluorescence value (RFU) for each trial.

E. Coli and *S. Aureus* OD₆₀₀ measurements were made to test equivalent CFU/mL for each strain. An OD₆₀₀ 0.003-0.006 for both *E. Coli* and *S. Aureus* was chosen as the experimental condition for further tests, as it was determined to be the sensitivity limit for the calibration curves. OD₆₀₀ to CFU/mL conversions can be found in **Table 7**.

Table 7 Optical Density (OD_{600}) to Colony Forming Unit (CFU/mL) conversion table. Based on *E. Coli* conversion factor OD_{600} of 1.0 = 8×10^8 cells/ml and *S. Aureus* conversion factor OD_{600} of 1.0 = 1.6×10^8 cells/ml. Conversion factors were verified via plating and colony counting in triplicate.

	OD₆₀₀	CFU/mL
<i>E. Coli</i>	0.03	2.4×10^7
	0.015	1.2×10^7
	0.003	2.4×10^6
<i>S. Aureus</i>	0.15	2.4×10^7
	0.075	1.2×10^7
	0.015	2.4×10^6
	0.003	4.8×10^5

Only dyes that had an increase in normalized fluorescence greater than 1 were considered for further assays, ruling out all dyes tested except for PicoGreen and Sybr Gold. Of those two dyes, PicoGreen showed the highest increase in fluorescence with increasing ratios of dead cells (0 % to 100 % dead). It is worth noting that Ethidium Bromide and *S. Aureus* also exhibited a normalized fluorescence value slightly higher than one, however due to inconsistent trends between fluorescence and cell concentration it was discarded as a viable dye.

We observed that *S. Aureus* exhibited brighter fluorescence compared to *E. Coli* at the same concentrations (for example, **Figure 23, (m)** versus **(n)**, and **(o)** versus **(p)**.) This difference is likely due to the higher levels of extracellular DNA in *S. Aureus*. Both *E. Coli* and *S. Aureus* release DNA during cell lysis, but as a Gram-positive bacterium, *S. Aureus* releases significantly more extracellular DNA, which is essential for its biofilm stability. In contrast, *E. Coli*, a Gram-negative bacterium, retains more DNA inside the cell, protected by its outer membrane.

3.4 Fluorescence Batch Experiments

The Batch Fluorescence Assay was performed with 30 mL of bacterial solution (working solution) under experimental conditions of bTiO₂ and white light (**Figure 36 (a)**), along with control conditions. Controls included bTiO₂ in the dark, glass filter (GF) under light and dark conditions, and nothing (no GF or bTiO₂) under light and dark conditions. Working solutions for each condition were swirled on a wellplate oscillator for up to 180 minutes with aliquots removed at various intervals. Bacterial inactivation was measured using PicoGreen fluorescence (**Figure 24**) compared to calibration curves performed for each set of conditions (not included). It was then verified using colony counting for intermittent aliquots (**Figure 25**). The goal of these tests was to establish a proof-of-concept of the bactericidal properties of bTiO₂ under visible irradiation, and a baseline of control conditions. Additionally, it was our first test where we applied the novel PicoGreen Assay to real (bTiO₂ and white light) reaction conditions. We were looking for increasing bacterial death as exposure time increased.

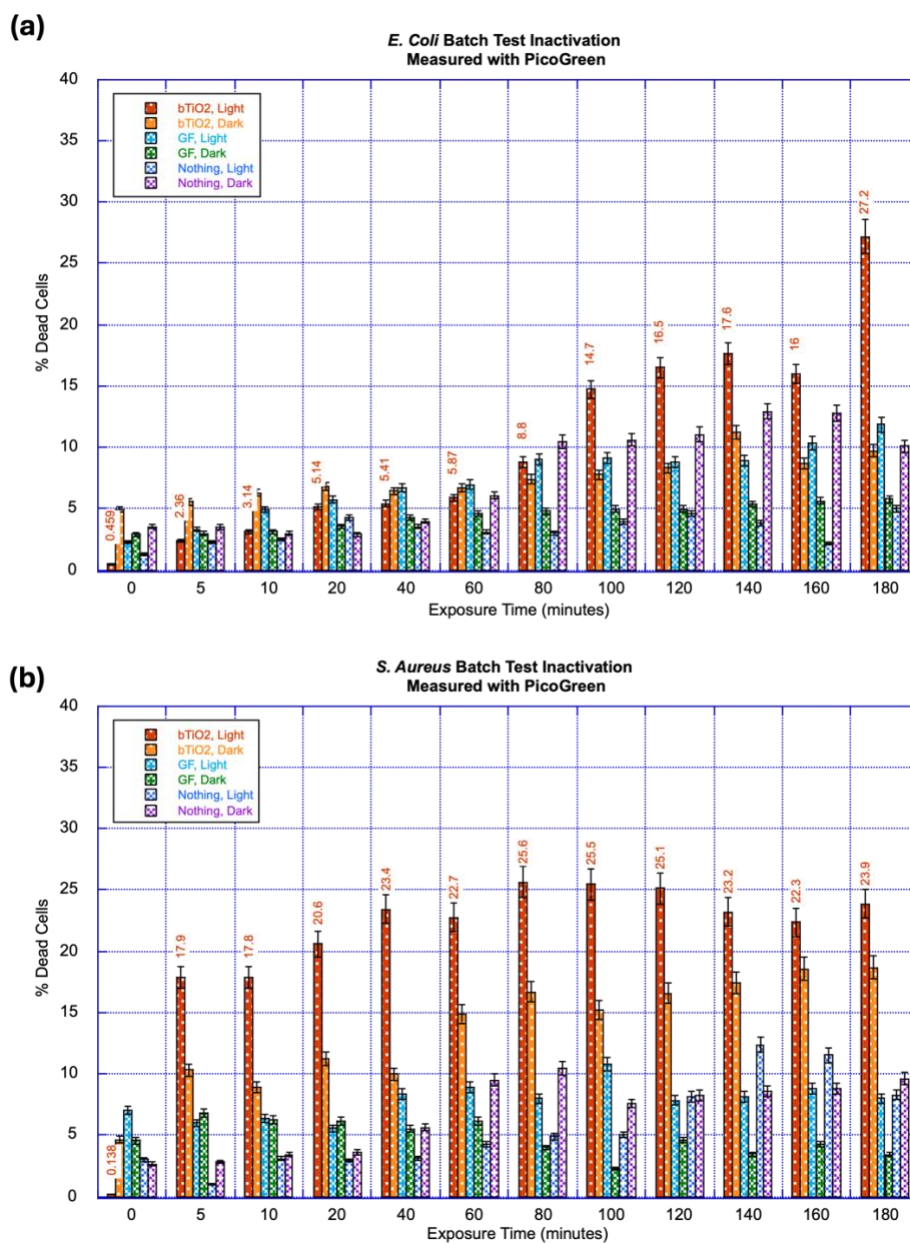


Figure 24 *E. Coli* (a) and *S. Aureus* (b) inactivation batch test results measured with PicoGreen fluorescence. Bacteria in DL Lactate media (30 mL, OD₆₀₀ 0.003) was oscillated at room temperature either under light or dark conditions (**Figure 7** Experimental batch setup diagram) Red bars represent experimental conditions; bTiO₂ on glass filter (GF) support and white LED light (**Figure 36**). All other conditions were represented other colours (bTiO₂ Dark, GF light and dark, and nothing - no catalyst and no GF). Bacteria were exposed to conditions for 180 minutes with 1 mL aliquots taken at minutes 0, 5, 10, 20, 40, 60, 80, 100, 120, 140, 160, and 180 minutes. Dilute PicoGreen (50 μ L) was added to each 1 mL aliquot for a total concentration of 6.4 μ M, left at room temperature in the dark for ten minutes, and fluorescence was read. Aliquots were taken in triplicate with error bars representing standard deviation. Statistical analysis using ANOVA and Tukey's HSD test ($p < 0.05$) showed that bTiO₂ significantly reduced viability compared to GF and 'nothing' conditions.

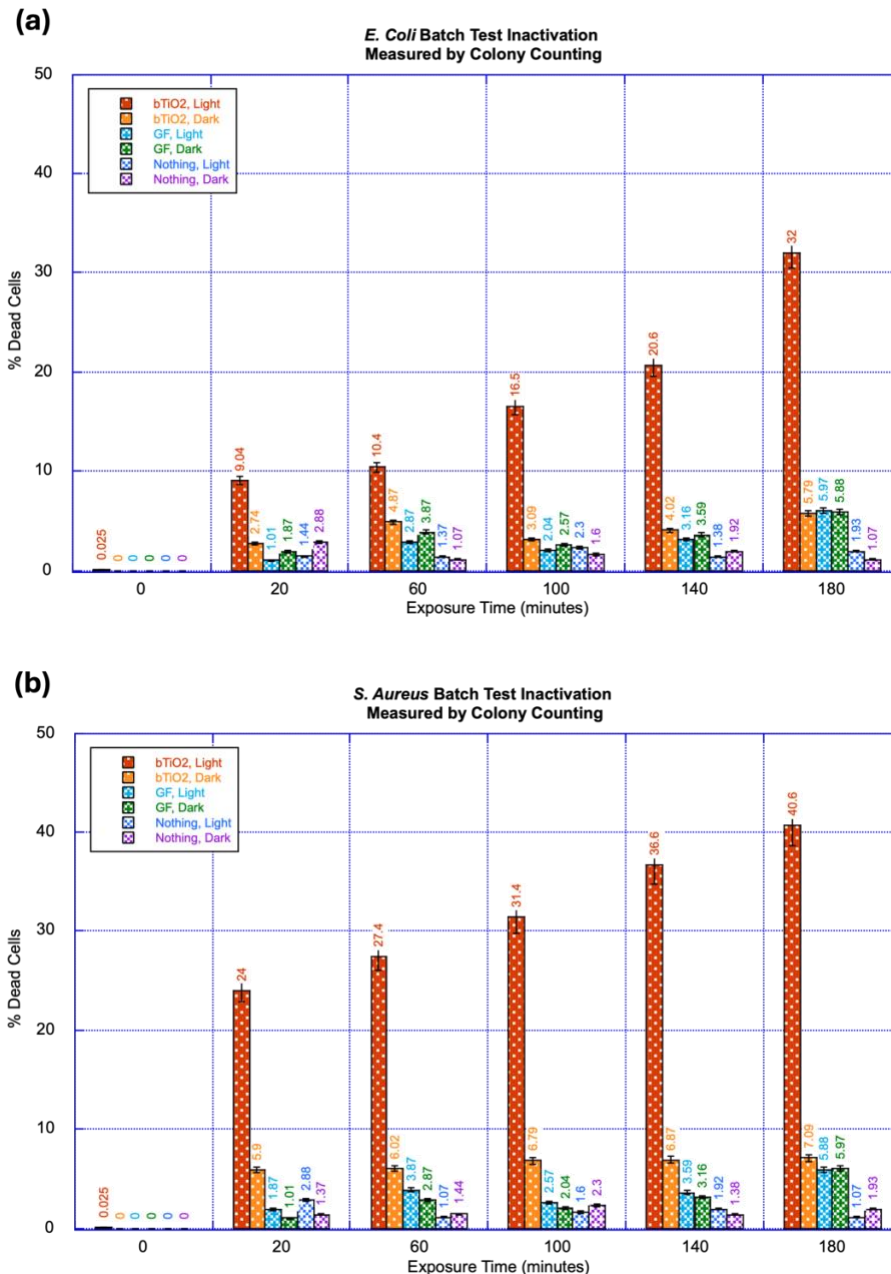


Figure 25 *E. Coli* (a) and *S. Aureus* (b) inactivation batch test results measured with plating and colony counting. Bacteria in DL Lactate media (30 mL, OD₆₀₀ 0.003) was oscillated at room temperature either under light or dark conditions (**Figure 7** Experimental batch setup diagram) Red bars represent experimental conditions; bTiO₂ on glass filter (GF) support and white LED light (**Figure 36**). All other conditions were represented other colours (bTiO₂ Dark, GF light and dark, and nothing - no catalyst and no GF). Bacteria were exposed to conditions for 180 minutes with 1 mL aliquots taken at minutes 0, 5, 10, 20, 40, 60, 80, 100, 120, 140, 160, and 180. Drops of working solution (10 μL) in various dilutions were plated, incubated for 14h and counted. Aliquots were taken in triplicate with error bars representing standard deviation. Statistical analysis using ANOVA and Tukey's HSD test ($p < 0.05$) showed that bTiO₂ and white light significantly reduced viability compared to control conditions.

Tests under experimental conditions demonstrated an increase in bacterial inactivation for both *E. Coli* and *S. Aureus* as exposure time increased. This was particularly notable when using colony counting (**Figure 25**), which showed cell inactivation up to 32 % for *E. Coli*, and 40.6 % for *S. Aureus*. Comparatively, **Figure 24** measured with PicoGreen, demonstrated a maximum percent inactivation of 27.2 % for *E. Coli*, and 25.6 % for *S. Aureus*. There was an observed increase in percent cell inactivation for both methodologies, with a more consistent trend shown with the colony counting assay.

In subsequent experiments, controls without a catalyst or glass wool were omitted due to the definitive absence of bacterial inactivation observed in initial tests. However, controls using a glass filter and dark conditions were consistently included in all further assays to ensure experimental reliability.

3.5 Fluorescence Flow Experiments Results

3.5.1 Flow 1.0, Recycled Solution

Flow 1.0 was designed to test the bactericidal capabilities of bTiO₂ under experimental conditions (white light- **Figure 36 (a)**) in a recycled flow. This meant solution was passed through the tube and returned to a beaker to be re-flowed through the same tube. Each pass through the tube was equivalent to 3 minutes of exposure to reaction conditions. This mimicked the effect of having multiple tubes for a single pass, as bacterial solution was exposed multiple times to the catalyst. That said, recycled flow is not our end goal, as most water purification technologies are single pass. These tests were therefore helpful in determining whether a flow system was worth pursuing, but ultimately required more optimization, which was performed in Flow 2.0 and Flow 3.0 testing.

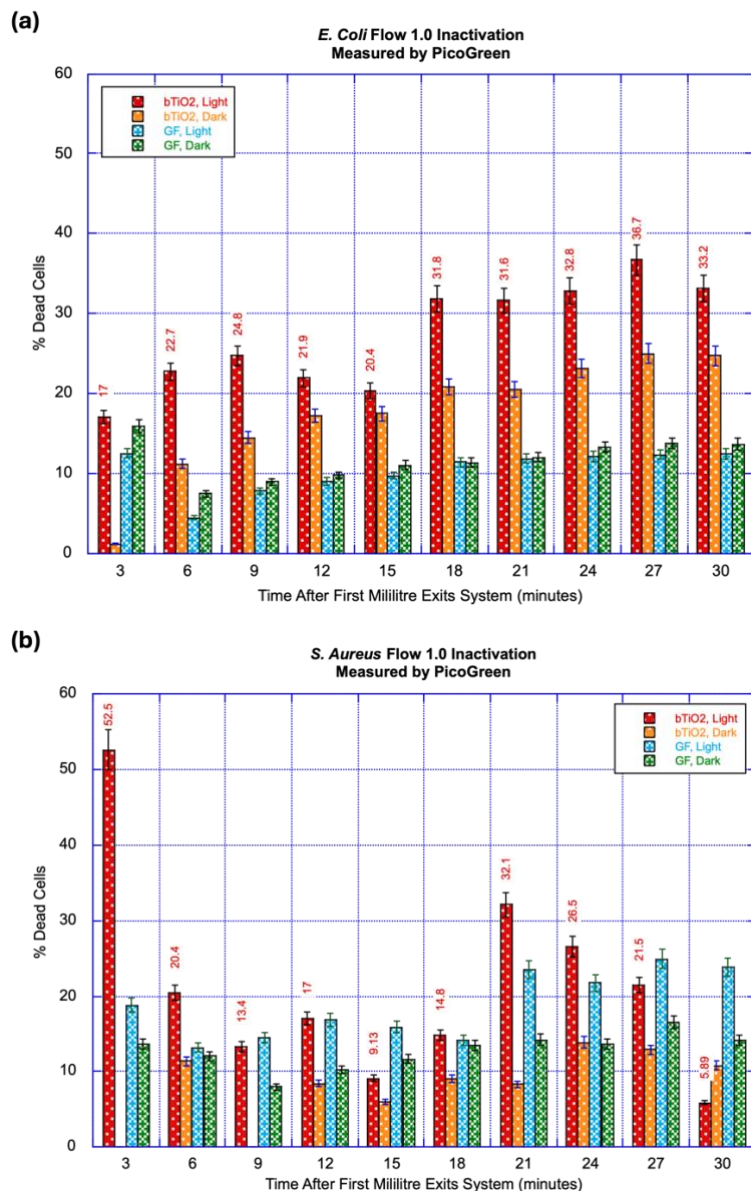


Figure 26 *E. Coli* (a) and *S. Aureus* (b) inactivation Flow 1.0 test results measured with PicoGreen fluorescence. Bacteria in DL Lactate media (70 mL, OD₆₀₀ 0.003) was pumped at 6 mL/min from a beaker over catalyst or glass filter at room temperature under either light or dark conditions (Figure 8) Upon exiting the flow tube, solution was returned to the beaker to be recycled. One millilitre aliquots were collected from the beaker. Aliquot times represent the number of minutes after the first millilitre of solution returned to the recycling beaker. Red bars represent experimental conditions; bTiO₂ on glass filter (GF) support and white LED light (Figure 36). All other conditions were represented other colours (bTiO₂ Dark, GF light and dark). Dilute PicoGreen (50 µL) was added to each 1 mL aliquot for a total dye concentration of 6.4 µM, left at room temperature in the dark for ten minutes, and fluorescence was read. Aliquots were taken in triplicate with error bars representing standard deviation. Statistical analysis using ANOVA and Tukey's HSD test ($p < 0.05$) showed that bTiO₂ reduced viability compared to control conditions for *E. Coli*.

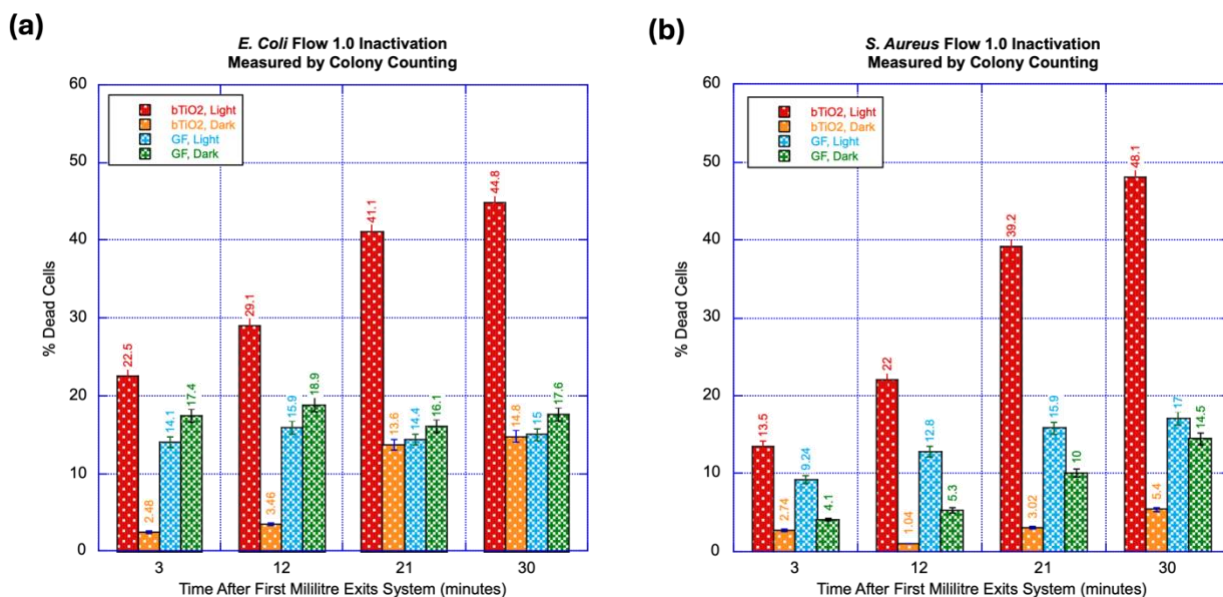


Figure 27 *E. Coli* (a) and *S. Aureus* (b) inactivation Flow 1.0 test results measured with plating and colony counting. Bacteria in DL Lactate media (70 mL, OD₆₀₀ 0.003) was pumped at 6 mL/min from a beaker over catalyst or glass filter at room temperature under either light or dark conditions (**Figure 8**). Upon exiting the flow tube, solution was returned to the beaker to be recycled. One millilitre aliquots were collected from the beaker. Aliquot times represent the number of minutes after the first millilitre of solution returned to the recycling beaker. Red bars represent experimental conditions; bTiO₂ on glass filter (GF) support and white LED light (**Figure 36**). All other conditions were represented other colours (bTiO₂ Dark, GF light and dark). Drops of working solution (10 µL) in various dilutions were plated, incubated for 14h and counted. Drops were plated in triplicate with error bars representing standard deviation. Statistical analysis using ANOVA and Tukey's HSD test ($p < 0.05$) showed that bTiO₂ and white light significantly increased bacterial inactivation compared to control conditions.

Flow 1.0 proved a success, in that the percent bacterial inactivation was higher than shown in the batch tests. Maximum percent inactivation seen in **Figures 26** and **Figure 27** were as follows: *E. Coli* showed 36.7 % with PicoGreen and 44.8 % with colony counting, whereas *S. Aureus* showed 32.1 % with PicoGreen (discarding the first datapoint) and 48.1 % with colony counting. The first datapoint in **Figure 26 (b)** was initially ignored due to its inconsistencies with the upwards trend observed in both batch and other Flow 1.0 tests. We theorized that it was higher due to inconsistent mixing of the recycling beaker, an experimental error. Due to the end goal of

a single pass system, Flow 1.0 was discarded, and single pass experiments commenced (Flow 2.0 and Flow 3.0).

3.5.2 Flow 2.0, Single Pass

Flow 2.0 was designed to optimize single pass bacterial inactivation mimicking real-world water purification strategies, but on a benchtop scale. *E. Coli* and *S. Aureus* were both flowed through a quartz tube (20 mL) at various flow speeds (**Table 8**) PicoGreen fluorescence for each flow speed was then evaluated. The goal was to achieve 2 log units of bacterial inactivation 30minute residence time or less, in accordance with WHO guidelines¹. With this goal in mind, three aliquots were taken at the beginning of the flow for all flow speeds, but only the 30-minute residence time was continued for an additional 1.75 hours. Aliquots were taken at various volumes after the first millilitre of working solution exited the tube. They were taken directly from the end of the system, with no recycled flow.

No colony counting assay was conducted for Flow 2.0. This decision was made because, despite some inconsistencies, the trends observed in prior PicoGreen assays aligned sufficiently with the corresponding plating and colony counting assay trends. This strategy was deemed adequate as a proof-of-concept screening tool, so we were able to prioritize expediting the assay and optimizing the experimental conditions over performing additional colony counting. Colony counting assays were resumed in the next iteration of the flow setup.

Table 8 Flow rates and equivalent residence times for Flow 2.0 and 3.0 experimental setups.

Flow Rate (mL/min)	Residence Time (min)
1.33	15
0.66	30
0.35	60

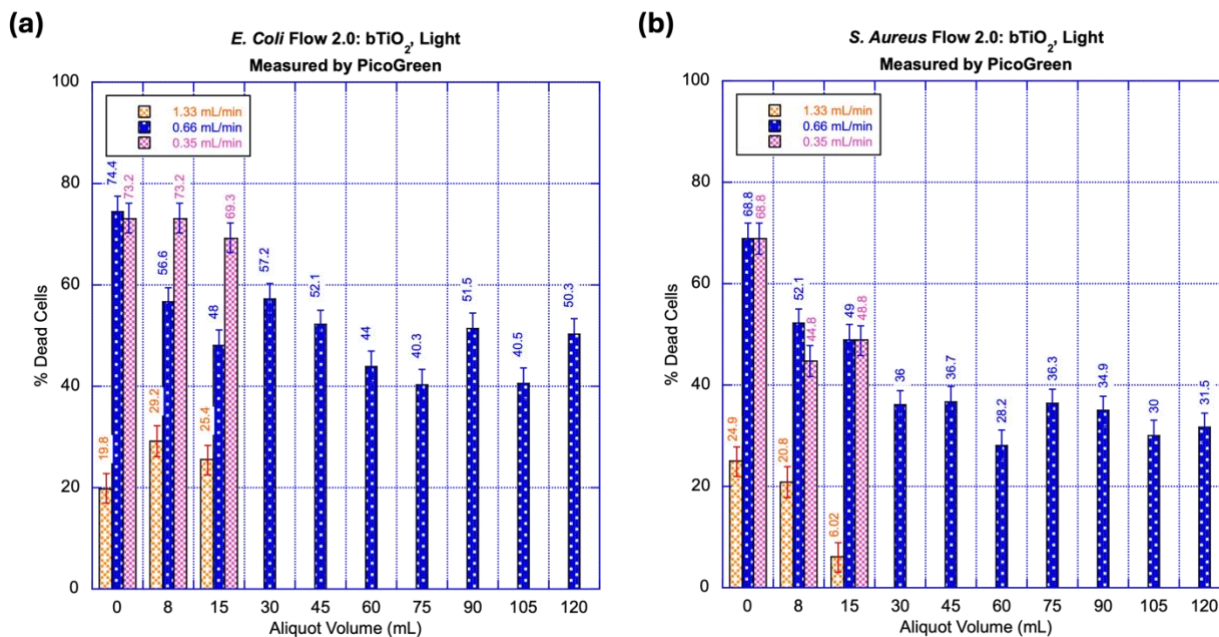


Figure 28 Flow 2.0 Bacterial Inactivation at various flow speeds, under white LED and bTiO₂ measured by PicoGreen. *E. Coli* and *S. Aureus* working solutions (OD₆₀₀ 0.003-0.006) were flowed through a 20 mL quartz tube at varying flow rates. Experiments were conducted under a "tent lamp" white LED light source (**Figure 36**) in the presence of bTiO₂ on glass filter support. Dilute PicoGreen (50 μL) was added to each 1 mL aliquot for a total dye concentration of 6.4 μM, followed by resting in the dark at room temperature for 10 minutes prior to fluorescence measurement. Statistical analysis using ANOVA and Tukey's HSD test ($p < 0.05$) showed that both flow speeds of 0.35 and 0.66 mL/min significantly increased bacterial inactivation compared to 1.33 mL/min. Note that the absence of bars for 0.35 and 1.33 mL/min at times longer than 15 minutes signifies that the measurement was not performed (as opposed to the reading being zero).

Figure 28 shows screening conditions for inactivating bacteria at varying flow speeds. For the sake of optimization three initial aliquots were taken for all flow speeds. However, after observing similar results for flow speeds of 0.66 mL/min and 0.35 mL/min, only the 0.66 mL/min was continued for an additional 120 mL of flow. Additionally, our goal flow rate was 0.66 mL/minute as this aligns with the WHO guidelines for water purification¹.

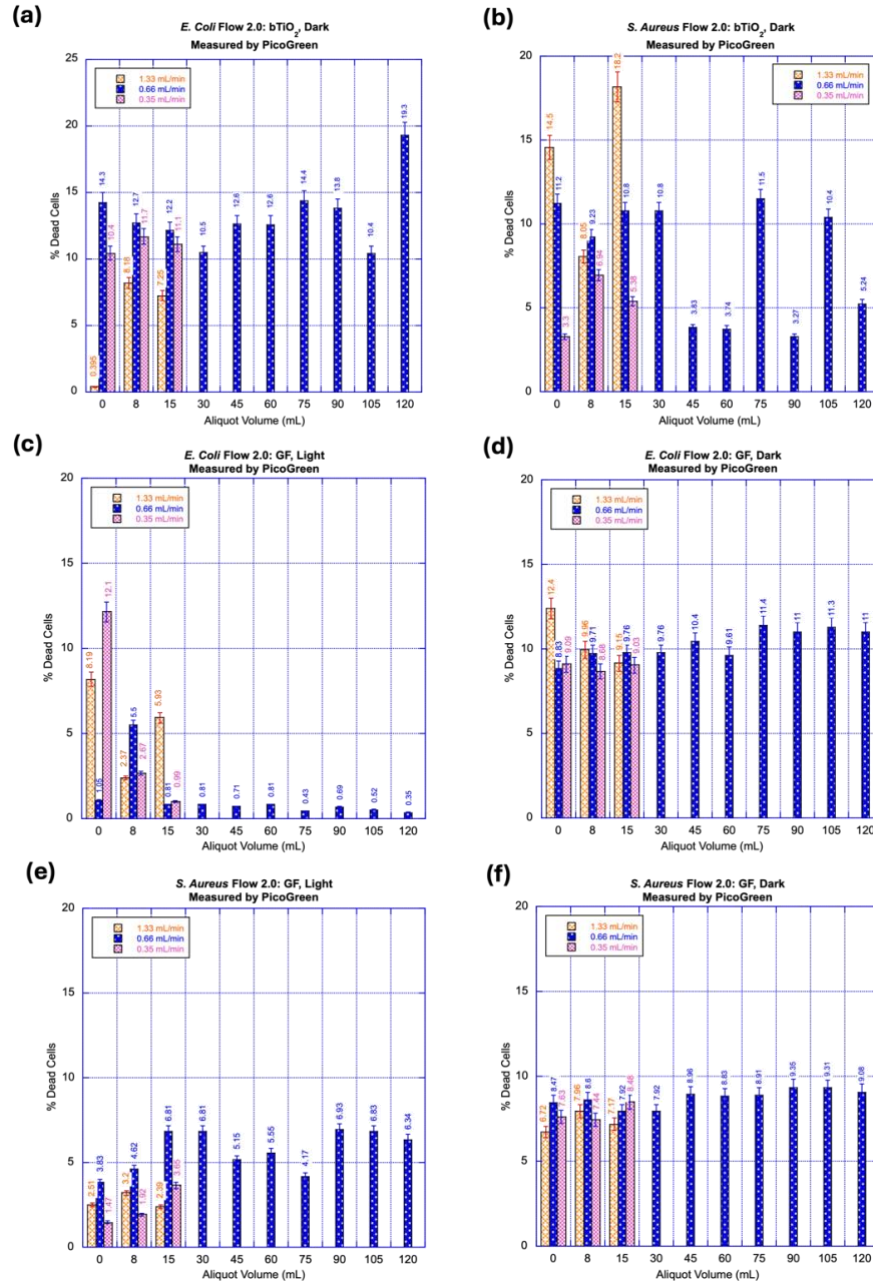


Figure 29 Control experiments for Flow 2.0 bacterial inactivation, measured by PicoGreen, under bTiO₂ (dark conditions) and glass filter (GF) support in both dark and light conditions. E. Coli and S. Aureus working solutions (OD₆₀₀ 0.003-0.006) were flowed through a 20 mL quartz tube at varying flow rates. For bTiO₂ controls experiments were conducted in the absence of illumination, while for GF controls, experiments were conducted under both "tent lamp" white LED light (**Figure 36**) and dark conditions. Dilute PicoGreen (50 μL) was added to each 1 mL aliquot for a total dye concentration of 6.4 μM, followed by rest in the dark at room temperature for 10 minutes prior to fluorescence measurement. Statistical analysis using ANOVA and Tukey's HSD test ($p < 0.05$) showed that bTiO₂ and white light significantly increased bacterial inactivation compared to all control conditions at any speed.

E. Coli demonstrated a maximum percent inactivation of 74.4 %, seen at a flow rate of 0.66 mL/min (**Figure 28**). Similarly, *S. Aureus* demonstrated a maximum percent inactivation of 68.8 % at 0.66 mL/min (**Figure 28**). While it is clear the 1.33 mL/min flow is too fast to be effectively bactericidal, there is no statistical difference (measured by two-way ANOVA) between the first aliquots flowed at 0.66 versus 0.35 mL/min (**Figure 28**).

Over a two-hour period, the working solution flowing at a rate of 0.66 mL/min appeared to reach a plateau. This observation may indicate either the depletion of a critical reagent or that the bacterial flow is too laminar, preventing sufficient interaction between the cells and the bTiO₂ surface to enable exposure to the bactericidal effects of the generated reactive oxygen species (ROS). To counteract this, air or oxygen bubbles were added to the flow, both increasing the amount of available ROS generating species, and making the flow more turbulent. Thus, Flow 3.0 was born.

3.5.3 Flow 3.0, Single Pass with Gas

Flow 3.0 used the same quartz tube system as Flow 2.0 but turned so the tube faced vertically. This allowed gas to be added to the system via a 0.5 mm needle through the bottom septum. All bacterial working solutions were pumped at 0.66 mL/min and all gasses were added at 1.33 mL/min resulting in small, champagne-like bubbles rising through the system. The gas bubbles (either air or oxygen) allowed for more turbulent flow, as well as increasing the available oxygen in the system for ROS generation. At room temperature equilibrium, oxygen generally has a solubility of 1.0 mM in water⁴⁴. The goal was to determine if additional turbulence and ROS availability would allow for more efficient bacterial inactivation.

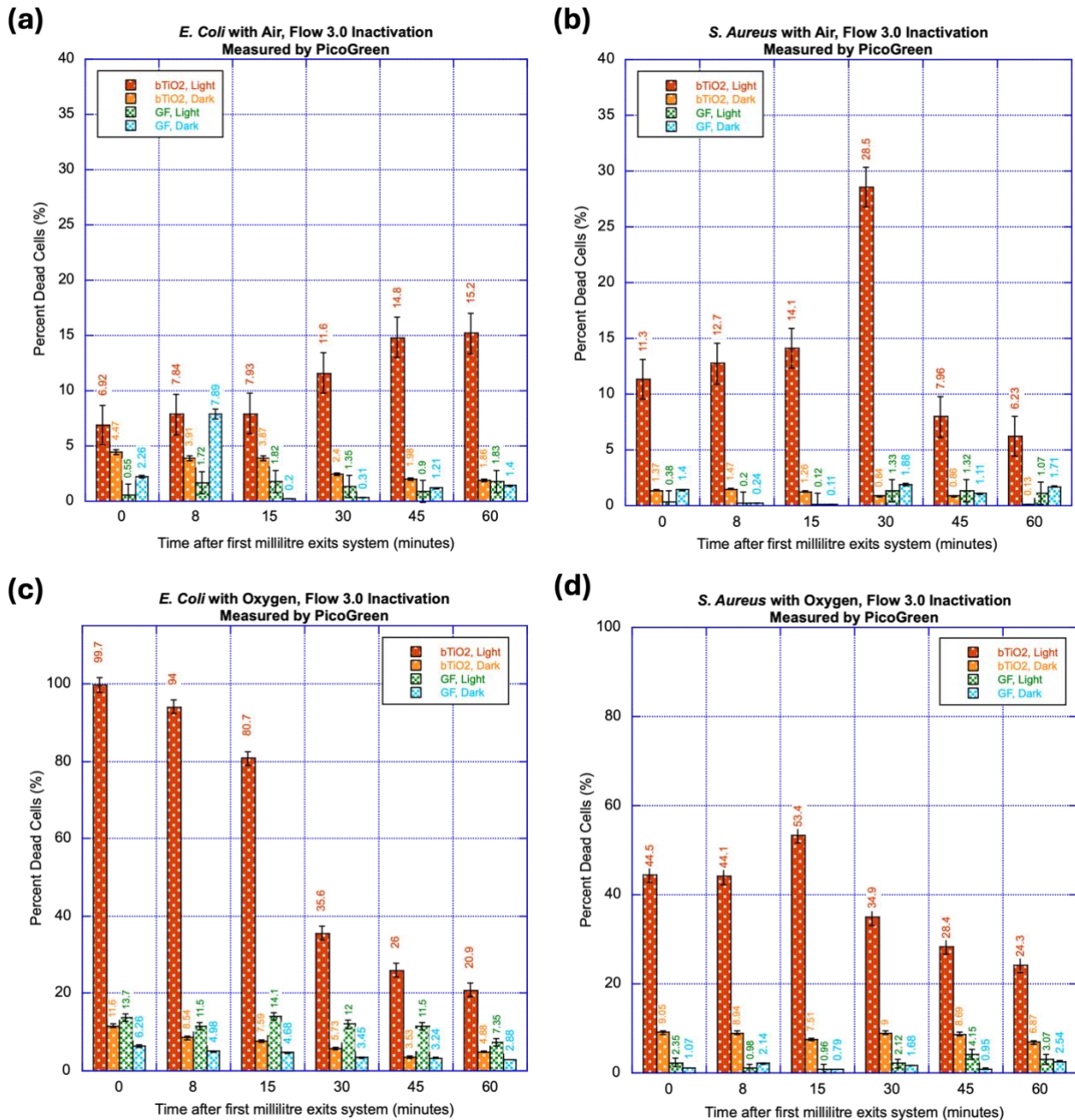


Figure 30 Flow 3.0 *E. Coli* and *S. Aureus* inactivation measured by PicoGreen with air or oxygen bubbled. *E. Coli* was flowed at 0.66 mL/min (30 minutes exposure time) with air (a) or oxygen (c) bubbled at 1.33 mL/min. *S. Aureus* was flowed under the same conditions with air (b) or oxygen (d). Dilute PicoGreen (50 μ L) was added to each 1 mL aliquot for a total dye concentration of 6.4 μ M, followed by resting in the dark at room temperature for 10 minutes prior to fluorescence measurement. Aliquots were measured in triplicate with error bars representing standard deviation. Statistical analysis using ANOVA and Tukey's HSD test ($p < 0.05$) showed that bTiO₂ and white light significantly increased bacterial inactivation compared to control conditions.

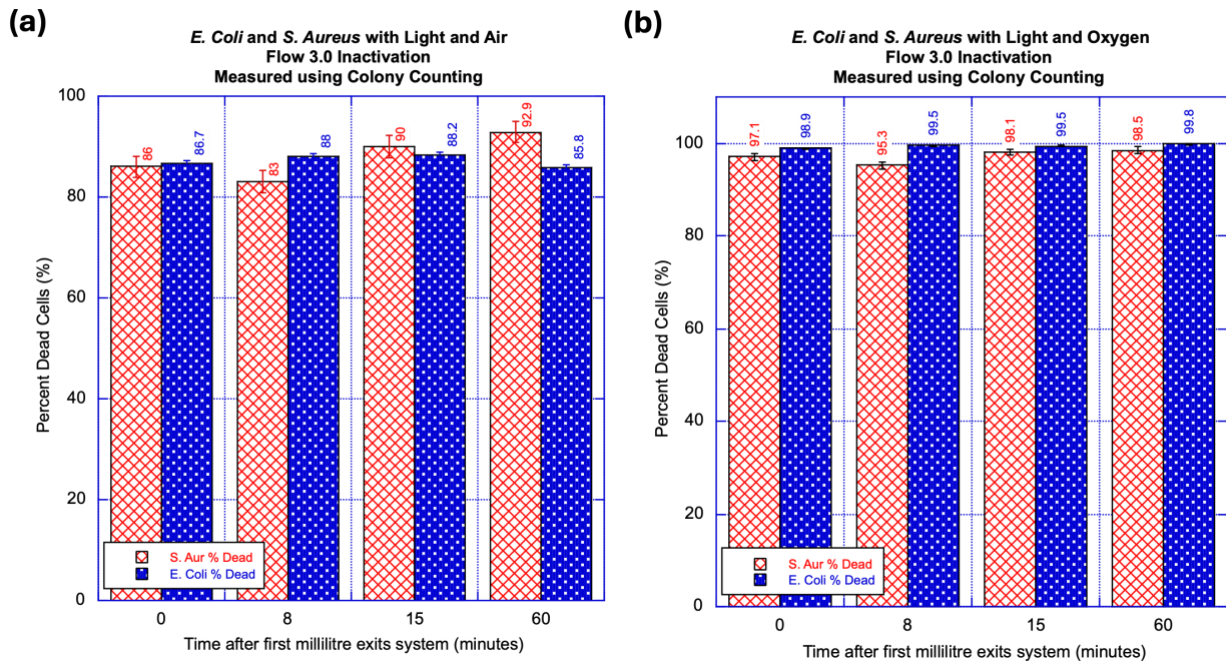


Figure 31 Flow 3.0 colony counting results for *E. Coli* and *S. Aureus* inactivation under white light illumination with $bTiO_2$ in the presence of either air (a) or oxygen (b). Drops of working solution ($10 \mu L$) in various dilutions were plated, incubated for 14h and counted. Drops were plated in triplicate with error bars representing standard deviation.

Figure 30 showed a dramatic change between the assay with air versus with pure oxygen. Surprisingly, the maximum percent bacterial inactivation seen for *E. Coli* with air was 15.2 %, whereas with oxygen 99.7 % were inactivated when measured with PicoGreen. Similarly, *S. Aureus* demonstrated a maximum percent bacterial inactivation of 28.5 % with air, versus 53.4 % with pure oxygen. These values, however, paled in comparison to the colony counting tests (**Figure 31**), which showed upwards of 83 % bacterial inactivation for *E. Coli* and *S. Aureus* under both air and oxygen flow conditions. Furthermore, the PicoGreen tests with oxygen still showed a decrease in bacterial inactivation after the first three aliquots, counter to our theory from Flow 2.0. Thankfully, the control conditions (**Figure 30**) still showed less than 12 %

inactivation for all conditions tested, with a statistical difference between experimental and control conditions (ANOVA).

We noted that the trend that the difference between the PicoGreen assay and the colony counting assay became more pronounced as we moved from Flow 1.0 to Flow 3.0, indicating the addition of gas played a large role in bacterial inactivation, but perhaps also impacted the PicoGreen assay. Due to discrepancies between the PicoGreen Assay and Colony Counting assay when gas was added to the system, mechanistic investigation was undertaken using FLIM.

3.6 FLIM Studies

Fluorescence Lifetime Imaging Microscopy (FLIM) allowed us to examine both the lifetimes and the white light images of bacteria under various conditions. To analyze various mechanisms of bacterial inactivation, both strains of bacteria were subjected to isopropanol, heat, UVC irradiation, and white light with oxygen and bTiO₂. Only the oxygen bubbled experimental conditions were explored via FLIM as they were observed to have the highest percent cell death in colony counting tests. The cells exposed to oxygen were thus hypothesized to have the highest ROS-induced cell inactivation.

Fluorescence lifetimes in **Figure 32** and **Figure 33** were taken and averaged from ten areas of interest per sample. An area of interest was qualitatively identified as a region with fluorescence and minimal noise. Lifetime therefore corresponds to the areas of fluorescence and not the entire sample image. Contrast on white light microscopy images was increased 45% for ease of viewing. The instrument response function (IRF) with PicoGreen was found to be $\tau = 0.36$ ns.

Additional testing was performed with Rhodamine B to visualize all cells present (live and dead), however these images were omitted from this thesis due to dye uptake differences between *E. Coli* and *S. Aureus*. We suggest additional tests be undertaken with a metabolically active dye for more consistent imaging.

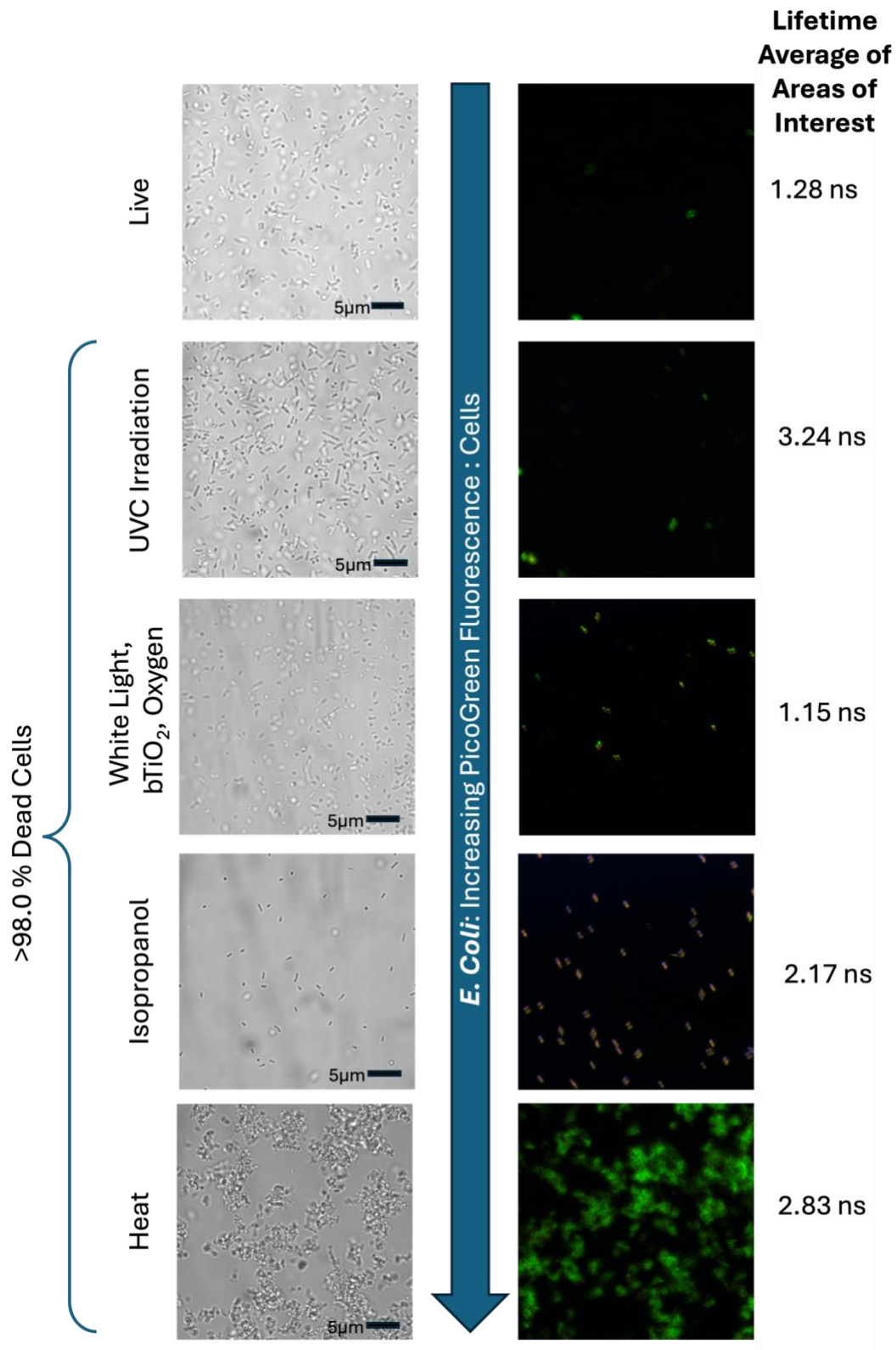


Figure 32 *E. Coli* inactivation by various methods using white light microscopy and FLIM. Percent inactive (dead) cells was verified using plating and colony counting.

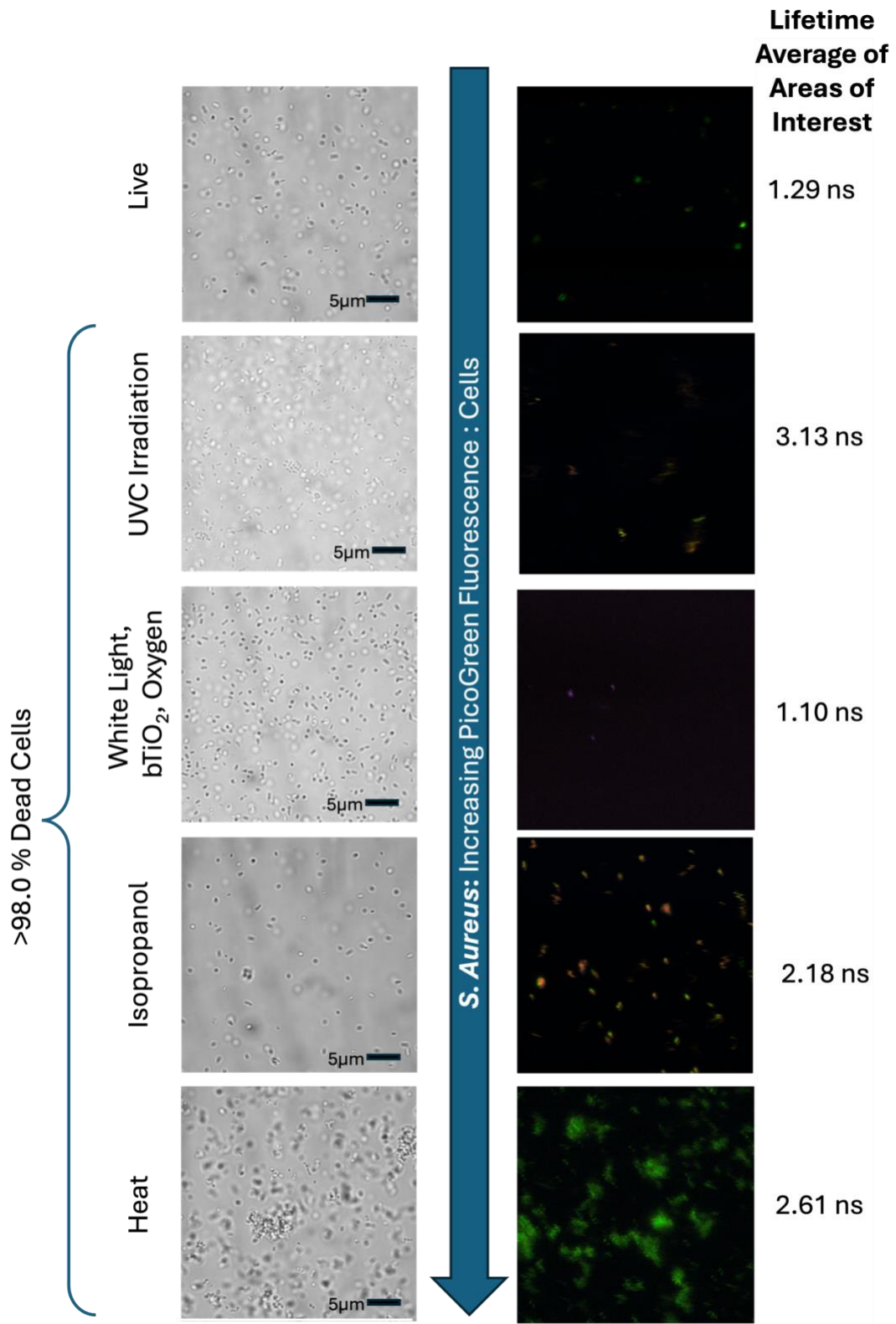


Figure 33 *S. Aureus* inactivation by various methods using white light microscopy and FLIM. Percent inactive (dead) cells was verified using plating and colony counting.

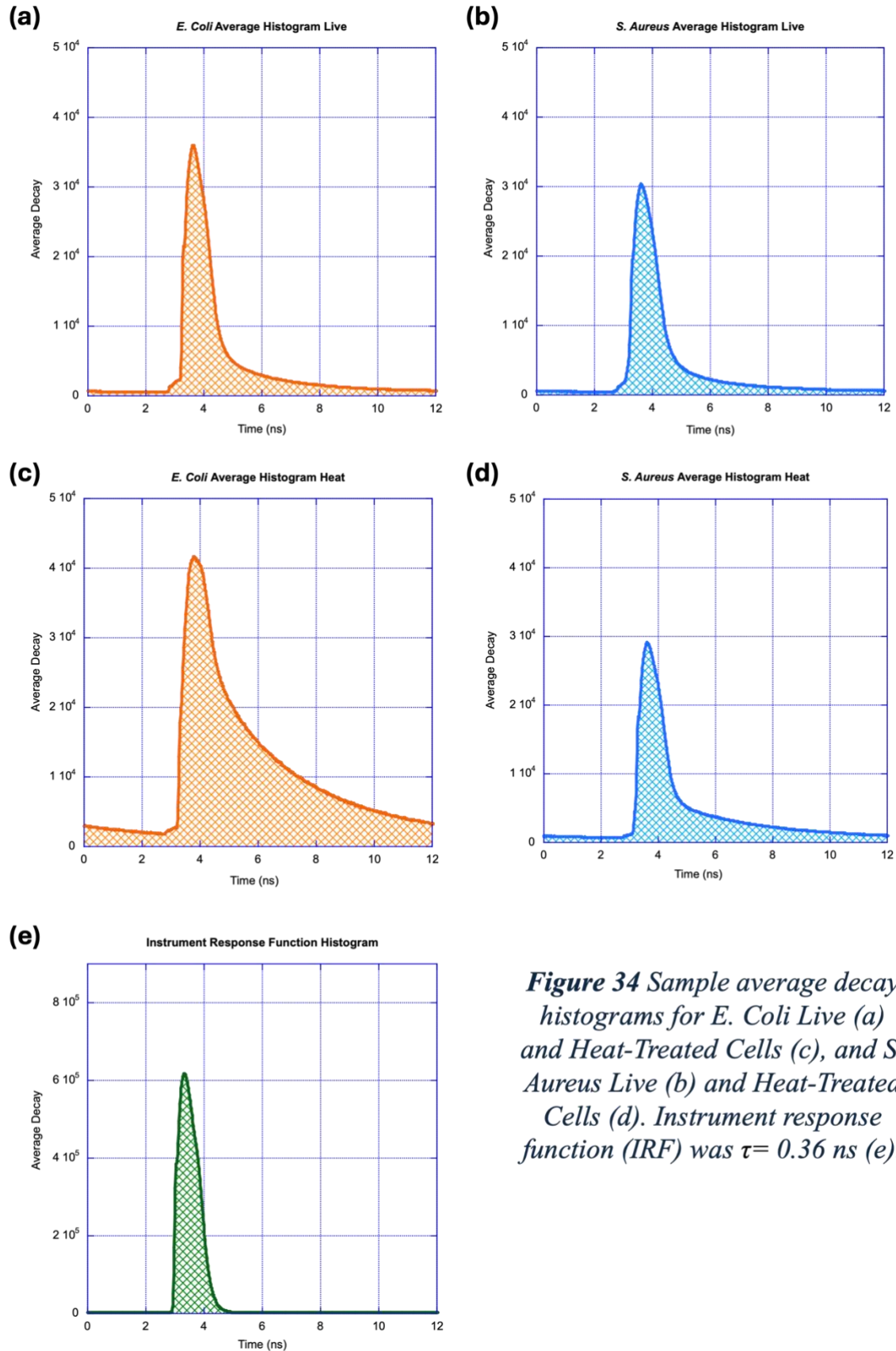


Figure 34 Sample average decay histograms for *E. Coli* Live (a) and Heat-Treated Cells (c), and *S. Aureus* Live (b) and Heat-Treated Cells (d). Instrument response function (IRF) was $\tau = 0.36$ ns (e).

Averages for sample histograms in **Figure 34** are taken from all ten areas of interest chosen for each sample, and lifetimes are reflected in **Figure 32** and **Figure 33**. All other histograms available in the Annex (**Figure 53**).

As stated before, exposure to either physical or chemical stressors can induce biological mechanisms for cellular inactivation. Biological cellular inactivation mechanisms include apoptosis, necrosis, autophagy, immune cell mediated inactivation, phagocytosis, viral infection, and senescence. All the above mechanisms except lysis and apoptosis were outside the scope of our research, so will not be discussed. Lysis is the opening of the cellular membrane due to external factors, such as osmotic pressure, physical damage, or infection²⁰. It is known that exposure to isopropanol causes lysis⁴⁴. Apoptosis is preprogrammed cellular destruction. It can be initiated by cellular stress or DNA damage, and causes cell shrinkage, chromatic condensation, membrane blebbing, and the formation of apoptotic bodies. These apoptotic bodies are then engulfed by phagocytes without spilling their intracellular contents, due to apoptosis being an anti-inflammatory response²¹. Apoptosis is known to be triggered by ROS exposure⁴⁵, which can occur under UVC irradiation as well as irradiated TiO₂ exposure. Based on the above information, we can assume that lysis-induced cell inactivation can be measured by PicoGreen fluorescence, but that apoptosis-induced cell inactivation is inconsistent in its response to the PicoGreen assay.

4.0 DISCUSSION

4.1 Optical Density Growth Assay

High throughput experiments are difficult in biological assays and, like plating, are often labour intensive. Despite this challenge, it is important to develop high throughput screening tests to quickly test conditions for initial proof of concept. The optical density growth assay was chosen for its high throughput capabilities, and low labour time. While current methods of bacterial quantification typically run less than five samples at once, the growth assay run in a 96-wellplate allowed us to study up to 32 conditions simultaneously with each condition in triplicate.

We observed a trend of *S. Aureus* fluorescing more brightly than *E. Coli* at the equivalent concentrations. This can be explained by the higher presence of extracellular DNA on *S. Aureus* compared to *E. Coli*. While both *E. Coli* and *S. Aureus* release DNA upon lysis, *S. Aureus* typically releases more extracellular DNA, owing to its Gram-positive structure and greater dependence on extracellular DNA for biofilm stability. *E. Coli*, as a Gram-negative bacterium, retains more DNA intracellularly due to its outer membrane barrier⁴⁶.

The assay was effective in determining the bacterial inactivation of *E. Coli* to be 99.9% and *S. Aureus* to be 65.9% after 180 minutes of batch exposure to target experimental conditions of bTiO₂ and white light. All controls demonstrated bacterial increase of up to 250%, indicating the control conditions did not kill the bacteria but that they instead grew while under 37 °C incubation. Additionally, this shows that the DL-Lactate media was only bacteriostatic at room temperature. Only the target experimental conditions demonstrated any bacterial inactivation, although this only had a significant impact after 60 minutes for *E. Coli* and 180 minutes for *S.*

Aureus. The observed lag time was likely due to experimental setup, where a small strip of catalyst was swirled in solution.

This batch setup allowed only a small portion of the working bacterial solution to be in proximity to the catalyst at a given time. The lifetimes of most ROS are nanoseconds to milliseconds⁴⁷, meaning they travel a maximum amount of a couple hundred nanometres in aqueous media before reacting or being quenched. This limits their antibacterial capabilities to cells within a few hundred nanometres to the catalyst, making batch tests a poor choice for thorough explorations of bactericidal properties of catalysts.

The method of stirring also had an impact on the measured antimicrobial properties of bTiO₂. Oscillation of the entire Erlenmeyer flask was chosen over a stir bar due to the mechanical properties of bTiO₂ and of GF by itself. According to unpublished flow studies performed by N. Rutajoga, a PhD student in the Scaiano Lab, bTiO₂ is stable in suspension for up to a year, but the glass filter support is susceptible to damage or structural failure upon impact. Glass filter alone is even more fragile in solution, with fibre debris leaching observed visually even under oscillation. This limited the amount of stirring possible in solution, which allowed for potential inhomogeneity while we took aliquots. The assay demonstrated that bacterial inactivation was not observed in the earlier aliquots due to an uneven distribution of inactivated bacteria throughout the solution. Consequently, aliquots taken at these earlier time points may have contained a disproportionate number of viable bacteria, leading to results that were not representative of the overall bacterial population in the solution.

The main disadvantage of the growth assay was the 16-hour growth time. Current standard methods for bacterial quantification (total coliform tests or colony counting) require at least 14

hours of incubation to yield results. The growth assay, while much higher throughput, had a similar incubation time to standard methods.

The optical density growth assay improved upon current methods and served as a useful starting point for evaluating the antimicrobial properties of bTiO₂ under white light. However, there was still potential for optimization, especially considering the urgent need to address water purification challenges efficiently.

4.2 SEM Images

SEM images were captured as a visual and qualitative method to assess bacterial settling. All catalyst strips used for imaging were freshly prepared to minimize contamination. If left unchecked, settled bacteria tend to form biofilms, which could potentially deactivate the bTiO₂ catalyst. While biofilm formation falls outside the scope of this thesis, the SEM analysis provided insight into the advantages of flow systems over batch systems, with the aim of preventing bacterial settling.

The images captured showed bacteria generally settled on the flat surfaces of the bTiO₂ structure. They also demonstrated that with even one manual rinse, the bacteria present on the catalyst decreased significantly. Due to the limited number of SEM images, we could not quantify the decrease in bacterial settling. This said, after 1.5 hours oscillating in solution and one rinse with Milli-Q water there were no observable bacteria left on the catalyst surface. After 3 hours in solution and a rinse clusters of bacteria were significantly reduced. Flow was therefore chosen over batch to minimize bacterial settling.

4.3 Fluorescent Dyes

The fluorescence assay was developed to provide a faster, more accessible, and less labour intensive method for measuring bacterial inactivation. These goals were largely achieved, despite some limitations. Fluorescence testing is significantly faster than standard methods, requiring only 10 minutes of incubation compared to the traditional 14–16 hours. The cost per sample was reasonable, totaling \$1.88 when using PicoGreen, the most effective dye tested. Additionally, the assay is straightforward to perform, requiring no specialized training or expensive equipment like flow cytometers. It also reduces labour by eliminating the need to plate multiple dilutions of bacterial solutions. **Figure 35** illustrates the factors considered when dyes were being tested. Ultimately, PicoGreen was selected as the best dye, due to its sensitivity and relative safety.

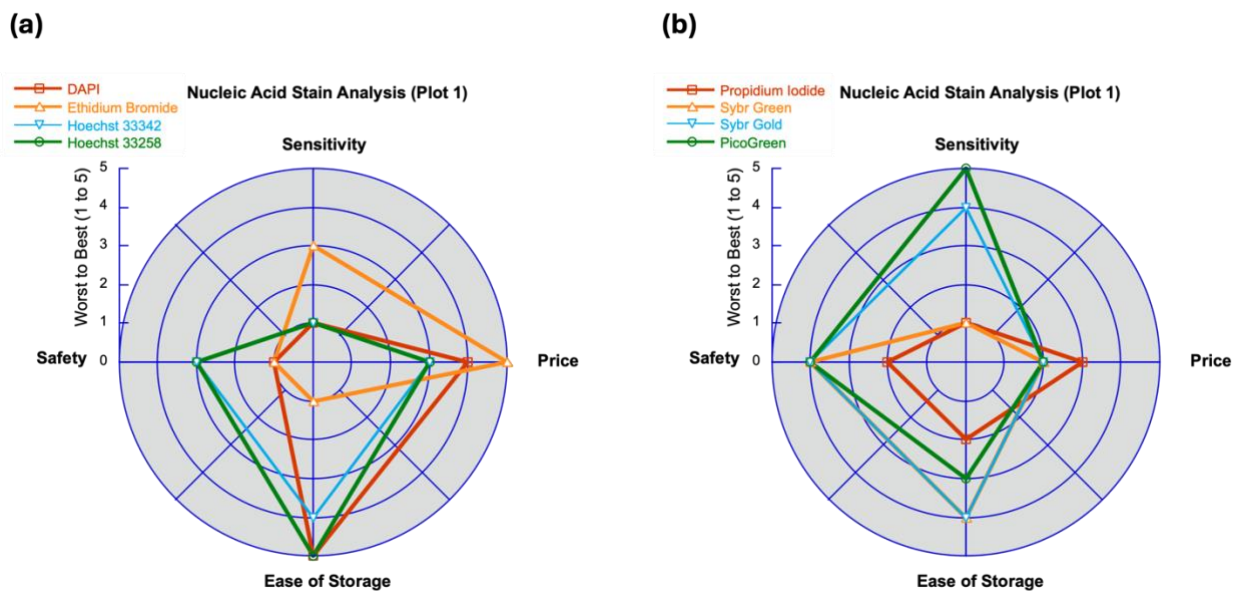


*Figure 35 Radar plots with decision factors for dye selection. Factors include Price (information sourced from Sigma Aldrich), Sensitivity (found using normalized RFU, **Figure 23**), Ease of Storage, and Safety (toxicity, temperature, and light conditions located on MSDS sheet, Sigma Aldrich). Plotted with Kaleidagraph v5.0.*

Fluorescence changes were quantified in relative fluorescence units (RFU). For each triplicate, the average RFU value was normalized to the RFU of the 0% dead cell control and subsequently baseline-corrected to account for background fluorescence. Dyes with a normalized fluorescence change of less than one were considered insufficiently fluorescent to detect low concentrations of bacteria. As a result, only Sybr Gold and PicoGreen were identified as viable options for the assay (**Figure 23**). PicoGreen was selected over Sybr Gold due to its high sensitivity with *S. Aureus* (**Figure 35**). This enabled us to further reduce the concentration of *S. Aureus* from 2.4×10^6 CFU/mL to 4.8×10^5 CFU/mL (or OD₆₀₀ 0.003) in subsequent assays, bringing it closer to the bacterial concentrations typically found in real river water¹⁶. The sensitivity limit of PicoGreen with *E. Coli* was found to be 2.4×10^6 CFU/mL or OD₆₀₀ 0.003. Later experiments were all performed with an OD₆₀₀ of 0.003-0.006 for both *E. Coli* and *S. Aureus*.

4.4 Fluorescence Tests for Batch Experiments

Batch tests with PicoGreen were conducted on *E. Coli* and *S. Aureus* with a small strip of bTiO₂ in 30 mL of working DL Lactate solution. The percent bacterial inactivation was then verified using plating and colony counting. PicoGreen assay demonstrated an increase in percent inactivation with longer exposure times up to 180 minutes. *E. Coli* was inactivated up to 27.2 % at 180 minutes. *S. Aureus* was inactivated up to 25.6 % at 80 minutes and 23.9 % at 180 minutes, where inactivation remained between 22.7 % and 25.6 % after 40 minutes exposure to bTiO₂ and white LED light. This plateau was also observed in later PicoGreen flow tests with both *E. Coli* and *S. Aureus* without added air or oxygen.

Colony counting tests demonstrated a consistent increase in bacterial inactivation over the course of the exposure to the working conditions for both *E. Coli* and *S. Aureus*. The highest

inactivation was seen at 180 minutes of exposure with *E. Coli* showing 32.2 % and *S. Aureus* showing 40.6 % inactivation. The discrepancy between PicoGreen and colony counting inactivation was seen in experimental conditions but not under control conditions, which demonstrated less than 20% bacterial inactivation in both PicoGreen and colony counting tests. This discrepancy has not fully explored at this point in the research but will be addressed in section 4.6 .

We hypothesized that the plateau observed with *S. aureus* and PicoGreen was caused by insufficient contact between the bacteria and the catalyst. To address this, flow tests were introduced.

4.5 Fluorescence Tests for Flow Experiments (Flow 1.0, 2.0, and 3.0)

Flow tests 1.0 and 2.0 were run without added air or oxygen to explore the theory that increased contact with the catalyst would heighten inactivation of the bacteria. Flow 1.0 was set up as a proof-of-concept, with a glass tube and connective silicone tubing (**Figure 8**). The solution was flowed at 6.00 mL/min with recycled flow, meaning solution was returned to the beaker after passing through the tube. Aliquots were taken from the working solution beaker at three-minute intervals up to 30 minutes. The beaker was exposed to ambient air.

Using PicoGreen, *E. Coli* exhibited a maximum inactivation of 36.7% at 27 minutes of flow, while *S. Aureus* reached a maximum inactivation of 32.1% at 21 minutes of flow. The first aliquot of *S. Aureus*, which showed 52.5% inactivation, was excluded due to experimental error. These results indicated a modest increase in bacterial inactivation compared to batch tests.

Colony counting showed a percent inactivation of 44.8 % for *E. Coli* and 48.1 % for *S. Aureus*, both increases from the batch tests.

Flow 2.0 involved some systemic changes. The tube used was switched to a quartz tube with rubber septum to allow for addition of gas in Flow 3.0 testing. The lamp was also replaced for the 'tent lamp' setup (**Figure 9**), which had two lamps arranged 5-7 cm from the tube. This increased visible irradiation (W/m^2) by a factor of 3.4. While not quantified, previous studies have demonstrated higher photochemical activity of bTiO_2 with increased irradiation³. Due to the end goal of water purification, single pass flow was preferred over recycled flow, therefore aliquots were taken directly from the exit of the system.

Flow experiments were conducted at three flow rates, corresponding to residence times of 15, 30, and 60 minutes. At a 15-minute residence time, the maximum inactivation was 29.2% for *E. Coli* and 24.9% for *S. Aureus*. For a 30-minute residence time, maximum inactivation increased to 74.4% for *E. Coli* and 68.8% for *S. Aureus*. Similarly, at a 60-minute residence time, maximum inactivation was 73.2% for *E. Coli* and 68.8% for *S. Aureus*. These results suggest that *E. Coli* and *S. Aureus* exhibit comparable responses to reactive oxygen species (ROS) under these conditions.

Under Flow 2.0 conditions, particularly with the longer 30-minute residence time experiments, the plateau became very noticeable. *E. Coli* inactivation decreased after the first aliquot and settling between 40-57 % and *S. Aureus* inactivation settled between 28-54 %. Besides the initial aliquot, this remained true for the entirety of the following 180-minute flowed. Due to the air present with the first aliquot but not subsequent ones, the plateau was believed to be caused by a reduction in the rate of ROS generation over time. We also considered that the flow may still be

too laminar, not allowing enough interaction between the bacteria and the catalyst for significant impact of ROS on the cells prior to being quenched.

With this observation, Flow 3.0 was born. Gas was added through the rubber septum at the bottom of the tube and flowed in small bubbles up the catalyst. This added more turbulence to the flow, as well as providing more oxygen for ROS creation by the bTiO₂.

To our surprise, the addition of air did not result in an increase in PicoGreen measured inactivation. Instead, it showed a marked decrease, with *E. Coli* having a maximum inactivation of 15.2 % after flowing for 60 minutes. *S. Aureus* showed similar trends, with a maximum of 28.5 % inactivation. This, when compared to the 80-93 % inactivation seen with colony counting, raised suspicions about the PicoGreen assay.

Adding pure oxygen to the flow, while better than just air, showed a maximum inactivation of 99.7 % for *E. Coli* and 53.4 % with *S. Aureus*. While the *E. Coli* increased dramatically in inactivation, *S. Aureus* showed less inactivation with oxygen than it did without any gas at all. When compared to the colony counting assay, *E. Coli* achieved 99.8 % inactivation and *S. Aureus* achieved 98.5 %.

It was demonstrated that our optimization was successful, with the bTiO₂ system achieving bacterial inactivation of up to two log units within 30 minutes of exposure. While the calibration curves and dye tests with PicoGreen had shown a high degree of reliability, discrepancies emerged between the results of the PicoGreen assay and colony counting under all working conditions. These inconsistencies became more pronounced with the introduction of gas into the system. A false positive, which would indicate an overestimation of bacterial inactivation, could lead to disastrous consequences, such as the premature validation of ineffective water treatment,

posing risks to health and safety. Conversely, a false negative, while undesirable, merely underscores the need for further optimization without endangering the integrity of the disinfection process. PicoGreen demonstrated false negative results, never overestimating the bacterial inactivation. Despite this, the irregularities still raised concerns about the fidelity of the PicoGreen assay, prompting further investigation using fluorescence lifetime imaging microscopy (FLIM).

4.6 Fluorescence Lifetime Imaging Microscopy (FLIM) Tests

The combination of white light images and fluorescent microscopy images can give a great indicator of fluorophore behavior. FLIM was performed on *E. Coli* and *S. Aureus* cells under the following conditions: live, UVC irradiated, exposed to experimental conditions, heat, and isopropanol. As cells die their membrane can open and DNA is released. Based on the mechanism of cell death the released DNA is either intact or can be further fragmented. Generally, longer fluorescence lifetimes can indicate a few things; cell lysis and the release of genetic material can increase fluorescent lifetimes of DNA intercalating dyes. Lysis also implies damage to the cellular membrane proteins, which when intact, are known to quench fluorophores⁴⁸. Therefore, as they are damaged (either by heat, detergent, or ROS) the fluorophore lifetime increases, as demonstrated by our control experiments.

Cells that were live showed the least number of fluorescent cells to cells present, which makes sense since their membranes are still intact, and the surrounding extracellular proteins are known to quench fluorescence⁴⁷. Fluorescence from live cells comes from their extracellular DNA, which is present on both strains of bacteria used, but in much smaller quantities than the DNA inside the cell. Intact proteins and extracellular matrix material can quench fluorophores

intercalated to extracellular DNA, leading to shorter lifetimes⁴⁸. Overall, live cells had average PicoGreen Fluorescence lifetimes of $\tau_{avg}= 1.28$ ns for *E. Coli* and $\tau_{avg}= 1.29$ ns for *S. Aureus*.

Isopropanol and heat demonstrated the highest degree of fluorescence to cells present.

Isopropanol causes lysis. This impacts the cellular membrane but not the internal components of the cell, leaving DNA intact for dye intercalation. FLIM results corroborated this by showing most cells present in the frame fluorescing with PicoGreen. Cells that were heated could experience lysis-like cell death involving degradation of the cellular membrane or cytoplasm, protein denaturing, and agglomeration⁴⁹. What was *not* seen with one minute heat shock, was significant DNA degradation. This allowed PicoGreen molecules to intercalate to all released DNA and fluoresce brightly and from all cell agglomerations seen under white light.

UVC irradiation - much like bTiO₂, oxygen, and white light exposure - promotes ROS formation, effectively inactivating cells. ROS are highly cytotoxic and cause damage to a variety of cellular components. Lipid peroxidation damages the membrane of the cell, protein oxidation damages amino acids causing enzymatic disruption, and oxidative stress response overload can lead to cellular collapse. Most importantly, extensive exposure to ROS causes DNA damage via fragmentation in an apoptosis-like effect⁵⁰. ROS can also damage cells up to an hour after exposure due to internal ROS multiplication and post-stress bacterial death⁵¹. Cells with fragmented DNA are inactive but may not intercalate fluorescent dyes as well as those with intact DNA. A decrease in PicoGreen intercalation leads to a less expressive fluorophore, and if DNA fragmentation is inconsistent then fluorescent results can become inconsistent.

The fluorescence lifetimes of PicoGreen under different cell death conditions provide insights into the behavior of DNA in each sample. For UVC-irradiated cells, lifetimes were measured at

$\tau_{\text{avg}} = 3.24$ ns for *E. Coli* and $\tau_{\text{avg}} = 3.13$ ns for *S. Aureus*—significantly longer than those observed under reaction conditions, which were $\tau_{\text{avg}} = 1.15$ ns for *E. Coli* and $\tau_{\text{avg}} = 1.10$ ns for *S. Aureus*.

This contrast suggests either varying extents of DNA damage or UVC-induced dimerization of neighboring cyclobutane pyrimidines⁵². Further investigation is required to fully understand the differences in fluorescence lifetimes between these two mechanisms of cell death.

Cells exposed to lysis-inducing treatments, such as isopropanol or heat, exhibited similar fluorescence lifetimes. Specifically, isopropanol-treated cells demonstrated lifetimes of $\tau_{\text{avg}} = 2.17$ ns for *E. Coli* and $\tau_{\text{avg}} = 2.18$ ns for *S. Aureus*. In comparison, heat-shocked cells displayed lifetimes of $\tau_{\text{avg}} = 2.83$ ns for *E. Coli* and $\tau_{\text{avg}} = 2.61$ ns for *S. Aureus*. Additionally, A paired ttest was performed to compare the bacterial viability of *E. Coli* and *S. Aureus* under identical experimental conditions. The mean values for *E. Coli* and *S. Aureus* were 2.044 and 2.062, respectively, with no statistically significant difference observed ($t = -0.313$, $p = 0.770$). These findings suggest that the experimental conditions affected both bacterial species similarly. There was also high correlation between the groups ($r = 0.989$, $p = 0.0014$). These comparable fluorescence lifetimes, along with paired T-Test results, reinforce the conclusion that both heat and isopropanol act as effective lysis-inducing agents, and that both gram-positive and gram-negative bacterium are impacted similarly by our experimental conditions (bTiO₂ and white light).

5.0 CONCLUSIONS

Bacterial inactivation of *E. Coli* and *S. Aureus* was tested under batch conditions and three variations of flow systems. A novel PicoGreen fluorescence viability assay was developed to quantify bacterial inactivation across all experiments. This assay proved to be quick, simple, and cost-effective, with results verified in part by plating and colony counting.

Overall, bacterial inactivation using bTiO₂ was successful, with the highest inactivation achieved during Flow 3.0 tests when oxygen bubbles were introduced. *E. Coli* showed up to 99.9% inactivation, surpassing the WHO threshold for bactericidal processes (99% inactivation within 30 minutes¹), while *S. Aureus* reached 98.5%, falling just 0.5% short.

However, a notable trend emerged: as ROS generation and bacterial inactivation became more optimized, the PicoGreen assay's precision decreased. For instance, during Flow 3.0 with air, plating results indicated upwards of 80% inactivation for both bacterial strains, whereas the PicoGreen assay reported less than 28% inactivation. This disparity was much smaller under batch conditions, where *E. Coli* showed a maximum inactivation of 27.7% with PicoGreen compared to 32.2% with colony counting. Similarly, *S. Aureus* demonstrated a maximum inactivation of 25.6% with PicoGreen versus 40.6% with colony counting. While PicoGreen has been shown to produce false negatives under certain conditions, it has never yielded false positives, ensuring that bacterial inactivation is not overestimated. This makes it a promising method for further investigation, as false positives could compromise disinfection validation, whereas false negatives merely indicate the need for further optimization.

FLIM results provided further insights, showing that cells exposed to bTiO₂, oxygen, and white light fluoresced with shorter lifetimes and fewer fluorescent cells per image compared to other

inactivation methods. This suggests that while the PicoGreen assay reliably measures lysis, results become compromised when cells are inactivated through processes like apoptosis or DNA damage. Notably, this limitation has not been previously reported in the scientific literature, where PicoGreen has typically been viewed as a universal solution for cell quantification regardless of the inactivation mechanism.

Future research should explore both PicoGreen assay optimization and alternative dyes for fluorescence assays to improve sensitivity across different inactivation mechanisms. Testing all currently available dyes against various bacterial inactivation pathways, including lysis, apoptosis, and oxidative stress, would provide a comprehensive understanding of their efficacy. As an alternative use, PicoGreen could be applied to future research to quickly differentiate between lysed versus apoptotic cells. Additionally, optimizing the flow system to reduce inactivation delays and studying biofilm formation under extended operational conditions could further enhance the practical application of bTiO_2 in water purification technologies.

A particular focus should be placed on addressing boil water advisories in northern Canada, where collaboration with Indigenous communities is essential to ensure solutions meet their specific needs. Involving engineers in developing sustainable water purification systems is crucial, particularly when considering material selection. Catalytic performance improvements should prioritize non-toxic, environmentally safe materials such as doped black TiO_2 with iron or copper, avoiding highly toxic elements. Additionally, LED-based solutions may offer more consistent efficacy than sunlight, making them a promising avenue for future development. Performance tests should be conducted on-site to ensure long-term effectiveness, prioritizing reliability over speed in real-world conditions.

Key Takeaways: Our novel photocatalyst, bTiO₂, combined with white light effectively kills both Gram-positive (*S. Aureus*) and Gram-negative (*E. Coli*) bacteria, particularly when ROS generation is enhanced by oxygen flow. The PicoGreen assay is a valuable alternative to traditional bacterial quantification methods for water quality assessment but is only reliable when cell inactivation does not involve extensive DNA damage.

6.0 APPENDIX

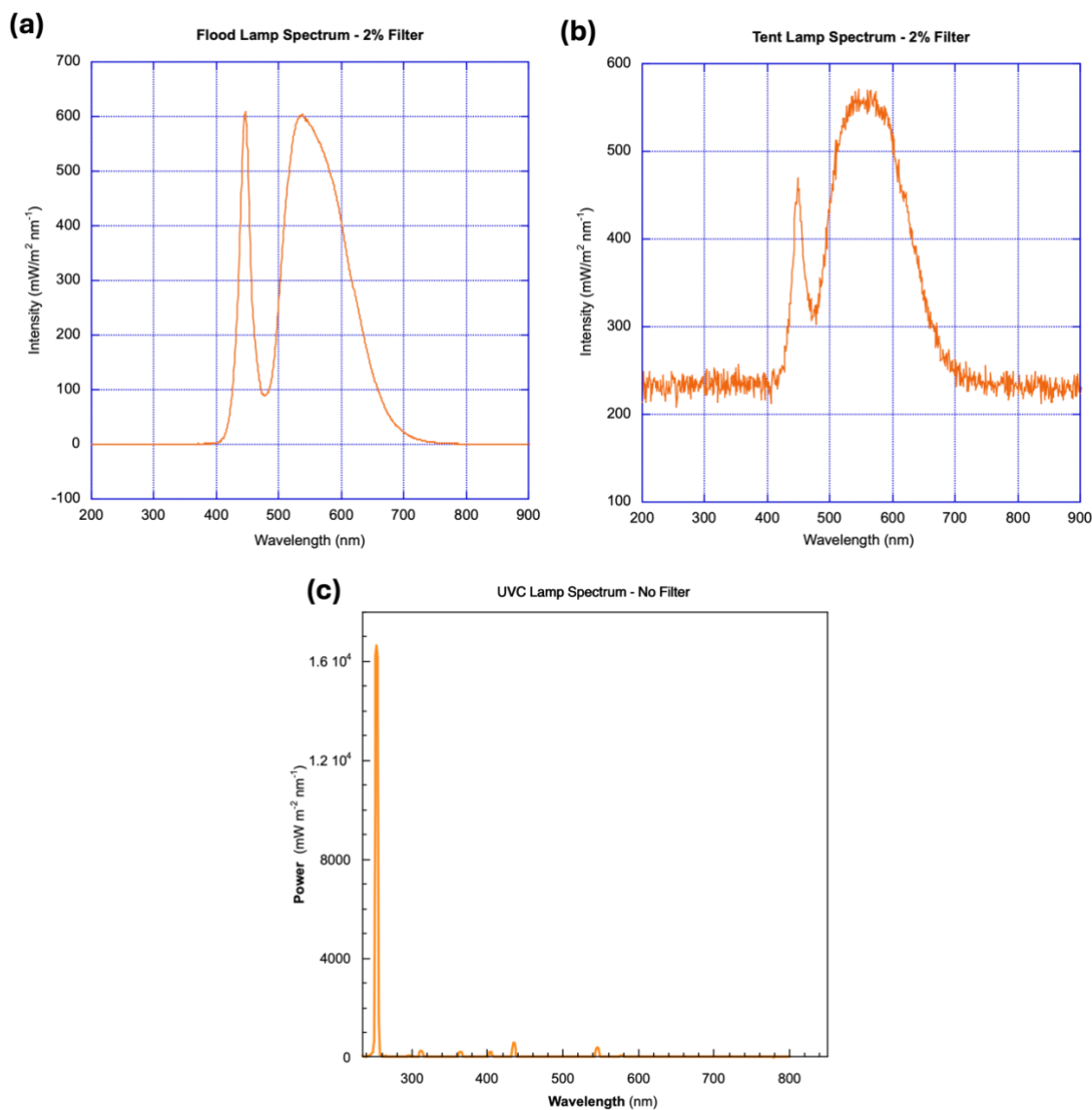


Figure 36 Intensity Spectra for 'Flood Lamp' (a) 'Tent Lamp' (b), and UVC lamp (c). Measured using LUZCHEM SPR-01-235-850nm Spectroradiometer. The 'Flood Lamp' was used for Growth Assay, Fluorescence Batch, and Fluorescence Flow 1.0 experiments. The bottom of the 'Tent Lamp' was coated with aluminum foil, and this setup was used for Fluorescence Flow 2.0 and 3.0 experiments. The UVC lamp was used exclusively for FLIM test cell inactivation at a distance of 5.0 cm, spectrum used was from Luzchem⁵³. A 2% filter was used to prevent overexposure for (a) and (b).

Figures 37 through 52 conform to methods in section **2.5 Optical Density Growth Assay**. The Optical Density Growth Assay measured the growth of *E. Coli* and *S. Aureus* exposed to bTiO₂

strips by graphing OD₆₀₀ over 8 hours. Bacteria (OD₆₀₀ 0.03) were exposed to bTiO₂ at room temperature for 5–180 minutes with oscillation. Aliquots were collected, stored in the dark, plated in triplicate on a 96-well plate, and incubated in a 37 °C plate reader with OD₆₀₀ measured every 20 minutes. Growth data were compared to calibration curves to assess bacterial viability. All control conditions shown below demonstrated no bacterial inactivation, instead demonstrating up to 250 % growth. It can therefore be determined that only the experimental conditions (bTiO₂ and white light) were effectively bactericidal.

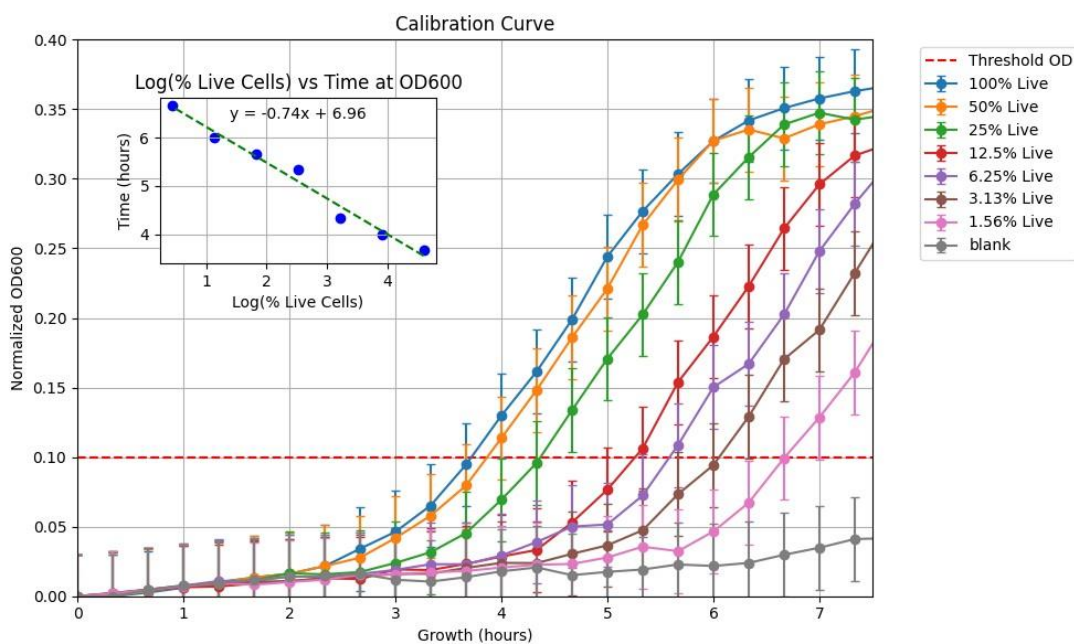


Figure 37 Growth Assay Calibration Curve Graph 3. OD₆₀₀ was monitored via wellplate reader over the course of 16 hours. *E. Coli* live cells (OD₆₀₀ 0.003) were diluted with dead cells (prepared as described in section 2.3 Bacteria Incubation and Preparation.) Longer lag times correspond to smaller fractions of live cells compared to dead cells. Inset datapoints refer to the time when each sample reaches the threshold value of OD₆₀₀ 0.1 versus the log(percent live cells). Inset trendlines were used to calculate the percent inactive bacteria for experimental and control conditions.

Figure 37 corresponds to **Figure 38** and **Figure 39** for growth assay with *E. Coli*, bTiO₂ exposure, in the dark, as well as *E. Coli*, glass filter, and white LED light (**Figure 36 (a)**). Inset refers to the time when each sample reaches the threshold value of OD₆₀₀ 0.1 versus the log(percent live cells).

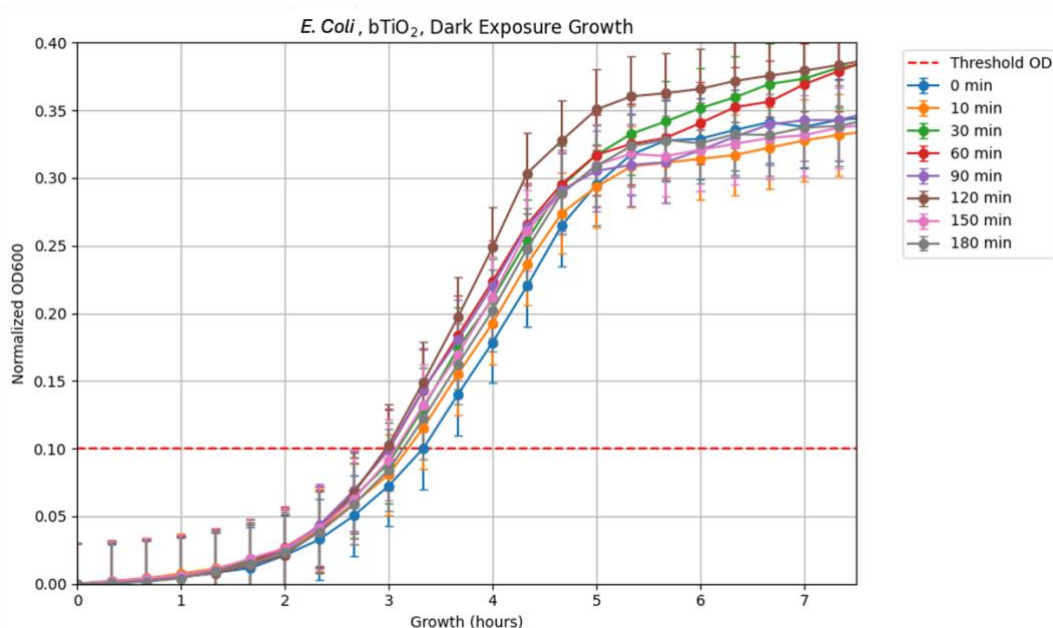


Figure 38 Growth assay results for *E. Coli* exposure to bTiO₂ under dark conditions. Aliquots were plated, incubate at 37°C, and OD₆₀₀ were read in a wellplate reader every 20 minutes for 16 hours. Datapoints after 8 hours show a plateau so were discarded. Times when each sample crossed the OD₆₀₀ threshold of 0.1 were noted and compared to the respective calibration curve to determine percent bacterial inactivation.

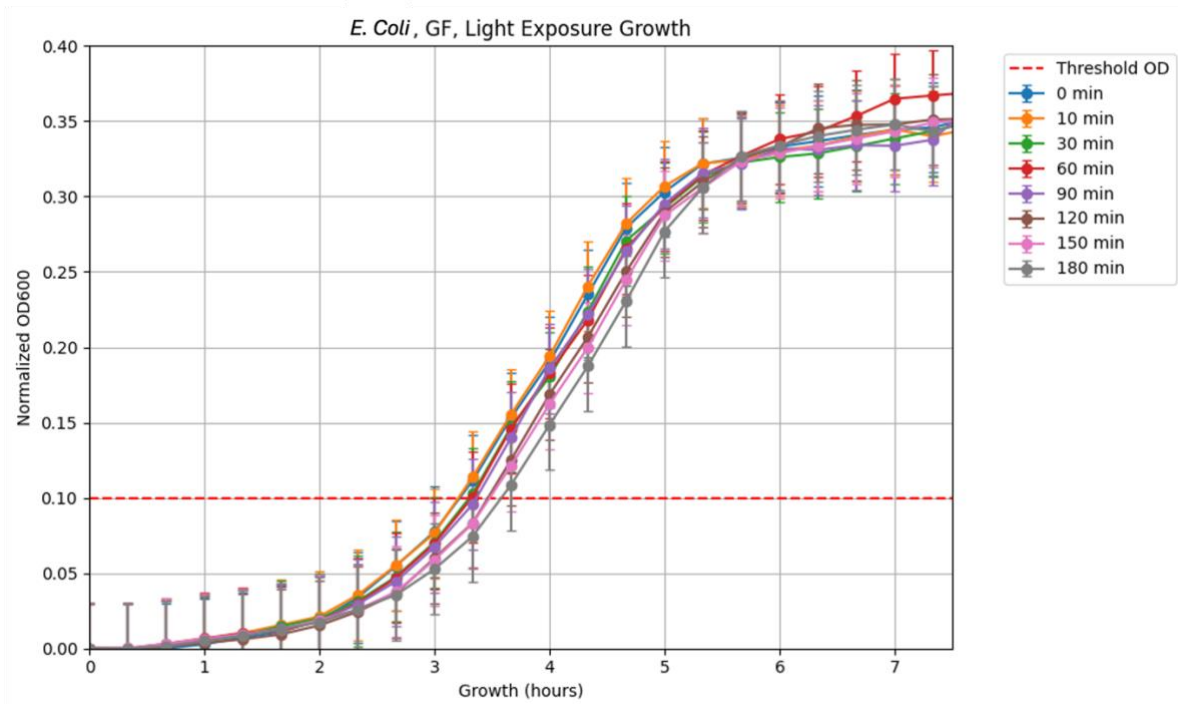


Figure 39 Growth assay results for *E. Coli* exposure to glass filter under white LED conditions (Figure 36 (a)). Aliquots were plated, incubate at 37°C, and OD₆₀₀ were read in a wellplate reader every 20 minutes for 16 hours. Datapoints after 8 hours show a plateau so were discarded. Times when each sample crossed the OD₆₀₀ threshold of 0.1 were noted and compared to the respective calibration curve to determine percent bacterial inactivation.

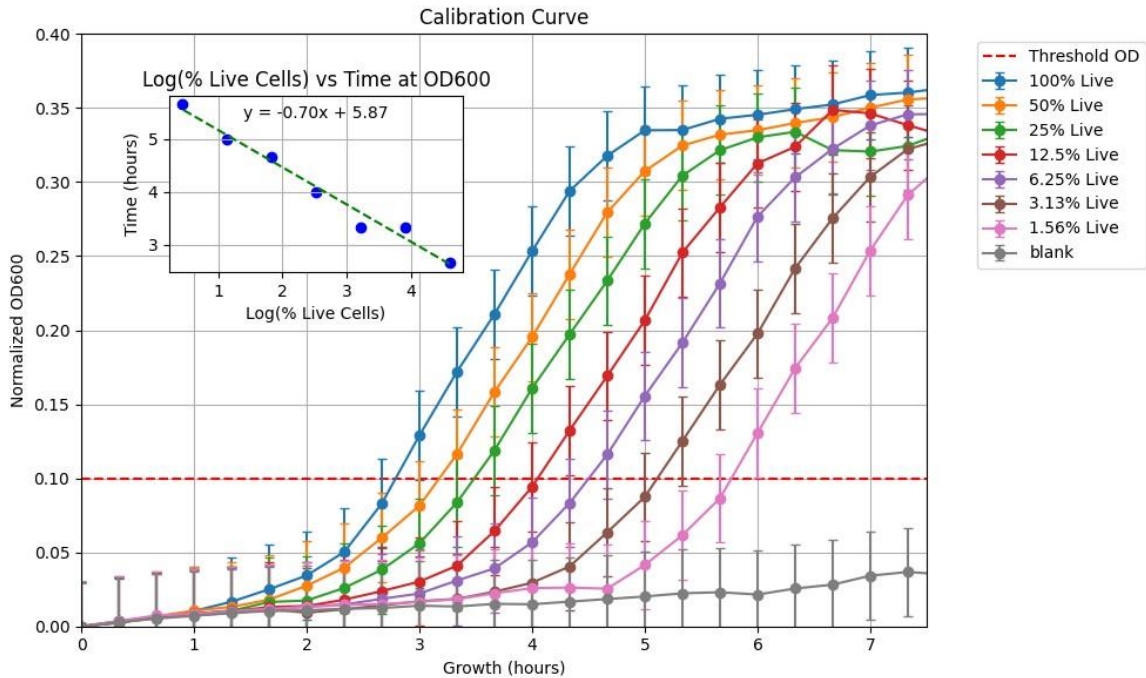


Figure 40 Growth Assay Calibration Curve Graph 4. OD_{600} was monitored via wellplate reader over the course of 16 hours. Data after 8 hours demonstrates a plateau, so was discarded. *E. Coli* live cells (OD_{600} 0.003) were diluted with dead cells (prepared as described in section 2.3 Bacteria Incubation and Preparation.) Longer lag times correspond to smaller fractions of live cells compared to dead cells. Inset datapoints refer to the time when each sample reaches the threshold value of OD_{600} 0.1 versus the log(percent live cells). Inset trendlines were used to calculate the percent inactive bacteria for experimental and control conditions.

Figure 40 corresponds to **Figure 41** and **Figure 42** for growth assay with *E. Coli*, no catalyst or glass filter, under white LED, as well as *E. Coli*, glass filter, under dark conditions. Inset refers to the time when each sample reaches the threshold value of OD_{600} 0.1 versus the log(percent live cells).

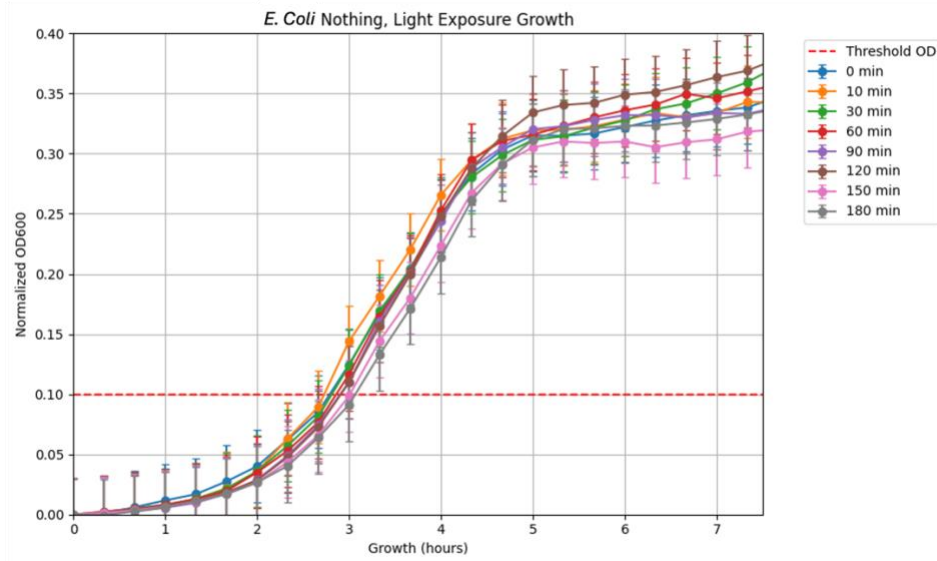


Figure 41 Growth assay results for *E. Coli* without catalyst or glass filter under white LED conditions (**Figure 36 (a)**). Aliquots were plated, incubate at 37°C, and OD₆₀₀ were read in a wellplate reader every 20 minutes for 16 hours. Datapoints after 8 hours show a plateau so were discarded. Times when each sample crossed the OD₆₀₀ threshold of 0.1 were noted and compared to the respective calibration curve to determine percent bacterial inactivation.

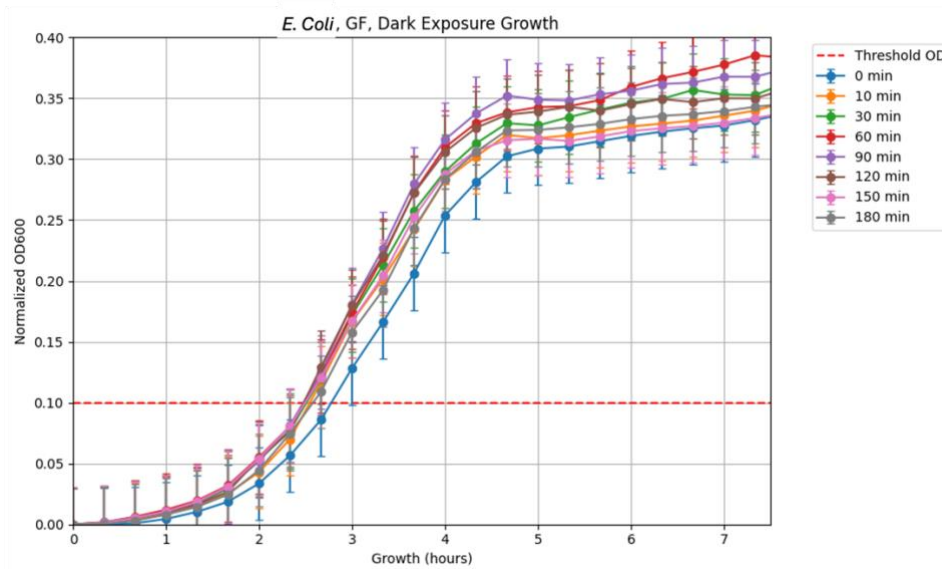


Figure 42 Growth assay results for *E. Coli* exposure to glass filter under dark conditions. Aliquots were plated, incubate at 37°C, and OD₆₀₀ were read in a wellplate reader every 20 minutes for 16 hours. Datapoints after 8 hours show a plateau so were discarded. Times when each sample crossed the OD₆₀₀ threshold of 0.1 were noted and compared to the respective calibration curve to determine percent bacterial inactivation.

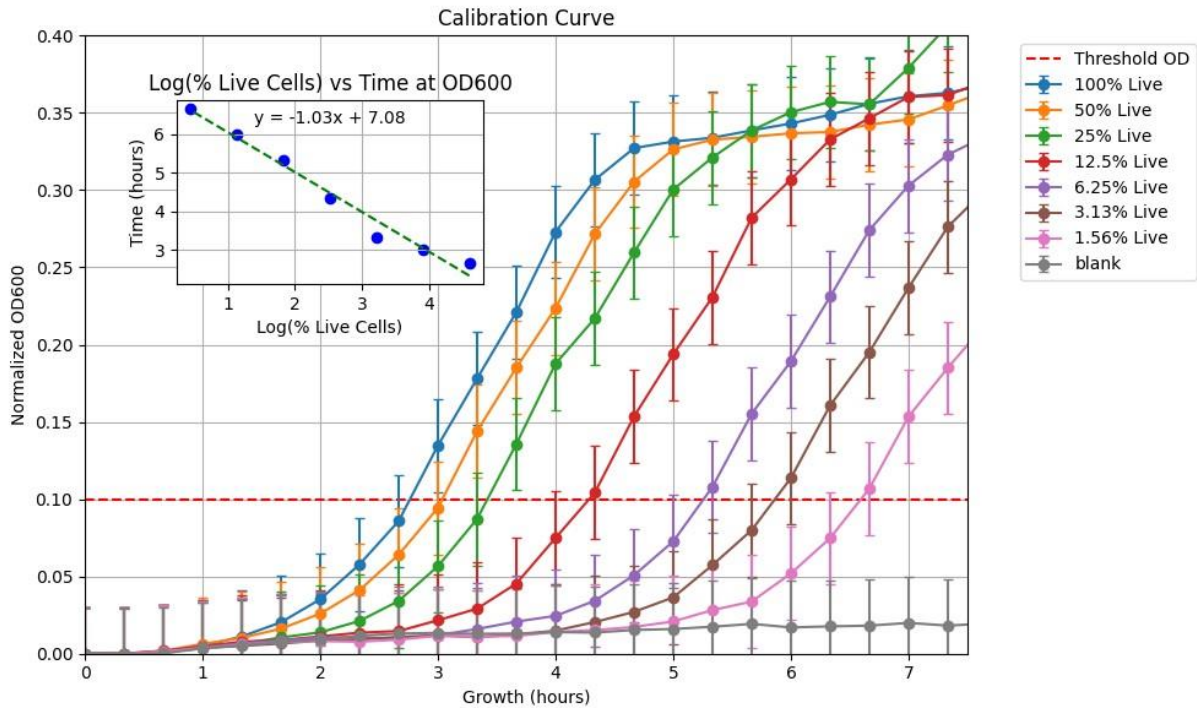


Figure 43 Growth Assay Calibration Curve Graph 5. OD_{600} was monitored via wellplate reader over the course of 16 hours. Data after 8 hours demonstrates a plateau, so was discarded. *E. Coli* live cells (OD_{600} 0.003) were diluted with dead cells (prepared as described in section 2.3 Bacteria Incubation and Preparation.) Longer lag times correspond to smaller fractions of live cells compared to dead cells. Inset datapoints refer to the time when each sample reaches the threshold value of OD_{600} 0.1 versus the log(percent live cells). Inset trendlines were used to calculate the percent inactive bacteria for experimental and control conditions.

Figure 43 corresponds to **Figure 44** for growth assay with *E. Coli*, no catalyst or glass filter, in the dark. Inset refers to the time when each sample reaches the threshold value of OD_{600} 0.1 versus the log(percent live cells).

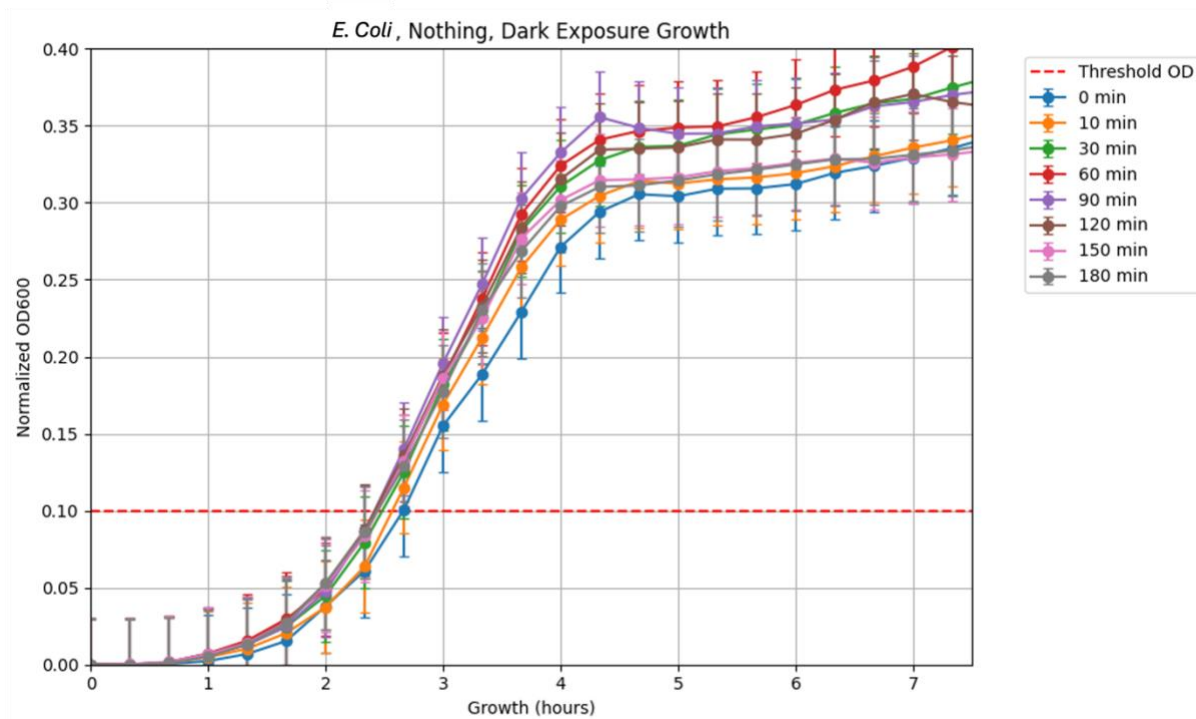


Figure 44 Growth assay results for *E. Coli* without catalyst or glass filter under dark conditions. Aliquots were plated, incubate at 37°C, and OD₆₀₀ were read in a wellplate reader every 20 minutes for 16 hours. Datapoints after 8 hours show a plateau so were discarded. Times when each sample crossed the OD₆₀₀ threshold of 0.1 were noted and compared to the respective calibration curve to determine percent bacterial inactivation.

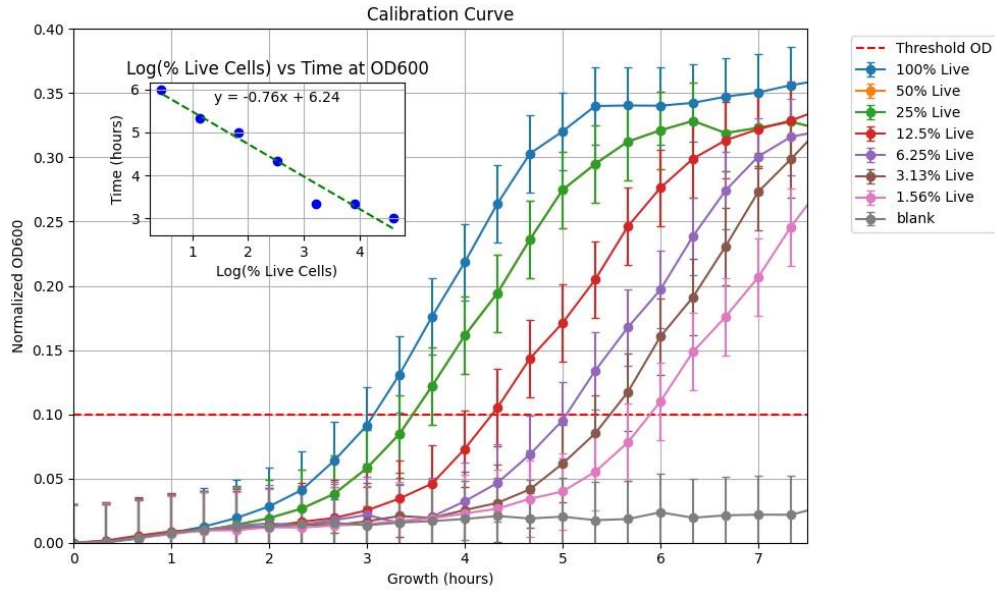


Figure 45 Growth Assay Calibration Curve Graph 6. OD_{600} was monitored via wellplate reader over the course of 16 hours. Data after 8 hours demonstrates a plateau, so was discarded. *S. Aureus* live cells (OD_{600} 0.003) were diluted with dead cells (prepared as described in section 2.3 Bacteria Incubation and Preparation.) Longer lag times correspond to smaller fractions of live cells compared to dead cells. Inset datapoints refer to the time when each sample reaches the threshold value of OD_{600} 0.1 versus the log(percent live cells). Inset trendlines were used to calculate the percent inactive bacteria for experimental and control conditions.

Figure 45 corresponds to **Figure 46** for growth assay with *S. Aureus*, glass filter, in the dark.

Inset refers to the time when each sample reaches the threshold value of OD_{600} 0.1 versus the log(percent live cells).

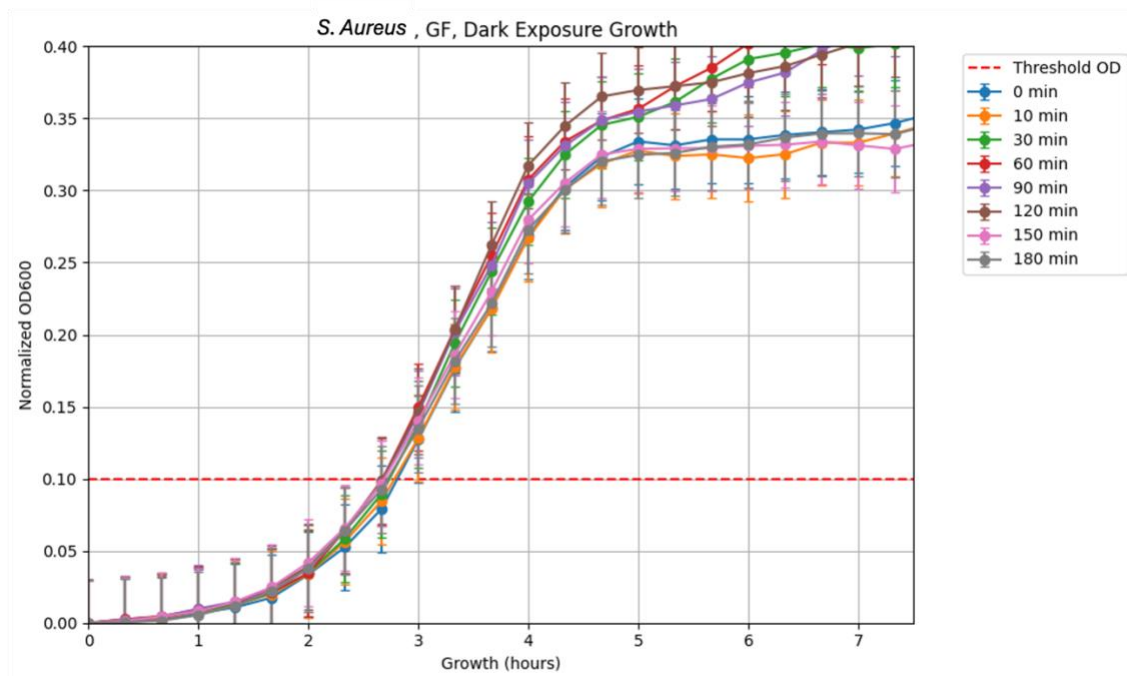


Figure 46 Growth assay results for *S. Aureus* exposure to glass filter under dark conditions. Aliquots were plated, incubate at 37°C, and OD₆₀₀ were read in a wellplate reader every 20 minutes for 16 hours. Datapoints after 8 hours show a plateau so were discarded. Times when each sample crossed the OD₆₀₀ threshold of 0.1 were noted and compared to the respective calibration curve to determine percent bacterial inactivation.

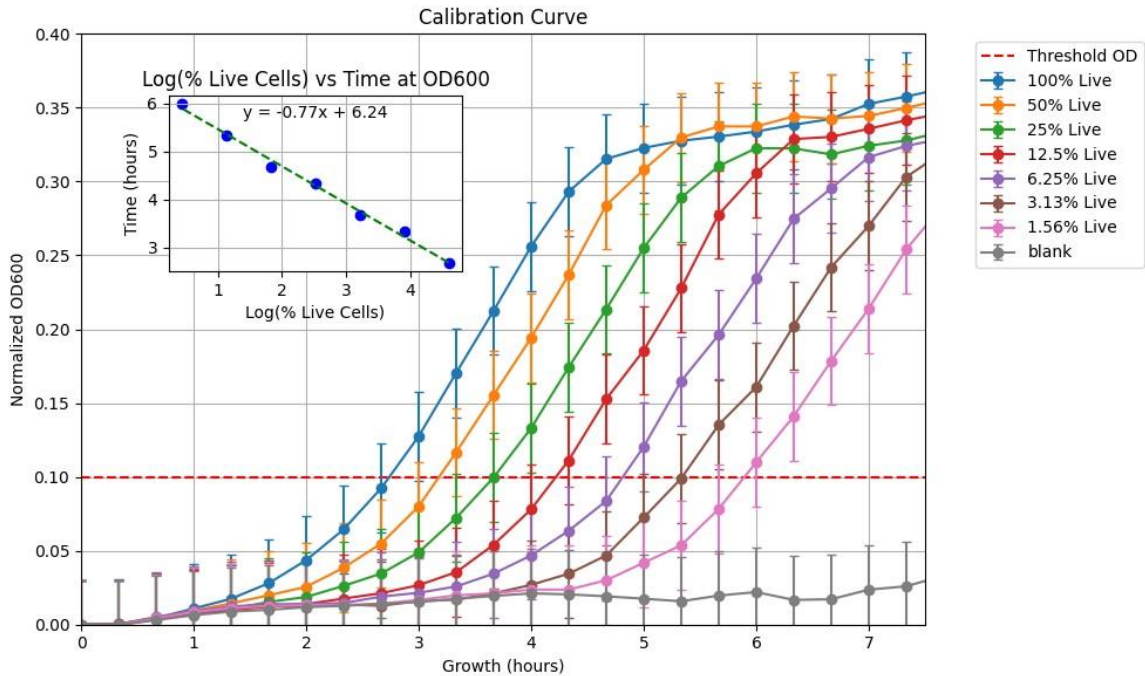


Figure 47 Growth Assay Calibration Curve Graph 7. OD_{600} was monitored via wellplate reader over the course of 16 hours. Data after 8 hours demonstrates a plateau, so was discarded. *S. Aureus* live cells (OD_{600} 0.003) were diluted with dead cells (prepared as described in section 2.3 Bacteria Incubation and Preparation.) Longer lag times correspond to smaller fractions of live cells compared to dead cells. Inset datapoints refer to the time when each sample reaches the threshold value of OD_{600} 0.1 versus the log(percent live cells). Inset trendlines were used to calculate the percent inactive bacteria for experimental and control conditions.

Figure 47 corresponds to **Figure 48** and **Figure 49** for growth assay with *S. Aureus*, bTiO₂, in the dark as well as with glass filter, under white LED illumination. Inset refers to the time when each sample reaches the threshold value of OD_{600} 0.1 versus the log(percent live cells).

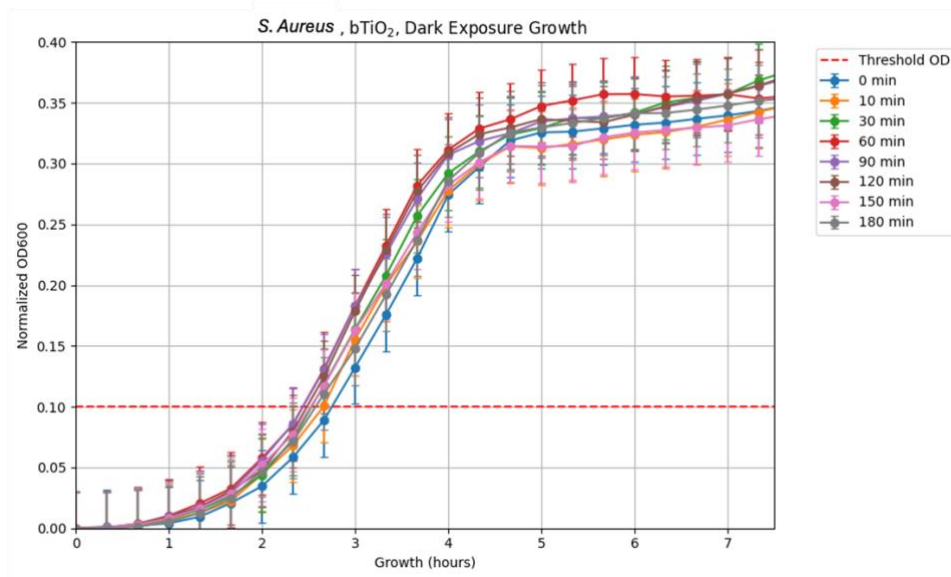


Figure 48 Growth assay results for *S. Aureus* exposure to $bTiO_2$ under dark conditions. Aliquots were plated, incubate at $37^\circ C$, and OD_{600} were read in a wellplate reader every 20 minutes for 16 hours. Datapoints after 8 hours show a plateau so were discarded. Times when each sample crossed the OD_{600} threshold of 0.1 were noted and compared to the respective calibration curve to determine percent bacterial inactivation.

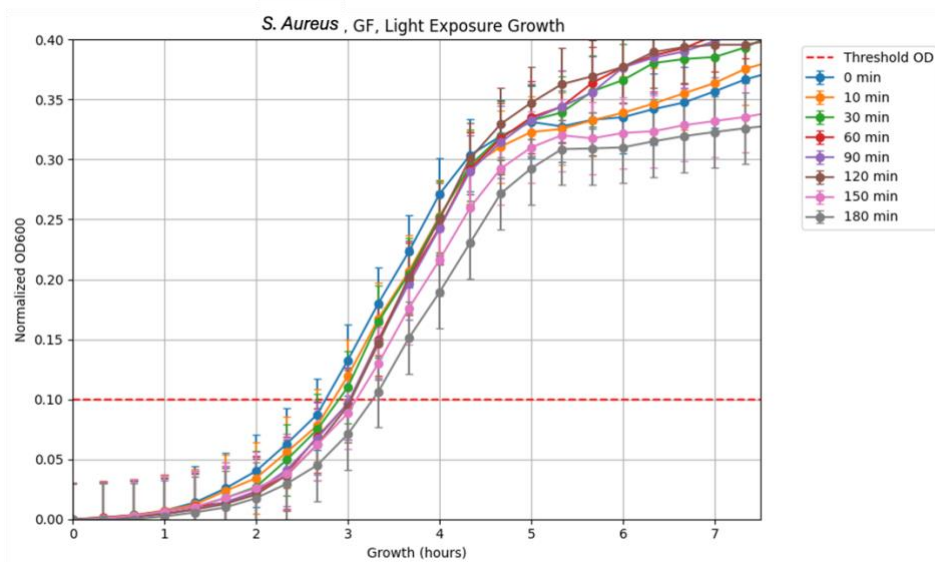


Figure 49 Growth assay results for *S. Aureus* exposure to glass filter under white LED conditions (**Figure 36 (a)**). Aliquots were plated, incubate at $37^\circ C$, and OD_{600} were read in a wellplate reader every 20 minutes for 16 hours. Datapoints after 8 hours show a plateau so were discarded. Times when each sample crossed the OD_{600} threshold of 0.1 were noted and compared to the respective calibration curve to determine percent bacterial inactivation.

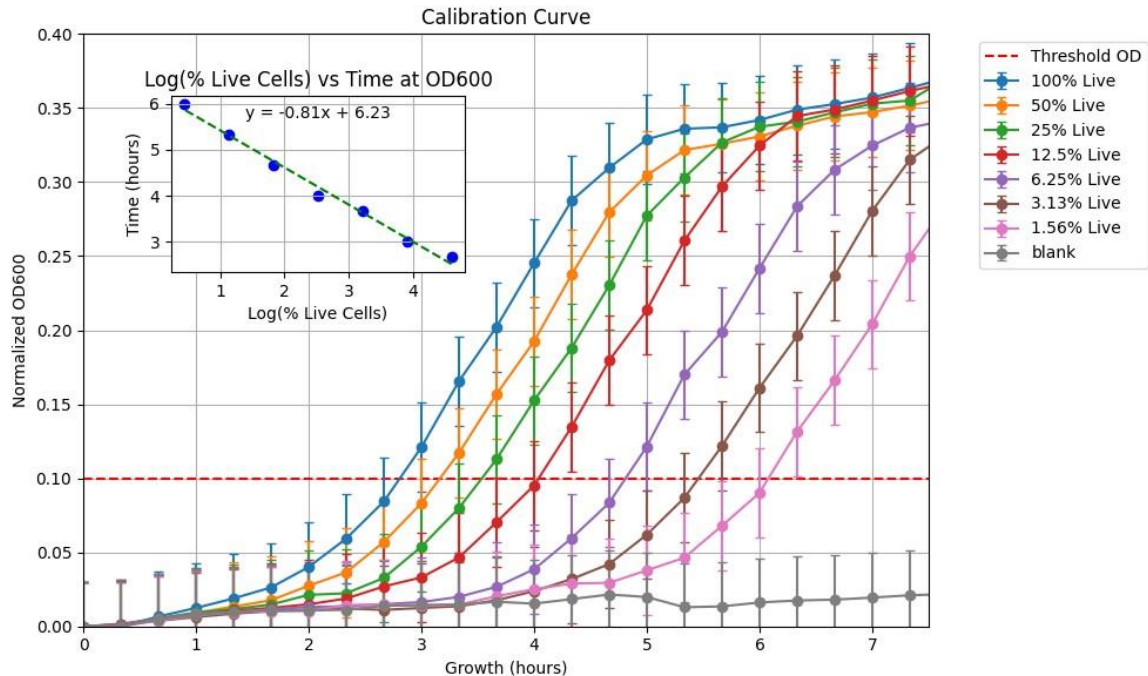


Figure 50 Growth Assay Calibration Curve Graph 8. OD_{600} was monitored via wellplate reader over the course of 16 hours. Data after 8 hours demonstrates a plateau, so was discarded. *S. Aureus* live cells (OD_{600} 0.003) were diluted with dead cells (prepared as described in section 2.3 Bacteria Incubation and Preparation.) Longer lag times correspond to smaller fractions of live cells compared to dead cells. Inset datapoints refer to the time when each sample reaches the threshold value of OD_{600} 0.1 versus the log(percent live cells). Inset trendlines were used to calculate the percent inactive bacteria for experimental and control conditions.

Figure 50 corresponds to **Figure 51** and **Figure 52** for growth assay with *S. Aureus*, no catalyst or glass filter under dark and white LED conditions. Inset refers to the time when each sample reaches the threshold value of OD_{600} 0.1 versus the log(percent live cells).

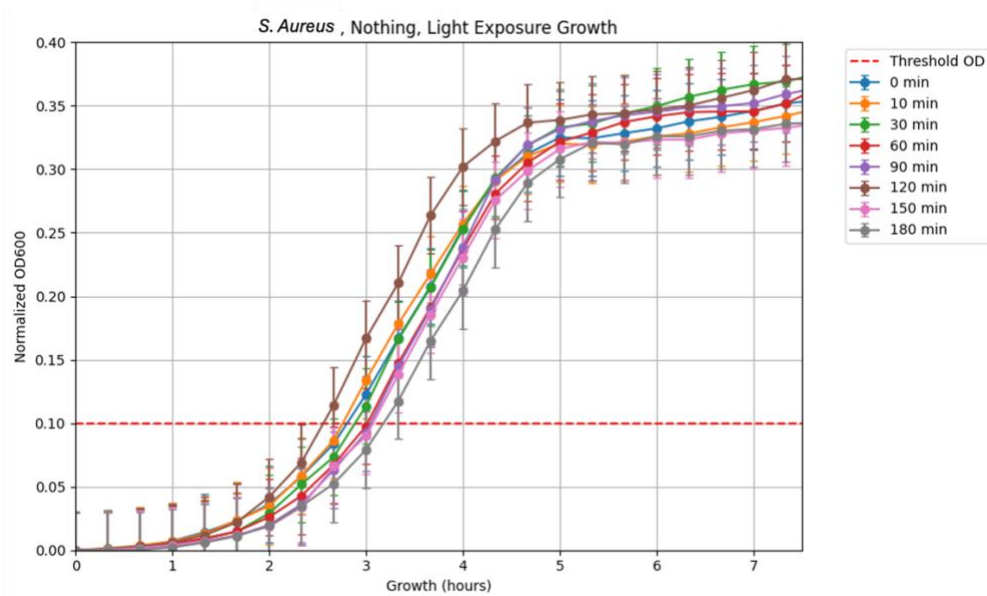


Figure 51 Growth assay results for *S. Aureus* without catalyst or glass filter under white LED conditions (**Figure 36 (a)**). Aliquots were plated, incubate at 37°C, and OD₆₀₀ were read in a wellplate reader every 20 minutes for 16 hours. Datapoints after 8 hours show a plateau so were discarded. Times when each sample crossed the OD₆₀₀ threshold of 0.1 were noted and compared to the respective calibration curve to determine percent bacterial inactivation.

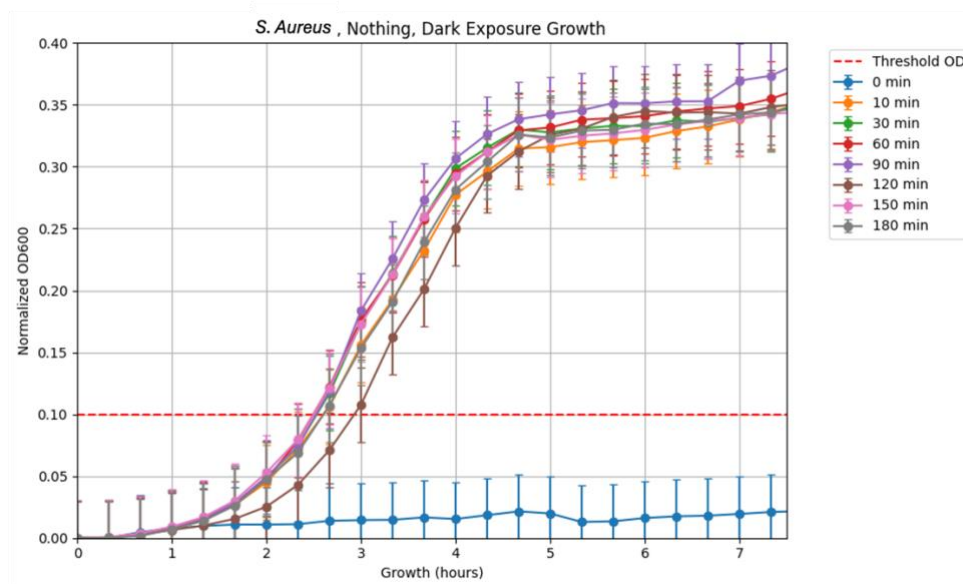


Figure 52 Growth assay results for *S. Aureus* without catalyst or glass filter under dark conditions. Aliquots were plated, incubate at 37°C, and OD₆₀₀ were read in a wellplate reader every 20 minutes for 16 hours. Datapoints after 8 hours show a plateau so were discarded. Times when each sample crossed the OD₆₀₀ threshold of 0.1 were noted and compared to the respective calibration curve to determine percent bacterial inactivation.

Table 9 One-Way ANOVA Results for all Batch Fluorescence tests. Comparisons used are from Tukey's HSD Test, where ANOVA results which rejected the null hypothesis ($P < 0.05$) indicated significant differences among treatment group means. PG is data measured with PicoGreen (Figure 24), and plating indicates data measured by plating and colony counting (Figure 25).

Comparison	P Value			
	<i>S. Aureus</i> , Batch, PG	<i>S. Aureus</i> , Batch, Plating	<i>E. Coli</i> , Batch, PG	<i>E. Coli</i> , Batch, Plating
bTiO ₂ , Light vs GF, Dark	< .0001	< .0001	0.0008058	< .0001
bTiO ₂ , Light vs Nothing, Light	< .0001	< .0001	0.007574	< .0001
bTiO ₂ , Light vs Nothing, Dark	< .0001	< .0001	0.4638	0.0003141
bTiO ₂ , Light vs GF, Light	< .0001	< .0001	0.5298	0.00051
bTiO ₂ , Light vs bTiO ₂ , Dark	< .0001	< .0001	0.5604	0.0008279
bTiO ₂ , Dark vs GF, Dark	< .0001	0.7836	0.1042	0.9547
bTiO ₂ , Dark vs Nothing, Light	< .0001	0.7871	0.3863	0.9565
bTiO ₂ , Dark vs Nothing, Dark	< .0001	0.9314	1	0.9988
bTiO ₂ , Dark vs GF, Light	0.0007284	0.9655	1	1
GF, Light vs GF, Dark	0.2161	0.9957	0.1159	0.9849
GF, Light vs Nothing, Light	0.5737	0.9959	0.4143	0.9858
GF, Light vs Nothing, Dark	0.964	1	1	1
Nothing, Dark vs GF, Dark	0.6807	0.9992	0.1452	0.9969
Nothing, Dark vs Nothing, Light	0.9604	0.9992	0.4783	0.9972
Nothing, Light vs GF, Dark	0.987	1	0.9827	1

Table 10 One-Way ANOVA Results for all Flow 1.0 Fluorescence tests. Comparisons used are from Tukey's HSD Test, where ANOVA results which rejected the null hypothesis ($P < 0.05$) indicated significant differences among treatment group means. PG is data measured with PicoGreen (**Figure 26**), and plating indicates data measured by plating and colony counting (**Figure 27**).

Comparison	P Value			
	<i>S. Aureus</i> , Flow 1.0, PG	<i>S. Aureus</i> , Flow 1.0, Plating	<i>E. Coli</i> , Flow 1.0, PG	<i>E. Coli</i> , Flow 1.0, Plating
bTiO ₂ , Light vs bTiO ₂ , Dark	0.002096	0.0009618	< .0001	0.0003565
bTiO ₂ , Light vs GF, Dark	0.0648	0.004338	< .0001	0.002655
bTiO ₂ , Light vs GF, Light	0.8576	0.02203	< .0001	0.006871
GF, Light vs bTiO ₂ , Dark	0.01523	0.1653	0.002607	0.1541
GF, Light vs GF, Dark	0.2842	0.6748	0.01659	0.8938
GF, Dark vs bTiO ₂ , Dark	0.4927	0.6565	0.8788	0.3946

Table 11 One-Way ANOVA Results for all Flow 3.0 Fluorescence tests measured with PicoGreen (PG) (**Figure 30**). Comparisons used are from Tukey's HSD Test, where ANOVA results which rejected the null hypothesis ($P < 0.05$) indicated significant differences among treatment group means.

Comparison	P Value			
	<i>S. Aureus</i> , Flow 3.0, PG, Air	<i>S. Aureus</i> , Flow 3.0, PG, Oxygen	<i>E. Coli</i> , Flow 3.0, PG, Air	<i>E. Coli</i> , Flow 3.0, PG, Oxygen
bTiO ₂ , Light vs GF, Light	0.0002709	< .0001	< .0001	0.0002629
bTiO ₂ , Light vs bTiO ₂ , Dark	0.0003321	< .0001	0.0002731	0.0004394
bTiO ₂ , Light vs GF, Dark	0.0003563	< .0001	0.0007952	0.001087
GF, Dark vs GF, Light	0.9988	0.2145	0.6777	0.8729
GF, Dark vs bTiO ₂ , Dark	1	0.3003	0.9391	0.9628
bTiO ₂ , Dark vs GF, Light	0.9995	0.9959	0.9428	0.9922

Table 12 Two-Way ANOVA Results for all Flow 2.0 Fluorescence tests measured with PicoGreen (PG) (

Figure 28, Figure 29). Comparisons used are from Tukey's HSD Test, where ANOVA results which rejected the null hypothesis ($P < 0.05$) indicated significant differences among treatment group means. Values in mL are aliquots, compared to residence times of 15, 30 or 60 minutes. Only comparisons with significant statistical differences are included in the table, all other values (controls and other experimental values) were found to be insignificant ($P > 0.05$).

	Comparisons	P Value
<i>E. Coli</i> , Light, bTiO ₂	0 mL:15 min vs. 0 mL:60 min	0.0257
	0 mL:60 min vs. 15 mL:15 min	0.0489
	8 mL:15 min vs. 8 mL:60 min	0.0257
	15 mL:15 min vs. 15 mL:60 min	0.0257
<i>S. Aureus</i> , Light, bTiO ₂	0 mL:15 min vs. 0 mL:30 min	0.0096
	0 mL:15 min vs. 8 mL:30 min	0.0105
	0 mL:15 min vs. 15 mL:30 min	0.0078
	0 mL:30 min vs. 0 mL:60 min	0.0123
	0 mL:60 min vs. 8 mL:30 min	0.0125
	0 mL:60 min vs. 15 mL:30 min	0.0091
	8 mL:15 min vs. 8 mL:30 min	0.0096
	8 mL:15 min vs. 15 mL:30 min	0.0228
	8 mL:30 min vs. 8 mL:60 min	0.0123
	8 mL:60 min vs. 15 mL:30 min	0.0281
	15 mL:15 min vs. 15 mL:30 min	0.0096
	15 mL:30 min vs. 15 mL:60 min	0.0123

The only exception to the insignificance of the controls for Flow 2.0 was observed in the Glass Filter, Light, and *S. Aureus* ANOVA. The overall ANOVA indicated a significant difference in residence times ($P = 0.043$), even though the post-hoc Tukey test detected no differences. This was attributed to the consistently low inactivation values across the dataset, where all bacterial

inactivations were less than 7 %. For example, differences such as 6 % versus 1 % could be detected as significant by the ANOVA test. However, these small differences did not appear significant when analyzing the entire dataset, which included both controls and experimental conditions.

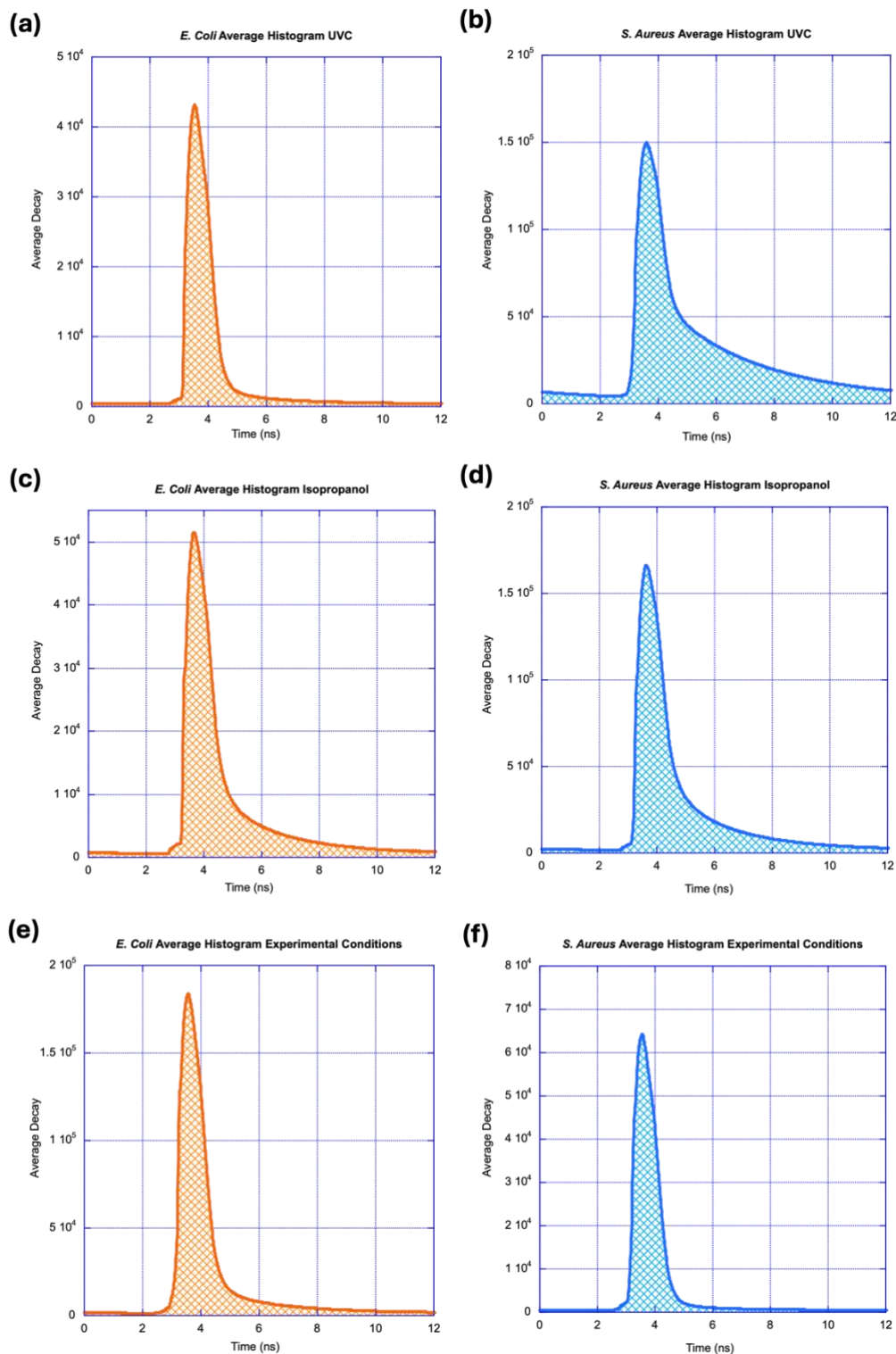


Figure 53 Sample average decay histograms for *E. Coli* treated with UVC (**Figure 36 (c)**) (a), isopropanol (c), and $bTiO_2$ and white light (**Figure 36 (b)**) (e), as well as *S. Aureus* treated with UVC (**Figure 36 (c)**) (b), isopropanol (d), and $bTiO_2$ and white light (**Figure 36 (b)**) (f).

REFERENCES

- (1) Health Organization, W. *Guidelines for Drinking-Water Quality: Small Water Supplies*.
- (2) Yaghmaei, M.; da Silva, D. R. C.; Rutajoga, N.; Currie, S.; Li, Y.; Vallieres, M.; Silvero, M. J.; Joshi, N.; Wang, B.; Scaiano, J. C. Innovative Black TiO₂ Photocatalyst for Effective Water Remediation Under Visible Light Illumination Using Flow Systems. *Catalysts* **2024**, *14* (11), 775. <https://doi.org/10.3390/catal14110775>.
- (3) Currie, S.; Scaiano, T. *Flow Photocatalyst Development for the Degradation of 17 β -Estradiol under Visible Light Using a Methylene Blue Surrogate*; 2021.
- (4) *Titanium Dioxide - Chemical Safety Facts*.
<https://www.chemicalsafetyfacts.org/chemicals/titanium-dioxide/#> (accessed 2024-11-21).
- (5) *Titanium(IV) oxide, 98.0-100.5% TiO₂, Thermo Scientific Chemicals*.
<https://www.thermofisher.com/order/catalog/product/277370010> (accessed 2024-11-21).
- (6) *Solar Energy Solutions in Kenya: Conquering Energy Shortages with 50%*.
<https://ariyafinergy.com/solar-energy-solutions-in-kenya/> (accessed 2024-11-21).
- (7) *Solar Panels Power Calculator for Ottawa, Ontario Canada*.
<https://solarcalculator.ca/report/Ontario/Ottawa/> (accessed 2024-12-19).
- (8) Science, S. *Radiation at Home, Outdoors and in the Workplace*.
- (9) Naldoni, A.; Altomare, M.; Zoppellaro, G.; Liu, N.; Kment, Š.; Zbořil, R.; Schmuki, P. Photocatalysis with Reduced TiO₂: From Black TiO₂ to Cocatalyst-Free Hydrogen Production. *ACS Catal* **2019**, *9* (1), 345–364. <https://doi.org/10.1021/acscatal.8b04068>.
- (10) Imlay, J. A. The Molecular Mechanisms and Physiological Consequences of Oxidative Stress: Lessons from a Model Bacterium. *Nature Reviews Microbiology*. July 2013, pp 443–454.
<https://doi.org/10.1038/nrmicro3032>.
- (11) Winterbourn, C. C. Reconciling the Chemistry and Biology of Reactive Oxygen Species. *Nature Chemical Biology*. Nature Publishing Group March 23, 2008, pp 278–286.
<https://doi.org/10.1038/nchembio.85>.
- (12) Yuan, J.; Shiller, A. M. *The Distribution of Hydrogen Peroxide in the Southern and Central Atlantic Ocean*; 2001; Vol. 48.
- (13) Wilkinson, F.; Brummer, J. G. Rate Constants for the Decay and Reactions of the Lowest Electronically Excited Singlet State of Molecular Oxygen in Solution. *J Phys Chem Ref Data* **1981**, *10* (4), 809–999. <https://doi.org/10.1063/1.555655>.
- (14) Silhavy, T. J. Classic Spotlight: Gram-Negative Bacteria Have Two Membranes. *Journal of Bacteriology*. American Society for Microbiology 2016, p 201.
<https://doi.org/10.1128/JB.00599-15>.
- (15) JM, M.; SO, W. Assessment of Dissolved Ions and Microbial Coliform in Water from Selected Sites of the Upper Athi River Sub-Catchment Area, Kenya. *IOSR Journal of Applied Chemistry* **2017**, *10* (05), 101–109. <https://doi.org/10.9790/5736-100502101109>.
- (16) Onyango, A. E.; Okoth, M. W.; Kunyanga, C. N.; Aliwa, B. O. Microbiological Quality and Contamination Level of Water Sources in Isiolo County in Kenya. *J Environ Public Health* **2018**, *2018*. <https://doi.org/10.1155/2018/2139867>.
- (17) Jang, J.; Hur, H. G.; Sadowsky, M. J.; Byappanahalli, M. N.; Yan, T.; Ishii, S. Environmental Escherichia Coli: Ecology and Public Health Implications—a Review. *Journal of Applied Microbiology*. September 1, 2017, pp 570–581. <https://doi.org/10.1111/jam.13468>.

- (18) Gutama, M.; Koliopoulos, J. *Staphylococcus Aureus, an Important Pathogen of Public Health and Economic Importance: A Comprehensive Review*; Vol. 4.
- (19) Paulton, R. J. L. The Bacterial Growth Curve. *J Biol Educ* **1991**, 25 (2), 92–94. <https://doi.org/10.1080/00219266.1991.9655183>.
- (20) Madigan, M. T.; Bender, K. S.; Buckley, D. H.; Sattley, W. M.; Stahl, D. A. *Brock Biology of Microorganisms*, 15th ed.; Pearson, 2018.
- (21) Elmore, S. *Apoptosis: A Review of Programmed Cell Death*.
- (22) Bayles, K. W. Bacterial Programmed Cell Death: Making Sense of a Paradox. *Nature Reviews Microbiology*. January 2014, pp 63–69. <https://doi.org/10.1038/nrmicro3136>.
- (23) Hu, Y.; Shao, J.; Dong, H.; Yang, D.; Dong, X. Bacterial Programmed Cell Death Induced by Nanotherapeutic Strategies. *ACS Materials Letters*. American Chemical Society September 2, 2024, pp 4209–4229. <https://doi.org/10.1021/acsmaterialslett.4c01165>.
- (24) Kroemer, G.; Martin, S. J. Caspase-Independent Cell Death. *Nature Medicine*. July 2005, pp 725–730. <https://doi.org/10.1038/nm1263>.
- (25) Cosa, G.; Focsaneanu, K.-S.; Mclean, J. R. N.; Mcnamee, J. P.; Scaiano, J. C. *Photophysical Properties of Fluorescent DNA-Dyes Bound to Single-and Double-Stranded DNA in Aqueous Buffered Solution ¶*; 2001; Vol. 73.
- (26) *Escherichia Coli (Migula) Castellani and Chalmers 25404™*. www.atcc.org.
- (27) *Staphylococcus Aureus Subsp. Aureus Rosenbach 12600™*. www.atcc.org.
- (28) Li, Y. Black Titanium Dioxide: Synthesis, Characterization and Applications, University of Ottawa, Ottawa, 2021. <https://ruor.uottawa.ca/server/api/core/bitstreams/aba87c42-93c9-4f95-8bc8-90f1321b5f3c/content> (accessed 2024-11-13).
- (29) *A/E glass fiber filters | Cytiva*. <https://www.cytivalifesciences.com/en/us/shop/lab-filtration/glass-and-quartz-microfiber-filter/binderless-glass-microfiber-filter/a-e-glass-fiber-filters-p-36479> (accessed 2024-11-13).
- (30) Qiu, T. A.; Guidolin, V.; Khoi, ‡; Hoang, N. L.; Pho, T.; Carra', A.; Villalta, P. W.; He, J.; Yao, X.; Hamers, R. J.; Balbo, S.; Feng, Z. V.; Haynes, C. L. *Supplementary Information Nanoscale Battery Cathode Materials Induce DNA Damage in Bacteria*; 2020.
- (31) *Petri dishes polystyrene 60 mm × 15 mm*. https://www.sigmaaldrich.com/CA/en/product/sigma/p5481?utm_source=google&utm_medium=organicshopping&gclid=CjwKCAiA3Na5BhAZEiWAZrfagKFFry-iXNN05_3I-ejls8xD00LPSfxlS0QuRUwp_APwgDVQA1p61RoCBLoQAvD_BwE (accessed 2024-11-13).
- (32) Qiu, T. A.; Nguyen, T. H. T.; Hudson-Smith, N. V.; Clement, P. L.; Forester, D. C.; Frew, H.; Hang, M. N.; Murphy, C. J.; Hamers, R. J.; Feng, Z. V.; Haynes, C. L. Growth-Based Bacterial Viability Assay for Interference-Free and High-Throughput Toxicity Screening of Nanomaterials. *Anal Chem* **2017**, 89 (3), 2057–2064. <https://doi.org/10.1021/acs.analchem.6b04652>.
- (33) *SpectraMax M Series Multi-Mode Microplate Readers | Molecular Devices*. <https://www.moleculardevices.com/products/microplate-readers/multi-mode-readers/spectramax-m-series-readers> (accessed 2024-11-15).
- (34) Gallagher, S. R.; Desjardins, P. R. Quantitation of DNA and RNA with Absorption and Fluorescence Spectroscopy. *Curr Protoc Mol Biol* **2006**, 76 (1). <https://doi.org/10.1002/0471142727.mba03ds76>.
- (35) Brakstad, O. G.; Aasbakk, K.; Maeland, J. A. Detection of Staphylococcus Aureus by Polymerase Chain Reaction Amplification of the Nuc Gene. *J Clin Microbiol* **1992**. <https://doi.org/10.1128/jcm.30.7.1654-1660.1992>.

- (36) *Glutaraldehyde Grade I, 70 water, specially purified for use as an electron microscopy fixative or other sophisticated use 111-30-8*.
<https://www.sigmaaldrich.com/CA/en/product/sial/g7776?srsId=AfmBOoo5BRW3SYO41ywb s7M1sFLgpqaUr7uWlaIWFTmxAvlkCgKkeINY> (accessed 2024-12-02).
- (37) *Pyrex® narrow-mouth graduated Erlenmeyer flask capacity 50 mL | Sigma-Aldrich*.
https://www.sigmaaldrich.com/CA/en/product/aldrich/cls498050?utm_source=google&utm_medium=organicshopping&srsId=AfmBOoo1Qm-RVas3_YQhiacF1FJycmYTL0C1__eP9hvOhy1oKYVpncP36cY (accessed 2024-11-15).
- (38) *50W LED Flood Light Outdoor, LED Work Light, Floodlight Fixture with Plug in IP66 Waterproof, 6500K 2Pack Security Light for Yard Garden Stadium Garage Playground : Amazon.ca: Tools & Home Improvement*. https://www.amazon.ca/Outdoor-Floodlight-Waterproof-Security-Playground/dp/B0BZNS9XV8/ref=sr_1_34?dib=eyJ2IjoiMSJ9.ENNmS7QxF7UxDWccdfH7448mg0kApwibK1QdCGyC5Nx76Fq4nYqJeotUAaT_4-GLELVEqkEJVxiJ7VVZuBGvH7pYy0GQNJe-hs4d5uWwfJ_vWcGWtRNCz4OjR_2m3KII2umTD01UaTTcMf8kycRFT6jrHbBPyhpQujTxZjHMbZUM5Cb09Iup1SML9IYqQUdfBIRnZdSCTwE2qKOJzUCpLWJvbBetiVWritA2JNpOxRVD4iU6GHbc6dBI_RDLAOn13vb7bnquEWlwYkgA6nyBwSI9va0a0S12PYHIYXesNOY.mkg-QRGjbwQQJCUuOjh9-zKjEuohzwrpfDqwqpl7BLk&dib_tag=se&hvadid=588926357657&hvdev=c&hvlocphy=9000668&hvnetw=g&hvqmt=e&hvrnd=16676235538649216291&hvtargid=kwd-327782349829&hydadcr=15804_13533858&keywords=50w%2Bled%2Bflood%2Blight%2Bwrm%2Bwhite&qid=1731776666&sr=8-34&th=1 (accessed 2024-11-15).
- (39) *VWR® Variable-Speed Peristaltic Pumps | VWR*. <https://us.vwr.com/store/product/4787969/vwr-variable-speed-peristaltic-pumps> (accessed 2024-11-16).
- (40) *SyringePump.com - NE-300 Just Infusion Syringe Pump*. https://www.syringepump.com/NE-300.php?gclid=Cj0KCQiA0fu5BhDQARIsAMXUBOKAUoR-gWFjWozz4QJv9T65_MaSVaXqSPpVJygVqIlbk_M00NCcUKwaAgWzEALw_wcB (accessed 2024-11-20).
- (41) *BD Syringes without Needle, 50 mL | Fisher Scientific*.
<https://www.fishersci.ca/shop/products/bd-syringes-luer-lok-tips-4/136898> (accessed 2024-11-20).
- (42) *Quartz Glassware –Luzchem Research*. <https://luzchem.com/products/quartz-glassware?variant=46779505443128> (accessed 2024-11-20).
- (43) Gibson, B.; Wilson, D. J.; Feil, E.; Eyre-Walker, A. The Distribution of Bacterial Doubling Times in the Wild. *Proceedings of the Royal Society B: Biological Sciences* **2018**, 285 (1880). <https://doi.org/10.1098/rspb.2018.0789>.
- (44) Reichardt, C. . *Solvents and Solvent Effects in Organic Chemistry*; Wiley-VCH, 2004.
- (45) Lewis, K. *Programmed Death in Bacteria*; 2000; Vol. 64.
- (46) Simon, H.-U.; Haj-Yehia, A.; Levi-Schaffer, F. *Role of Reactive Oxygen Species (ROS) in Apoptosis Induction*; Kluwer Academic Publishers, 2000; Vol. 5.
- (47) Molin, S.; Tolker-Nielsen, T. Gene Transfer Occurs with Enhanced Efficiency in Biofilms and Induces Enhanced Stabilisation of the Biofilm Structure. *Current Opinion in Biotechnology*. Elsevier Ltd 2003, pp 255–261. [https://doi.org/10.1016/S0958-1669\(03\)00036-3](https://doi.org/10.1016/S0958-1669(03)00036-3).
- (48) Andrés Juan, C.; Manuel Pérez de la Lastra, J.; Plou, F. J.; Pérez-Lebeña, E.; Reinbothe, S. Molecular Sciences The Chemistry of Reactive Oxygen Species (ROS) Revisited: Outlining

- Their Role in Biological Macromolecules (DNA, Lipids and Proteins) and Induced Pathologies. *Int. J. Mol. Sci* **2021**, *22*, 4642. <https://doi.org/10.3390/ijms>.
- (49) Berezin, M. Y.; Achilefu, S. Fluorescence Lifetime Measurements and Biological Imaging. *Chem Rev* **2010**, *110* (5), 2641–2684. <https://doi.org/10.1021/cr900343z>.
- (50) Mitsuzawa, S.; Deguchi, S.; Horikoshi, K. Cell Structure Degradation in Escherichia Coli and Thermococcus Sp. Strain Tc-1-95 Associated with Thermal Death Resulting from Brief Heat Treatment. *FEMS Microbiol Lett* **2006**, *260* (1), 100–105. <https://doi.org/10.1111/j.1574-6968.2006.00301.x>.
- (51) Kwun, M. S.; Lee, D. G. Bacterial Apoptosis-Like Death through Accumulation of Reactive Oxygen Species by Quercetin in Escherichia Coli. *J Microbiol Biotechnol* **2024**, *34* (7), 1395–1400. <https://doi.org/10.4014/jmb.2403.03057>.
- (52) Hong, Y.; Zeng, J.; Wang, X.; Drlica, K.; Zhao, X. Post-Stress Bacterial Cell Death Mediated by Reactive Oxygen Species. *Proc Natl Acad Sci U S A* **2019**, *116* (20), 10064–10071. <https://doi.org/10.1073/pnas.1901730116>.
- (53) Pfeifer, G. P. Mechanisms of UV-Induced Mutations and Skin Cancer. *Genome Instab Dis* **2020**, *1* (3), 99–113. <https://doi.org/10.1007/s42764-020-00009-8>.
- (54) Technical Release LUZCHEM Exposure Standard: LES-UVC-16.